AN ABSTRACT OF THE THESIS OF

Ho Sung Aum for the degree of Doctor of Philosophy in Mechanical Engineering presented on May 13, 1992.

Title: Parameters Affecting Mechanical Collisions

Redacted for Privacy

Abstract approved: ___

Charles E. Smith

Even though the elastic deformations that occur during the impact of colliding bodies may be small in comparison to their actual dimensions, they play an important role in mechanical collisions. During the time the bodies are in contact, elastic, friction, and inertia properties combine to produce a complex variation of sliding and sticking throughout the contact surface. Detailed analysis of this interaction is quite tedious, but would seem to be necessary for accurately predicting the impulse and velocity changes that occur during contact. However, a considerably-simplified model captures the essential characteristics of the elastic-friction interaction during contact, leading to predictions of impulse and velocity changes that agree well with those of more detailed analyses of a number of different collisions.

The model's simplicity enables an examination of parameters that affect a general class of collisions. For planar collisions, the

model contains five dimensionless parameters; the effects of four of these on the rebound velocity are examined here.

In addition, comparisons are made with a previously-used, somewhat simpler model, which neglects the tangential compliance in the region of contact.

Parameters Affecting Mechanical Collisions

by

Ho Sung Aum

A THESIS

submitted to

Oregon State University

in partial fulfillment of
the requirements for the
degree of

Doctor of Philosophy

Completed May 13, 1992

Commencement June 1993

APPROVED:

Redacted for Privacy

Professor of Mechanical Engineering in charge of major

Redacted for Privacy

Head of Department of Mechanical Engineering

Redacted for Privacy

Dean of Graduate School

Date thesis is presented May 13, 1992

Typed by the author Ho Sung Aum

ACKNOWLEDGEMENTS

"Where shall I begin, please your Majesty ?" she asked. "Begin at the beginning" the Queen said, very gravely, "and go on till you come to the end: then stop."

- Alice in Wonderland -

Despite three years break, Dr. Charles Smith, my major advisor, accepted me for doctoral program again. I am deeply grateful for his encouragement, kindness and patience throughout the duration of my study at OSU. Without his foresight and guidence this thesis could not be completed. I also would like to thank graduate council representative and all of my committee members for their excellent teaching.

I like to express my most sincere appreciation to Rev. Moon. He inspired me with courage and supported me financially during this study.

I am also indebt to my wife and two daughters for their understanding, sacrifice and patience even though they have been away. From the bottom of my heart I want to express special thanks to my parents for their support and endless love which provided me with the source of motivation.

TABLE OF CONTENTS

LIST OF FIGURES

NOMENCLATURE

a	the radius of contact area.
$\mathbf{a}_1$, $\mathbf{a}_2$	the engenvectors of $\mathbf{M}$.
b	the distance between contact point P and mass center G.
c	the radius of stick region in contact area.
c	the definition of the coefficient of restitution.
c_n, c_t	the normal and tangential compliance of contact surface.
d	the definition of the coefficient of restitution.
e	the definition of the coefficient of restitution.
$\mathbf{e}_1$, $\mathbf{e}_2$	a set of mutually perpendicular unit vector.
E, E_i	Young's modulus.
$\mathbf{F}$, F_n, F_t	the reaction force and its components.
$F_{t,non}$	the nondimensional tangential reaction force.
$\mathbf{g}$, g_n, g_t	the impulse and its components.
G	the center of mass.
G, G_i	the shear modulus
I_3, I_3'	the central moment of inertia of body B for $\mathbf{e}_3$.
K	the kinetic energy.
$\mathbf{K}$, K_{ij}	the stiffness matrix and its coefficients.
k_3	the central radius of gyration of rod.
L	the length of rod.
l_{ri}	the component of $\mathbf{v}_r$ in the $\mathbf{e}_1$ direction.
m	the equivalent mass, see equation (2.47).
$\mathbf{M}$	the inertia matrix in $\mathbf{e}_1$, $\mathbf{e}_2$, $\mathbf{e}_3$ direction.
M_1, M_2	the eigenvalues of $\mathbf{M}$.
m_{ij}	the inertia coefficients ingeneralized coordinates.

$\mathbf{n}$	the normal direction of the contact surface.
$\mathbf{N}$	the inverse of inertia matrix $\mathbf{M}$.
N_{ij}	the coefficients of $\mathbf{N}$.
N_1, N_2	the eigenvalues of $\mathbf{N}$.
P, P'	the contact points belonging to body B and B'.
P_r	the r^{th} component of generalized momentum.
p(r)	the pressure on contact surface by normal force.
q(r)	the tangential traction on the contact surface.
R, R_i	the radius of hemisphere at contact point.
s(t)	the displacement of tangential spring.
$\mathbf{t}$	the tangential direction of the contact surface.
T	the duration of impact.
t	the intant time during impact.
$\mathbf{u}(t)$, u_n, u_t	the displacement of contact point and its components.
u_r, u_s	the generalized speeds.
$\mathbf{v}$	the relative velocity between P and P' at the beginning of contact.
v, v_n, v_t	the magnitude and its components of $\mathbf{v}$.
$\mathbf{v}_r$	the r^{th} partial velocity of $\mathbf{v}$.
$\bar{\mathbf{v}}(t), \bar{v}_n, \bar{v}_t$	the velocity of contact point P at any instant time, $\dot{\mathbf{u}}(t)$, and its components
$\mathbf{w}$	the relative velocity between P and P' at the end of contact.
w_n, w_t	the components of $\mathbf{w}$.
W	the work done by contact force during impact.
W_n	the work done by normal contact force during impact.
W_{nc}, W_{nr}	the work done by the normal force during the compression and restitution phases.

α	the approach angle.
γ_n, γ_t	the nondimensional components of impulse $\mathbf{g}$.
γ_n', γ_t'	the nondimensional components of reaction force $\dot{\mathbf{g}}$.
δ_n, δ_t	the nondimensional components of displacement $\mathbf{u}$.
δ_n', δ_t'	the nondimensional components of velocity $\dot{\mathbf{u}}$.
ε	the nondimensional displacement of tangential spring s(t).
ε'	the nondimensional velocity of tangential spring s(t).
ε^*	the nondimensional displacement of tangential spring s(t) for limit friction force.
ε'^*	the nondimensional velocity of tangential spring s(t) for limit friction force.
θ	the angle between $\mathbf{n}$ and $\mathbf{a}_2$.
λ	the inertia coupling parameter.
μ	the friction coefficient.
ν	Poisson's ratio.
Φ_t	the ratio of tangentialforce and limiting friction force, see equation (4.55).
$\Psi_{1,2}$	the nondimensional incident and rebound angle.
τ	the nondimensional contact time during impact.
ω^B	the angular velocity of body B.

LIST OF TABLES

Parameters Affecting Mechanical Collisions

1. INTRODUCTION

From classical theory of the dynamics of colliding rigid bodies, the Newtonian concepts of impulse and momentum have been developed and the coefficient of restitution, which is the ratio of incident and rebound velocities in the normal direction, has been applied to obtain additional information. The coefficient of restitution, widely believed to have a value of one for a perfect elastic body and zero for a pure plastic body, has been considered as a material property from which changes of velocities can be computed. Since the impulse-momentum equations represent the first integral of motion, they contain no information of the trajectory. Also, this simple means of analysis can not be used to predict the rebound from a collision for a general configuration, due to the presence of a number of unknown effects, including friction, inertia coupling, and deformation of the contact area, among others.

Recent attempts have been made to study impact in the presence of friction [1,2]. There is no satisfactory method under the idea that the collision is instantaneous within the framework of rigid body mechanics. Whittaker [20] assumes that the relative tangential velocity is zero if the magnitude of the tangential impulse is less than the coefficient of friction times the magnitude of normal impulse and there exists the relative velocity when the magnitude of tangential impulse equals the coefficient times the magnitude of normal impulse.

This method is correct only when the initial slip does not stop and keeps constant direction throughout the collision. Kane and Levinson [7] use the same criteria with additional specification of static and kinetic friction. This approach, developed for a pendulum striking a fixed surface, leads to an increase of kinetic energy. Keller [8] explains that it is due to reverse slip during the impact, but the difficulty in using his theory arises in calculation. Thus, improper handling of friction in collision has often caused difficulties and has led to serious error.

Analysis of the means for graphic guidance of the tangential and normal impulse between two colliding bodies had been presented by Routh [15] in 1905, and has been developed recently in greater detail by Smith and Liu [17]. In this approach, tangential velocity is given by rigid body kinematics; slip or stick are not affected by deformations. Although this analysis has constituted a contribution to realistic solution for rebounds, it indicates that, under some circumstance, reverse slip occurs immediately after initial slip stops and the tangential force is subject to discontinuous changes as the sliding reverses direction. However, in practice, sudden changes in tangential force implied by ignoring tangential deformations of colliding bodies are unlikely to occur. Consequently, it has been evident that even the relatively small elastic deformations that occur during impacts have served to introduce effects that must be taken into account in the analysis of the elastic collisions.

Herzt developed a theory for the elastic deformations of bodies which are pressed together. Since Hertz theory of contact is

developed the quasi-static loading, it provides an adequate description of events in normal impact. This is described in Timoshenko and Goodier [19]. In turn, tangential compliance for the contact surface between two elastic spheres under the action of friction, keeping the normal force constant, is analyzed by Mindlin [13]. He shows that an annulus of micro-slip is generated at the edge of the contact area for even small relative tangential loads. When the tangential load is increased, the inner radius of this annulus reduces to zero and the bodies initiate sliding action. On the other hand, when the tangential force is subsequently decreased, this process would not simply reverse. Rather, micro-slip in the opposite direction would begin at the edge of the contact area. Hence, it is determined that the state of unloading is different from that of loading, and that the process is irreversible. The "irreversibility" implied by frictional slip demonstrates that the final state of contact depends on the previous history of loading and not only on the final values of the normal and tangential forces. In addition, Mindlin and Deresiewicz [14] have investigated changes in surface traction and compliance between spherical bodies in contact arising from various possible combinations of incremental changes of loads. Since the contact area is changed continuously, and neither the normal nor the tangential forces could be known previously, the interface conditions between the two bodies is more complex than might be expected.

To account for this complex interaction, Maw et al. [10,11,12] have developed a numerical method for the oblique impact of elastic spheres. By trial and error the solution is tested to see whether the

assumed divisions of slip and stick on the potential contact area divided into a series of equi-spaced concentric annuli are correct and converged. This approach is supported by experimental results, but limited only to the collision of spheres. Recently, Liu [9] has considered a finite element method, using ANSYS code for non-collinear elastic collisions, including wave propagation in the bodies. Like other numerical methods, it requires time-consuming process and sometimes leads to unstable output for extreme cases.

The interface between two colliding bodies resembles the behavior of a pair of mutually perpendicular, non-linear springs which react independently against each bodies, with the exception that the stiffness of the tangential "spring" is influenced by the normal compliance. Tangential and normal vibrations are dependent on the initial condition as well as the inertia of the colliding bodies. Thus, if the local deformations between colliding bodies were expressed in terms of "spring" stiffnesses in the normal and tangential directions, then the collision process could be solved as a spring-mass system, having a typical formulation of the form $[\mathbf{M}]\{\ddot{u}\} + [\mathbf{K}]\{u\} = 0$. This concept represents the starting point for this investigation.

The inertia of the colliding system [**M**], expressed in terms of two parameters for planar collisions, is formulated from the generalized impulse-momentum relationship, and the recognition and treatment of tangential restitution are considered in Chapter 2. In chapter 3, Hertz theory is presented for normal compliance, based upon the assumption that colliding bodies are perfectly elastic. In addition, based on contact mechanics [6], complicated tangential

compliance is investigated. Methods of modeling normal and tangential deformation in the region of the contact area, in which stiffness of local deformation for the contact area [**K**] is simplified by three different models for tangential compliance, are discussed in Chapter 4. All system equations are formulated nondimensionally for planar collisions in terms of four parameters which characterize the mechanical collision. In chapter 5, three coefficients of restitution are defined and various parameter values are compared for planar impacts. It is revealed that the coefficient of restitution, a ratio of the normal components of approach and separation velocities, is highly dependent upon the parameters of inertia coupling, friction and incident velocity and it could attain high value for the extreme parameters (i.e., much greater than 3.0).

2. GENERAL SYSTEM EQUATIONS FOR ELASTIC COLLISIONS

Assumptions used to develop general dynamic equations of colliding systems are discussed in this chapter. Based upon generalized coordinates and generalized speeds of a dynamic system introduced by Kane and Levinson [7], inertial properties of colliding system in a general configuration is formulated for any three dimensional coodinates. The relation between generalized impulse and generalized momentum, combining stiffness of local deformation for a half-space analysis, leads the system equations, which have the form of simple, ordinary differential equations.

2.1 Background for consideration of elastic collisions

Some typical assumptions are commonly made for the classical approach for collisions of rigid bodies. The duration of contact is sufficiently short that there is no change in configuration of bodies while velocities undergo the changes necessary for separation at the instant of collision. For many cases, this assumption of constant configuration during contact would be not responsible for serious discrepancies in the prediction of the rebound. In the absence of detailed knowledge of the deformations induced by the impulsive reaction force where the bodies contact one another, an additional assumption is made, that the coefficient of restitution (the ratio of the normal velocity of separation to the normal velocity of incidence) can be estimated. Assuming a value for this coefficient is necessary, since

the equations of rigid body kinetics are too few to predict the impulse and velocity changes. This ratio has often been regarded as "material constant" with the implication that it is independent of such considerations as system configuration, direction of approach velocity and friction. However, this assumption is true only under special circumstances.

For elastic analysis, the contact area is small compared with the size of the colliding bodies and surrounds the contact point of rigid body collision, and Hertz theory is applied for normal effects. Colliding bodies are assumed linearly elastic,implying that surface friction is the only source of energy dissipation related to the impact. In addition, there is no distinction between static and kinetic friction coefficients and the coefficient is assumed to be constant.

Other effects, including wave propagation, heat and sound are excluded from consideration in this investigation. Note that the Hertz theory considers only local deformations and neglects the effects of wave propagation. It is an excellent approximation for spherical or stocky bodies where the contact duration, t^*, is much greater than the natural periods of vibration of the system, thus avoiding amplification shown in Figure 1 [3]. Compared to the contact time for stocky bodies, the vibration periods of wave propagation are short and the effect of wave propagation could be neglected [5]. However, for consideration of a slender bar, the vibrational effects should in general be included for an impact analysis.

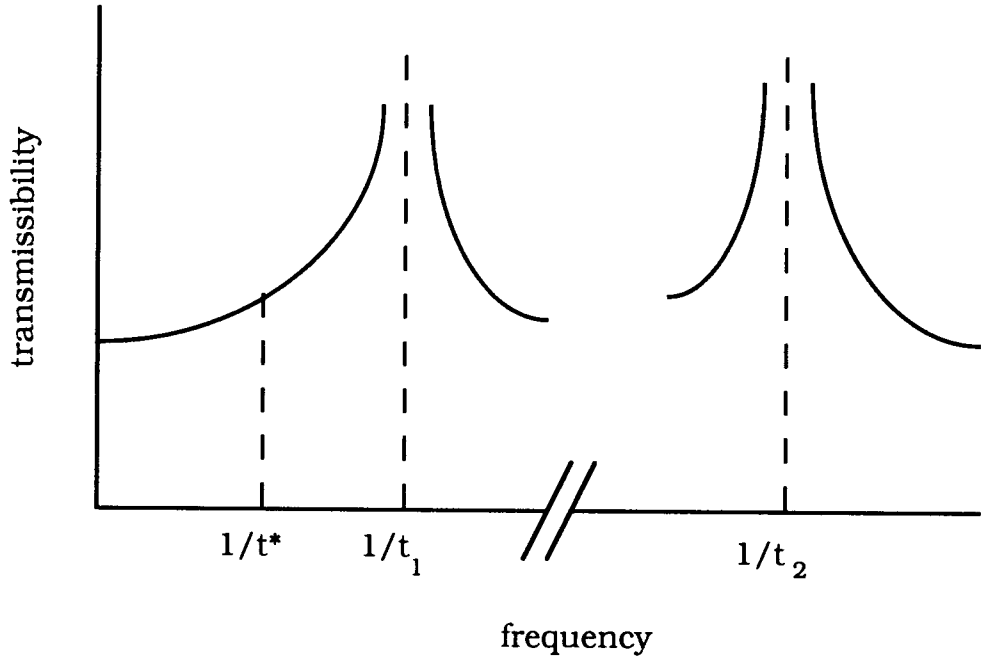

Figure 1. Transmissibility for multi-degree of freedom system

2.2 Generalized impulse, momentum and kinetic energy

Consider two rigid bodies B and B' colliding as the points P and P' on their respective surfaces move into coincidence. If this system S possesses n degrees of freedom, the velocities of the contact points P and P' can be written in terms of generalized speeds u_r as

$$\mathbf{v}^{P} = \sum_{r} \mathbf{v}_r^{P}\, u_r ,$$
$$\mathbf{v}^{P'} = \sum_{r} \mathbf{v}_r^{P'}\, u_r , \qquad (2.1)$$

where $\mathbf{v}_r^{P}$ and $\mathbf{v}_r^{P'}$ are the partial velocities. It is helpful to define the relative velocity $\mathbf{v}$ as

$$\mathbf{v} = \mathbf{v}^{P} - \mathbf{v}^{P'} , \tag{2.2}$$

from which

$$\mathbf{v} = \sum_{r} \mathbf{v}_r u_r , \tag{2.3}$$

where $\mathbf{v}_r = \mathbf{v}_r^{P} - \mathbf{v}_r^{P'}$. If the changes in configuration and contributions from forces other than the action-reaction at the contact point are neglected and the impulse of the force exerted on B by B' is denoted as $\mathbf{g}$, then the r^{th} component of generalized impulse can be expressed as

$$I_r = \mathbf{v}_r \cdot \mathbf{g} . \tag{2.4a}$$

Expressing the kinetic energy in terms of the selected generalized speeds, the inertia coefficients m_{rs} can be evaluated from

$$K = \frac{1}{2} \sum_{r} \sum_{s} m_{rs} u_r u_s . \tag{2.5}$$

According to the relationship

$$P_r = \frac{\partial K}{\partial u_r} , \tag{2.6}$$

this r^{th} component of generalized momentum can be rewritten as

$$P_r = \sum_{s} m_{rs} u_s . \tag{2.7}$$

The impulse-momentum laws can then be expressed as

$$I_r = \Delta P_r = \sum_{s} m_{rs} \Delta u_s , \tag{2.8}$$

where Δu_s denotes the change in u_s during the contact.

If $\mathbf{v}$ and $\mathbf{w}$ are used to denote the relative velocity between the contact points P and P' , at the beginning of contact and at the end of contact, then

$$\mathbf{w} = \mathbf{v} + \Delta\mathbf{v} \tag{2.9}$$

and

$$\Delta\mathbf{v} = \sum_r \mathbf{v}_r \Delta u_r \ . \tag{2.10a}$$

Then, let $\mathbf{e}_1$, $\mathbf{e}_2$ and $\mathbf{e}_3$ be a set of mutually perpendicular unit vectors, where $l_{ri} = \mathbf{v}_r \cdot \mathbf{e}_i$ and $g_i = \mathbf{g} \cdot \mathbf{e}_i$. Then, equations (2.3a), (2.4a) and (2.10a) can be written as

$$\begin{aligned}\mathbf{v} &= \mathbf{v}_1 u_1 + \mathbf{v}_2 u_2 + \ldots\ldots + \mathbf{v}_n u_n \\ &= (l_{11}\mathbf{e}_1 + l_{12}\mathbf{e}_2 + l_{13}\mathbf{e}_3)u_1 + \ldots\ldots + (l_{31}\mathbf{e}_1 + l_{32}\mathbf{e}_2 + l_{33}\mathbf{e}_3)u_3 \\ &= \left(\sum_r l_{r1}u_r\right)\mathbf{e}_1 + \left(\sum_r l_{r2}u_r\right)\mathbf{e}_2 + \left(\sum_r l_{r3}u_r\right)\mathbf{e}_3 \ ,\end{aligned} \tag{2.3b}$$

$$I_r = l_{r1}g_1 + l_{r2}g_2 + l_{r3}g_3 \ , \tag{2.4 b}$$

and

$$\Delta\mathbf{v} = \left(\sum_r l_{r1}\,\Delta u_r\right)\mathbf{e}_1 + \left(\sum_r l_{r2}\,\Delta u_r\right)\mathbf{e}_2 + \left(\sum_r l_{r3}\,\Delta u_r\right)\mathbf{e}_3 \ . \tag{2.10b}$$

So, the following matrix forms according to equations (2.3b), (2.4b), (2.5), (2.8) and (2.10b) become

$$\mathbf{v} = \mathbf{l}^T \mathbf{u} \ , \tag{2.11}$$

$$\mathbf{I} = \mathbf{l}\,\mathbf{g} \ , \tag{2.12}$$

$$K = \frac{1}{2}\ \mathbf{u}^T\mathbf{m}\mathbf{u} \ , \tag{2.13}$$

$$\mathbf{I} = \mathbf{m}\,\Delta\mathbf{u} \ , \tag{2.14}$$

and

$$\Delta\mathbf{v} = \mathbf{l}^T \Delta\mathbf{u} \ , \tag{2.15}$$

where **l**, **u** and $\Delta\mathbf{u}$ are (n x 1) matrices, **g**, **v** and $\Delta\mathbf{v}$ are (3 x 1) matrices, **l** is (n x 3) matrix, and **m** is (n x n) symmetric matrix for inertia. From equations (2.12) and (2.14),

$$\Delta\mathbf{u} = \mathbf{m}^{-1}\,\mathbf{l}\,\mathbf{g}\ , \tag{2.16}$$

and substituting equation (2.16) into (2.15),

$$\Delta\mathbf{v} = (\,\mathbf{l}^{T}\mathbf{m}^{-1}\mathbf{l})\,\mathbf{g} = \mathbf{N}\,\mathbf{g} \tag{2.17}$$

or

$$\mathbf{g} = (\,\mathbf{l}^{T}\mathbf{m}^{-1}\mathbf{l})^{-1}\,\Delta\mathbf{v} = \mathbf{M}\,\Delta\mathbf{v}\ , \tag{2.18}$$

where

$$\mathbf{N} = (\,\mathbf{l}^{T}\mathbf{m}^{-1}\mathbf{l}) = \mathbf{M}^{-1}\ . \tag{2.19}$$

Both **N** and **M** are (3 x 3) symmetric matrices and depend on the configuration of the system at initial contact, but not on the motion. Also, if the configuration does not change significantly during impact, the small dynamic deformations during contact, and consequently **g**, may be expected to depend on **v**, but not on the particular set of generalized speeds that contribute to **v**. Therefore, all pre-contact motions having the approach velocity **v** and the same configuration at the initial contact will result in the same impulse and corresponding separation velocity **w**. Once $\Delta\mathbf{v}$ has been determined, changes in the generalized speeds can be evaluated from equation (2.16), where

$$\Delta\mathbf{u} = \mathbf{m}^{-1}\,\mathbf{l}\,\mathbf{M}\,\Delta\mathbf{v}\ , \tag{2.20}$$

and corresponding changes in velocities and angular velocities of interest can be evaluated using the appropriate partial velocities and partial angular velocities. Thus, from any generalized speeds, impulse

and momentum relationships in equation (2.18) for the general configuration of the colliding system may be formulated in three dimensions.

The change in kinetic energy induced by the impulse is given by

$$\Delta K = \frac{1}{2} (\mathbf{u} + \Delta\mathbf{u})^T \cdot \mathbf{m} \cdot (\mathbf{u} + \Delta\mathbf{u}) - \frac{1}{2} \mathbf{u}^T \cdot \mathbf{m} \cdot \mathbf{u} \qquad (2.21)$$

and, through the relationship of generalized impulse and momentum described in this section, can also be expressed as:

$$\Delta K = \mathbf{g}^T \cdot \mathbf{v} + \frac{1}{2} \mathbf{g}^T \cdot \mathbf{M}^{-1} \cdot \mathbf{g} , \qquad (2.22a)$$

$$\Delta K = \mathbf{g}^T \cdot \frac{\mathbf{v} + \mathbf{w}}{2} , \qquad (2.22b)$$

and

$$\Delta K = \frac{1}{2} (\mathbf{w}^T \cdot \mathbf{M} \cdot \mathbf{w} - \mathbf{v}^T \cdot \mathbf{M} \cdot \mathbf{v}) . \qquad (2.22c)$$

2.3 Kinematics of planar collisions

To facilitate formulation of a contact law for planar collisions, as shown in Figure 2, substitute for $\mathbf{e}_1$ - $\mathbf{e}_2$ - $\mathbf{e}_3$, as developed in the previous section, a set of basis vectors $\mathbf{t}$ - $\mathbf{n}$ - $\mathbf{t}_1$, where $\mathbf{n}$ is a unit vector perpendicular to the common tangent to the surfaces at P and P' and directed from B' into B, $\mathbf{t}$ has the same direction as $\mathbf{n} \times (\mathbf{v} \times \mathbf{n})$, where $\mathbf{v}$ is the relative velocity between two contact points, and $\mathbf{t}_1 = \mathbf{t} \times \mathbf{n}$. The approach velocity can then be expressed as

$$\mathbf{v} = v_t \mathbf{t} + v_n \mathbf{n} . \qquad (2.23)$$

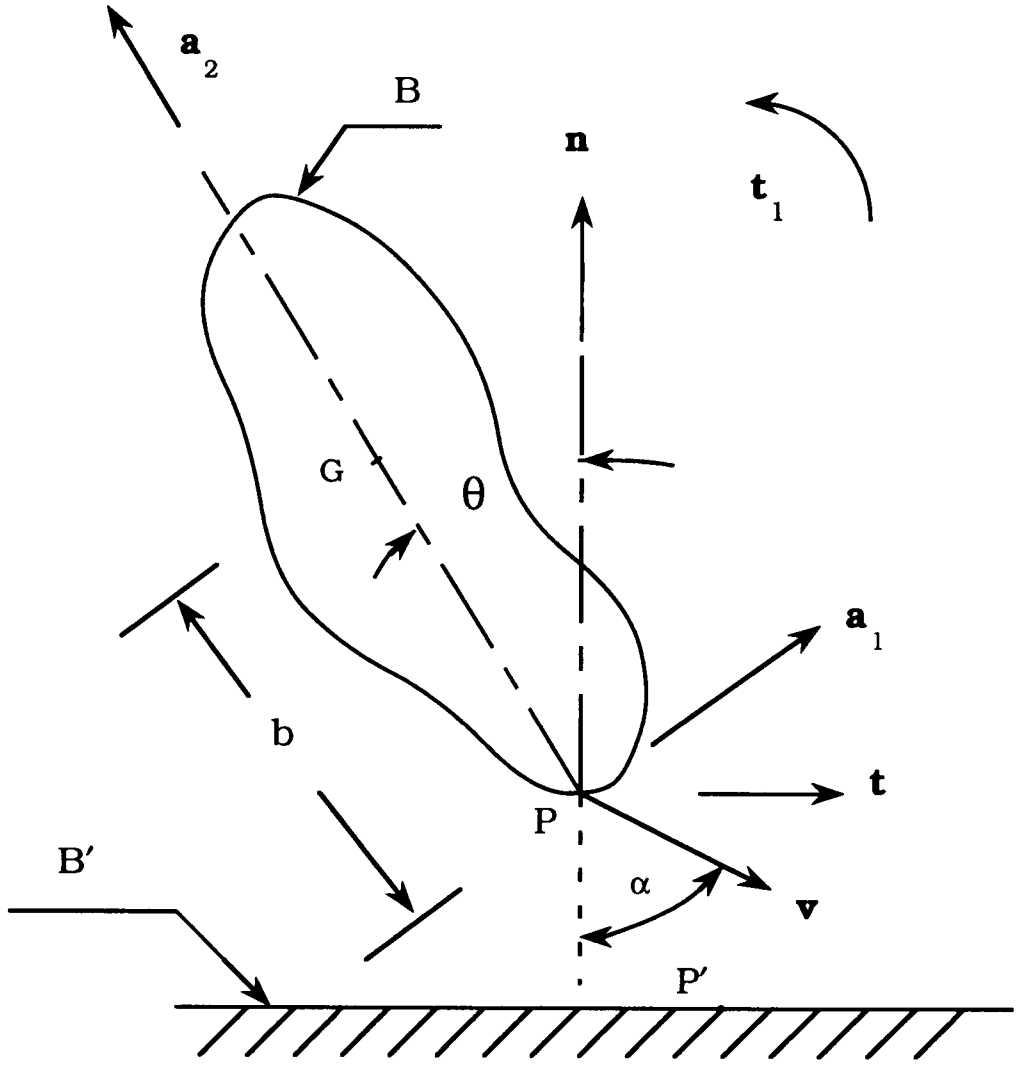

Figure 2. Planar collision between a rod and a flat plane

Subject to an appropriate coordinate transformation, all of the matrices developed in previous section can be evaluated in terms of the unit vectors $\mathbf{t}$ - $\mathbf{n}$ - $\mathbf{t}_1$. From equation (2.17), if there is no coupling of $\mathbf{N}$ between $\mathbf{t}_1$ and other directions, the relative velocity $\mathbf{w}$ and the impulse $\mathbf{g}$ could be expressed in terms of normal and tangential components as

$$\mathbf{w} = w_t\,\mathbf{t} + w_n\,\mathbf{n} \tag{2.24}$$

and

$$\mathbf{g} = g_t\,\mathbf{t} + g_n\,\mathbf{n} \tag{2.25}$$

Thus, equation (2.17) can be rewritten as

$$\begin{Bmatrix} \Delta v_t \\ \Delta v_n \end{Bmatrix} = \begin{bmatrix} N_{tt} & N_{tn} \\ N_{nt} & N_{nn} \end{bmatrix} \begin{Bmatrix} g_t \\ g_n \end{Bmatrix} \tag{2.26}$$

Based on the theory of Mohr's circle, two principal values N_1 and N_2 can be obtained, that is,

$$N_{1,2} = \frac{N_{tt} + N_{nn}}{2} \pm \sqrt{\left(\frac{N_{tt} - N_{nn}}{2}\right)^2 + N_{tn}^2}\,, \tag{2.27}$$

wherein N_1 is defined to be the larger of two. It follows that the expressions for the components of $\mathbf{N}$ are

$$N_{tt,\,nn} = \frac{N_1 + N_2}{2} \pm \left(\frac{N_1 - N_2}{2}\right)\cos 2\theta \tag{2.28}$$

and

$$N_{tn} = \left(\frac{N_1 - N_2}{2}\right)\sin 2\theta \tag{2.29}$$

where θ is the angle between $\mathbf{n}$ and the principal direction along with N_1 and

$$\tan 2\theta = \frac{2N_{tn}}{N_{tt} - N_{nn}}. \tag{2.30}$$

Thus, in terms of principal values, **N** can be expressed as

$$\mathbf{N} = \begin{bmatrix} N_{tt} & N_{tn} \\ N_{nt} & N_{nn} \end{bmatrix} = \frac{1}{m} \begin{bmatrix} 1+\lambda\cos 2\theta & \lambda\sin 2\theta \\ \lambda\sin 2\theta & 1-\lambda\cos 2\theta \end{bmatrix}, \tag{2.31}$$

where

$$m = \frac{2}{N_1 + N_2} = \frac{2}{N_{tt} + N_{nn}} \tag{2.32}$$

and

$$\lambda = \frac{N_1 - N_2}{N_1 + N_2} = \frac{\sqrt{(N_{tt} - N_{nn})^2 + 4N_{tn}^2}}{N_{tt} + N_{nn}}, \tag{2.33}$$

where m and λ are dependent upon the system configuration.

The relationship between **M** and **N** and the physical meanings of λ are illustrated as follows: Consider a rod which collides with an immobile body at the point P. As shown in Figure 2, the mass of the rod is denoted as m_B, the point G is the center of mass and the angle between the major axis of the rod and the normal vector of the contact surface is denoted as θ. One set of basis vectors shown in figure 2, in which vector $\mathbf{a}_2$ represents the major axis of the rod, is chosen and generalized speed is defined as:

$$\mathbf{v}^G = u_1 \mathbf{t} + u_2 \mathbf{n} \tag{2.34}$$

and

$$\omega^B = u_3 \mathbf{t} \times \mathbf{n}. \tag{2.35}$$

Let

$$\mathbf{r}_{GP} = b \sin\theta \mathbf{t} - b \cos\theta \mathbf{n} \tag{2.36}$$

and express the velocity of the contact point P as

$$\mathbf{v}^P = \mathbf{v}^G + \omega^B \times \mathbf{r}_{GP}$$

$$= u_1 \mathbf{t} + u_2 \mathbf{n} + u_3 (b\cos\theta \mathbf{t} + b\sin\theta \mathbf{n}) . \qquad (2.37)$$

The partial velocities for the relative velocity $\mathbf{v}$ become

$$\mathbf{v}_1 = \mathbf{t} ,$$

$$\mathbf{v}_2 = \mathbf{n} , \qquad (2.38)$$

$$\mathbf{v}_3 = b\cos\theta \mathbf{t} + b\sin\theta \mathbf{n} ,$$

and the matrix $\mathbf{l}$ becomes

$$\mathbf{l} = \begin{bmatrix} 1 & 0 \\ 0 & 1 \\ b\cos\theta & b\sin\theta \end{bmatrix} . \qquad (2.39)$$

The kinetic energy may be expressed as

$$K = \frac{1}{2} m_B \mathbf{v}^G \cdot \mathbf{v}^G + \frac{1}{2} I_3 \omega^B \cdot \omega^B \qquad (2.40)$$

where I_3 is the central moment of inertia of rod for $\mathbf{a}_3$. Denoting the central radius of gyration of rod as k_3, equation (2.40) may be rewritten as

$$K = \frac{1}{2} m_B (u_1^2 + u_2^2 + k_3^2 u_3^2) . \qquad (2.41)$$

From equation (2.19), hence, $\mathbf{m}^{-1}$ becomes

$$\mathbf{m}^{-1} = \frac{1}{m_B k_3^2} \begin{bmatrix} k_3^2 & 0 & 0 \\ 0 & k_3^2 & 0 \\ 0 & 0 & 1 \end{bmatrix} \qquad (2.42)$$

and the matrix $\mathbf{M}$ becomes

$$\mathbf{M} = \frac{m_B}{k_3^2 + b^2} \begin{bmatrix} k_3^2 + b^2\sin^2\theta & -b^2\cos\theta\sin\theta \\ -b^2\cos\theta\sin\theta & k_3^2 + b^2\cos^2\theta \end{bmatrix} . \qquad (2.43)$$

The two eigenvectors $\mathbf{a}_1$ and $\mathbf{a}_2$ of this operator are shown in Figure 2 and are related to the tangential and normal base vectors by

$$\mathbf{a}_1 = \cos\theta\, \mathbf{t} + \sin\theta\, \mathbf{n} ,$$
$$\mathbf{a}_2 = -\sin\theta\, \mathbf{t} + \cos\theta\, \mathbf{n} , \tag{2.44}$$

and corresponding eigenvalues are

$$M_1 = \frac{I_3}{I_3'} m_B = \frac{k_3^2}{k_3^2 + b^2} m_B ,$$
$$M_2 = m_B , \tag{2.45}$$

where I_3' is the moment of the inertia of rod about the axis through P' and perpendicular to the plane of motion.

Since $\mathbf{N} = \mathbf{M}^{-1}$ from equation (2.19), the eigenvalues of $\mathbf{N}$ are the reciprocals of those of $\mathbf{M}$:

$$N_1 = \frac{I_3'}{I^3} = \frac{k_3^2 + b^2}{k_3^2 m_B} ,$$
$$N_2 = \frac{1}{m_B} . \tag{2.46}$$

From equations (2.32) and (2.33), the values of m and λ become

$$m = \frac{2\, I_3 m_B}{I_3' + I_3} = \frac{2\, K_3^2 m_B}{2\, k_3^2 + b^2} \tag{2.47}$$

and

$$\lambda = \frac{I_3' - I_3}{I_3' + I_3} = \frac{b^2}{2\, k_3^2 + b^2} \tag{2.48}$$

From equations (2.33) and (2.48), λ can be seen to lie between zero to one and larger values of λ reflect more pronounced inertia coupling.

For contact between an end of an unconstrained, slender rod and an immobile body, $\lambda = 0.6$, while the value of λ for the double pendulum discussed in Smith [16] is 0.964 in the configuration considered there.

Another parameter that affects the collision is the angle α between $-\mathbf{n}$ and $\mathbf{v}$ shown in Figure 2. The initial velocity $\mathbf{v}$ can be expressed in terms of incident angle α.

$$\mathbf{v} = v\,(\sin\alpha\,\mathbf{t} - \cos\alpha\,\mathbf{n}) \tag{2.49}$$

so that this incident angle α is given by

$$\tan\alpha = v_t/(-v_n)\ . \tag{2.50}$$

Observe that a redundancy in results would occur if the sign of both the angles θ and α were reversed; in the following, this redundancy is avoided by restricting α to the range $(0, \pi/2)$ and considering values of θ throughout the range $(-\pi/2, \pi/2)$.

2.4 Local deformations of contact bodies

The formulations of impulse and momentum, as given in equation (2.18), provide fewer relationships than the unknown components of $\mathbf{g}$ and $\Delta\mathbf{v}$. In the absence of detailed analysis of surface forces and related deformation in the region of contact, assumptions about impulse and relative motion are needed to provide the additional equations from which $\mathbf{g}$ and $\mathbf{w}$ can be predicted. In classical analysis for rigid body collision, a commom assumption is that the ratio e of the normal component of $\mathbf{w}$ to the normal component of $\mathbf{v}$ is known;

thus, the relationship $\mathbf{w}_n = - e \mathbf{v}_n$ can be used directly in the calculation. This coefficient has been given as one for perfect elastic bodies and zero for pure plastic bodies. However, it should be noted that when the deformations may be fully analyzed properly for the contact region of colliding bodies this assumption is no longer necessary.

Despite the static, elastic nature of its derivation, Hertz theory has been used widely for the normal compliance during impact. For example, Timoshenko and Goodier [19] quote the analysis for the collinear impact of spheres based on Hertz theory. As soon as the spheres, in their motion toward one another, come in contact at a point, the compression force begins to act and the region near the contact point P deforms continuously until the velocity of approach becomes zero and returns to normal shape during restitution. The behavior during normal collision of elastic spheres may be represented as a half cycle for a mass- spring vibration system. Similarly this effect could be extended in the sense of tangential compliance when the work done in deflecting the surface tangentially due to the friction is stored as strain energy in the solid and, under suitable circumstances, it is recoverable in the same manner as the stain energy resulting from normal force and displacement. Since both bodies are subject to deformation, the effective "contact spring" between them is equal to the combination of the stiffness of each body regarded as an elastic half-space. Contrary to the complexity of contact deformation, a simplified conceptual model is presented in Figure 3, where the vertical and horizontal springs represent, respectively, the stiffness of

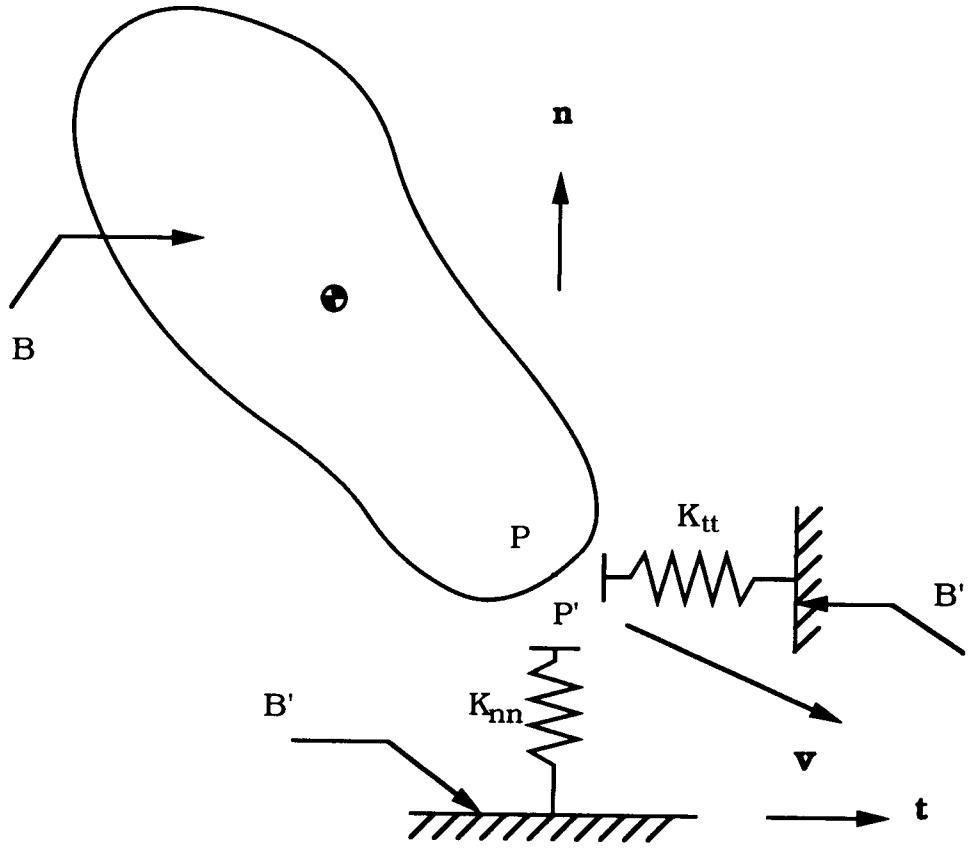

Figure 3. Modelling local deformation of contact area during impact

local deformations of the contacts in the normal and tangential directions.

Once the stiffness of deformation is known, equation (2.18) may be differentiated with respect to time and dynamic equations for mechanical collisions become simple ordinary differential equations. Thus,

$$[\mathbf{M}]\ d/dt\ \{\Delta \mathbf{v}\} = d/dt\ \{\mathbf{g}\}\ . \tag{2.51}$$

Substituting acting force $\{\mathbf{F}\} = -[\mathbf{K}]\ \{u\}$ into right side of equation (2.51), system equation could be expressed in terms of inertia [**M**] of configuration and stiffness [**K**] of local deformation at contact area for colliding bodies:

$$[\mathbf{M}]\ \{\ddot{u}\} + [\mathbf{K}]\ \{u\} = \{0\}\ , \tag{2.52}$$

where {u} is the displacement at contact point. In practical terms, this concept, which may be distingushied from the complex representation of contact surfaces during impacts, is seemingly too simplistic to provide for the prediction of collision rebounds. In the following chapters, the means to determine the coefficients for a stiffness matrix are demonstrated, including degree to which the results derived from this analysis are in agreement with more detailed analyses.

3. CONTACT MECHANICS OF ELASTIC BODIES

The subject of contact mechanics is concerned with the stresses and deformations which arise when the surfaces of two solid bodies are brought into contact. The contact area of colliding bodies is generally small in comparision to the dimensions of the colliding bodies. The resultant stresses and deformations are highly subject to concentration in the regions surrounding the contact zone and are not greatly influenced by the shape of the bodies at a distance from the contact area. Thus, each body can be regarded as an elastic half-space, loaded over a small region of its plane surface. In the absence of friction, a normal force F_n pressing the bodies together gives rise to area of contact, which would have dimensions given in Hertz theory. A sliding motion, or any tendency to slide, of real surface introduces a tangential force of friction, F_t, which acts upon each surface in a direction opposed to direction of motion. For the current investigation, each body has a steady sliding motion so that the force F_t represents the force of "kinetic friction" between the surfaces.

3.1 Normal contacts of elastic bodies: Hertz theory

The development of contact theory is necessary to predict the shape of the contact area and how it grows in size with increasing load. Hertz's analysis is based upon the assumptions of a normal load on the elastic and isotropic materials. According to the Hertz theory, the contact surface boundary is generaly regarded as an ellipse.

However, for simplicity of analysis, the current investigation is confined to the case of circular contact areas. Since the contact surfaces are assumed to be frictionless, the tangential traction and displacement due to normal force is neglected. Keeping a constant normal contact force, F_n, the elastic approach u_n, the radius of contact area a, and the distribution of pressure over the contact area p(r), as given in Hertz theory, are shown in Figure 4 and are determined from the following relationships [6]:

$$a = \left(\frac{3F_nR}{4E}\right)^{\frac{1}{3}}, \tag{3.1}$$

$$u_n = \frac{a^2}{R} = \left(\frac{9F_n{}^2}{16\,RE^2}\right)^{\frac{1}{3}} \tag{3.2}$$

and

$$F_n = \frac{4}{3}\sqrt{R}E\,u_n{}^{\frac{3}{2}} \tag{3.3}$$

For $r < a$,

$$p(r) = p_0\left\{1 - \left(\frac{r}{a}\right)^2\right\}^{\frac{1}{2}}, \tag{3.4}$$

otherwise, $p(r) = 0$. The maximum pressure p_0 is

$$p_0 = \frac{3F_n}{2\pi a^2} = \left(\frac{6F_nE^2}{\pi^3R^2}\right)^{\frac{1}{3}}, \tag{3.5}$$

where r is a distance from the origin. In turn, R and E are, respectively, relative curvature and Young's modulus for contact bodies, given as

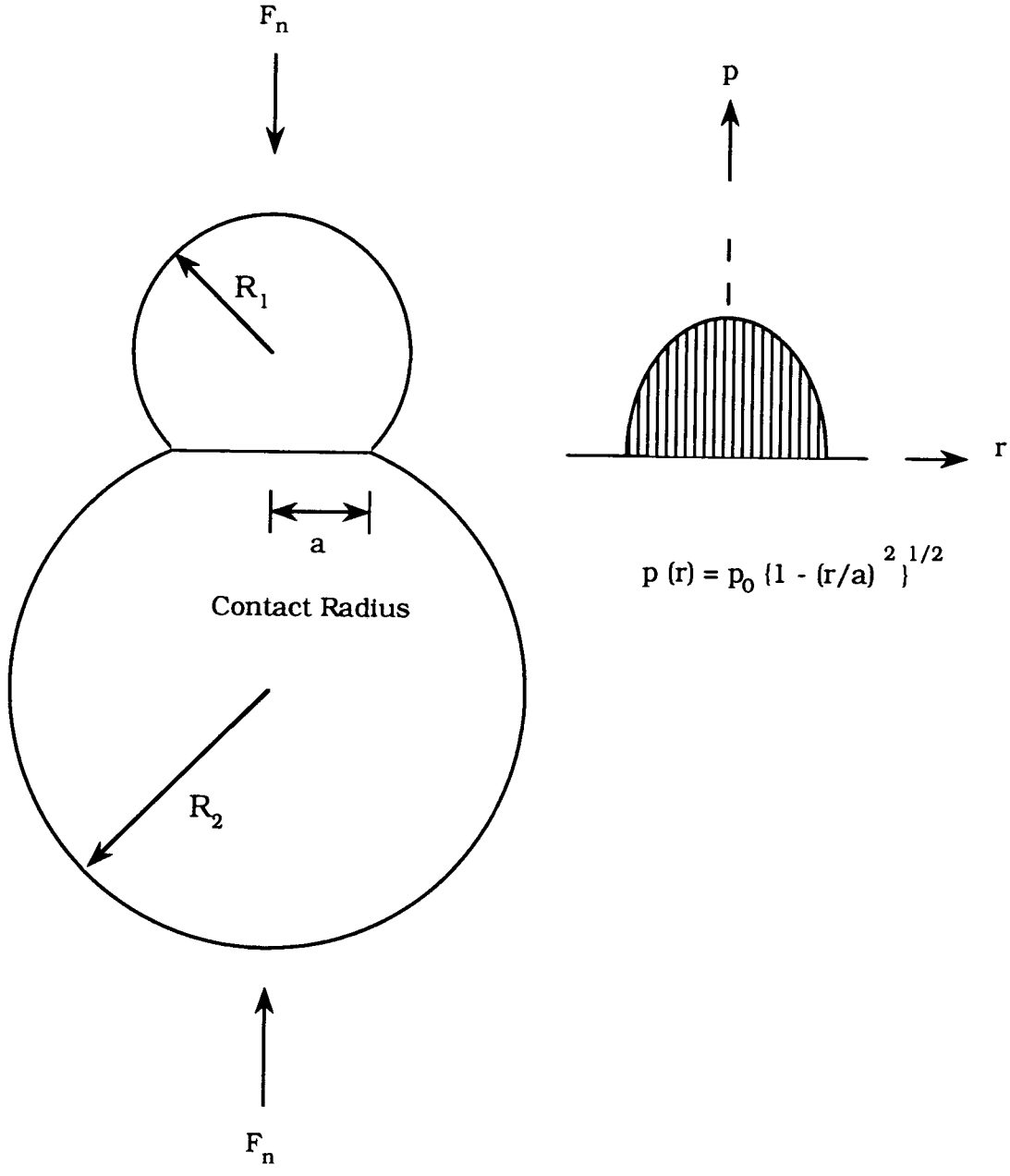

Figure 4. Deformation and pressure distribution of normal contact from Hertz theory

$$\frac{1}{E} = \frac{1 - \nu_1^2}{E_1} + \frac{1 - \nu_2^2}{E_2}$$

and

$$\frac{1}{R} = \frac{1}{R_1} + \frac{1}{R_2},$$

where ν_1 and ν_2 are Poisson's ratios.

Equation (3.3) demonstrates a nonlinear force-displacement relationship in the normal direction. Differentiating equation (3.2) with respect to the normal force F_n results in the normal compliance of colliding bodies; When these bodies have same material properties, then normal compliance is obtained as follows:

$$C_n = \frac{du_n}{dF_n} = \frac{2}{3}\left\{\frac{9}{4}\left(\frac{1-\nu^2}{E}\right)\left(\frac{1}{R_1}+\frac{1}{R_2}\right)\frac{1}{F_n}\right\}^{\frac{1}{3}} = \frac{(1-\nu)}{2Ga} \tag{3.6}$$

As shown in Figure 4, the direct central (i.e., collinear) impact of two elastic spheres was investigated by Timoshenko and Goodier [19] based upon the equations discussed in this section. The Hertz theory, originally developed for static loads, was applied to the quasi-static problem of impact in practice.

3.2. Tangential compliance of contact area

In this section, the effect of the tangential force for non-collinear impact is considered. Since the influence of tangential traction upon normal pressures at the contact area is generally small,

this interaction is neglected [6]. In addition, the stresses and deformations due to the normal pressures and tangential traction are assumed to be independent of each other and they may be superposed to determine the resultant stresses and deformations. In Coulomb's theory of friction, contact surfaces are either in a state of total stick or total slip, corresponding to the friction force less than or equal to the critical value of tangential force which is the coefficient μ times the normal force. Mindlin [13] considers a case in which two spheres are pressed together subject to the constant normal force, F_n, and are then subject to a tangential force, F_t, where $F_t < \mu F_n$. If the tangential force F_t, applied subsequently, causes elastic deformation without slip at the interface, then the tangential displacement at all points within the contact area should be a constant. The distribution of tangential traction which produces a uniform tangential displacement of a circle region on the surface of contact bodies has been found from the analysis of an elastic half-space. The state is analogous to the pressure on the face of a flat frictionless punch shown in Figure 5. In this case, tangential traction is radially symmetric in magnitude and everywhere parallel to the tangential plane. The tangential traction and displacement are given as follows:

$$q(r) = q_0 \left(1 - \frac{r^2}{a^2} \right)^{-\frac{1}{2}} , \tag{3.7}$$

and

$$u_t = \frac{\pi(2 - \nu)}{4G} q_0 a, \tag{3.8}$$

where

$$q_0 = \frac{F_t}{2\pi a^2} .$$

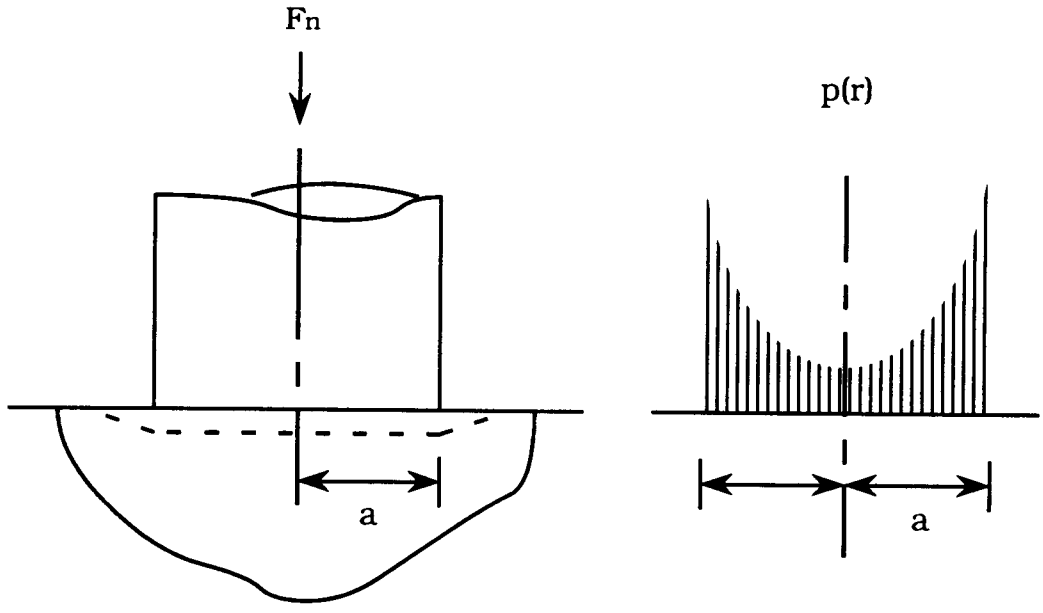

Figure 5. Pressure for constant deformation of flat rigid cylinder punch

The relative displacement for two elastic bodies in tangential direction becomes

$$u_t = u_{t_1} - u_{t_2} = \frac{F_t}{8a}\left(\frac{2 - \nu_1}{G_1} + \frac{2 - \nu_2}{G_2}\right). \tag{3.9}$$

The tangential traction necessary to prevent slip rises to a theoretically infinite value at the periphery of the contact circle. Since the infinite tangential traction at the edge of contact area can not be sustained, there must be some micro-slip and it occurs at the edge of the contact area as shown in the annulus in Figure 6. If the tangential force is increased to the limiting value μF_n, so that the two bodies are on the point of sliding, the tangential traction can be obtained from equation (3.4) as

$$q'(r) = \mu p_0 \left(1 - \frac{r^2}{a^2}\right)^{\frac{1}{2}}. \tag{3.10}$$

The response of collision in gross slip can then be determined from the application of simple rigid body theory. When the tangential force is less than the limiting friction force (i.e., $F_t < \mu F_n$), the region of stick and slip in the contact area can be determined as follows. Consider a distribution of traction acting over the circular area $r \le c$:

$$q''(r) = -\left(\frac{c}{a}\right)\mu p_0 \left(1 - \frac{r^2}{a^2}\right)^{\frac{1}{2}}. \tag{3.11}$$

The distribution of tangential traction q(r) then becomes

$$q(r) = q'(r) + q''(r), \tag{3.12}$$

and the resultant displacement within the circle, $r \le c$, is

$$u_t = \frac{\pi\mu\, p_0}{8Ga}\,(2 - \nu)\left(a^2 - c^2\right). \tag{3.13}$$

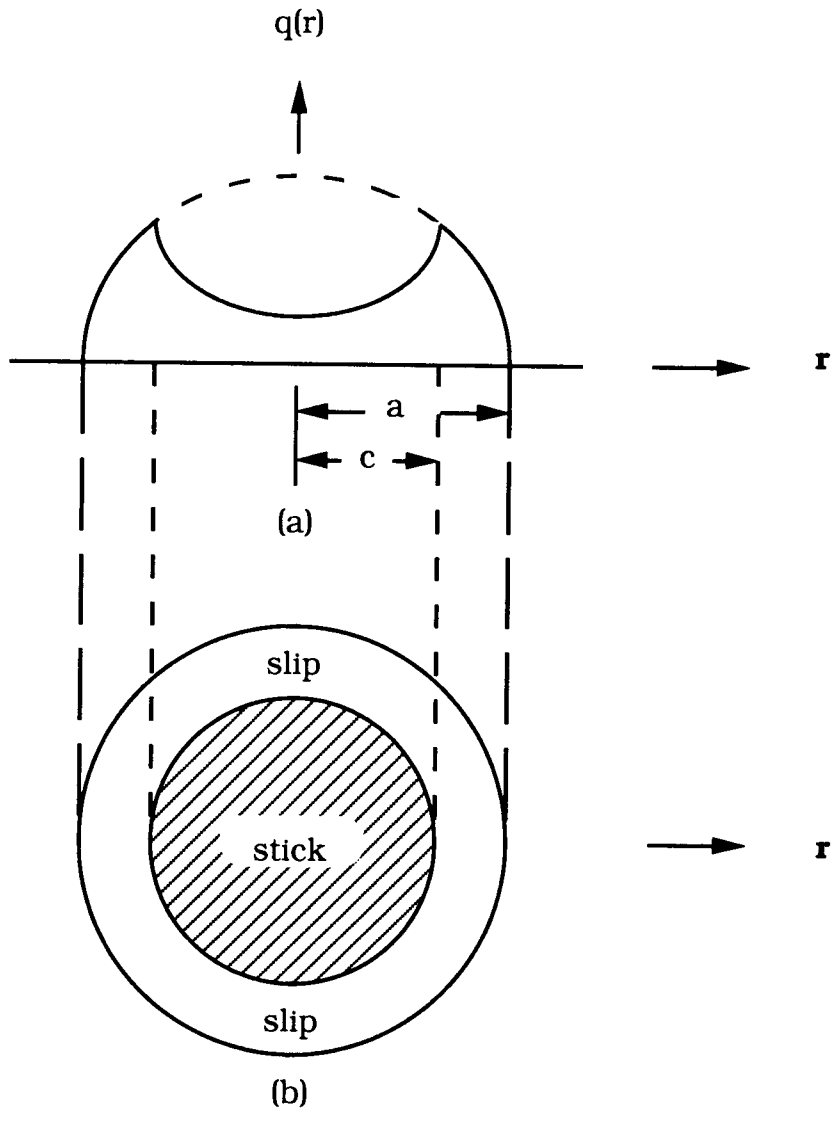

Figure 6. (a) Tagential traction distribution with partial slip
(b) Stick and slip region on the contact area

These displacements satisfy the condition for no-slip within the circle $r \le c$, with the result that

$$u_t = \frac{3\,\mu F_n}{16}\left(\frac{2-\nu_1}{G_1}+\frac{2-\nu_2}{G_2}\right)\frac{a^2-c^2}{a^3}. \tag{3.14}$$

Thus, the stick region is a circle of radius c, the value of which can be determined from the magnitude of the tangential force,

$$F_t = \int_0^a 2\pi q' r\,dr - \int_a^c 2\pi q'' r\,dr = \mu F_n\left(1-\frac{c^3}{a^3}\right), \tag{3.15a}$$

from which

$$\frac{c}{a} = \left(1-\frac{F_t}{\mu F_n}\right)^{\frac{1}{3}}. \tag{3.15b}$$

The relative tangential displacement for the two bodies can be found by substituting equation (3.15 b) into (3.14).

$$u_t = \frac{3\mu F_n}{16a}\left(\frac{2-\nu_1}{G_1}+\frac{2-\nu_2}{G_2}\right)\left\{1-\left(1-\frac{F_t}{\mu F_n}\right)^{\frac{2}{3}}\right\}. \tag{3.16}$$

The procedure described above is shown in Figure 7, and the nonlinear relationship of tangential displacement to force is plotted in Figure 8. For very small values of tangential force, when the slip annulus is very thin, it follows that the linear relationship for no-slip is given in equation (3.9). As F_t approaches μF_n, the tangential displacement progressively separates from that of the no-slip solution, until the point of sliding has been reached.

The tangential compliance for the case of constant normal force and monotonically increasing tangential force is the reciprocal of the slope of the curve B in Figure 8. For same material of colliding bodies, it is given by the formula

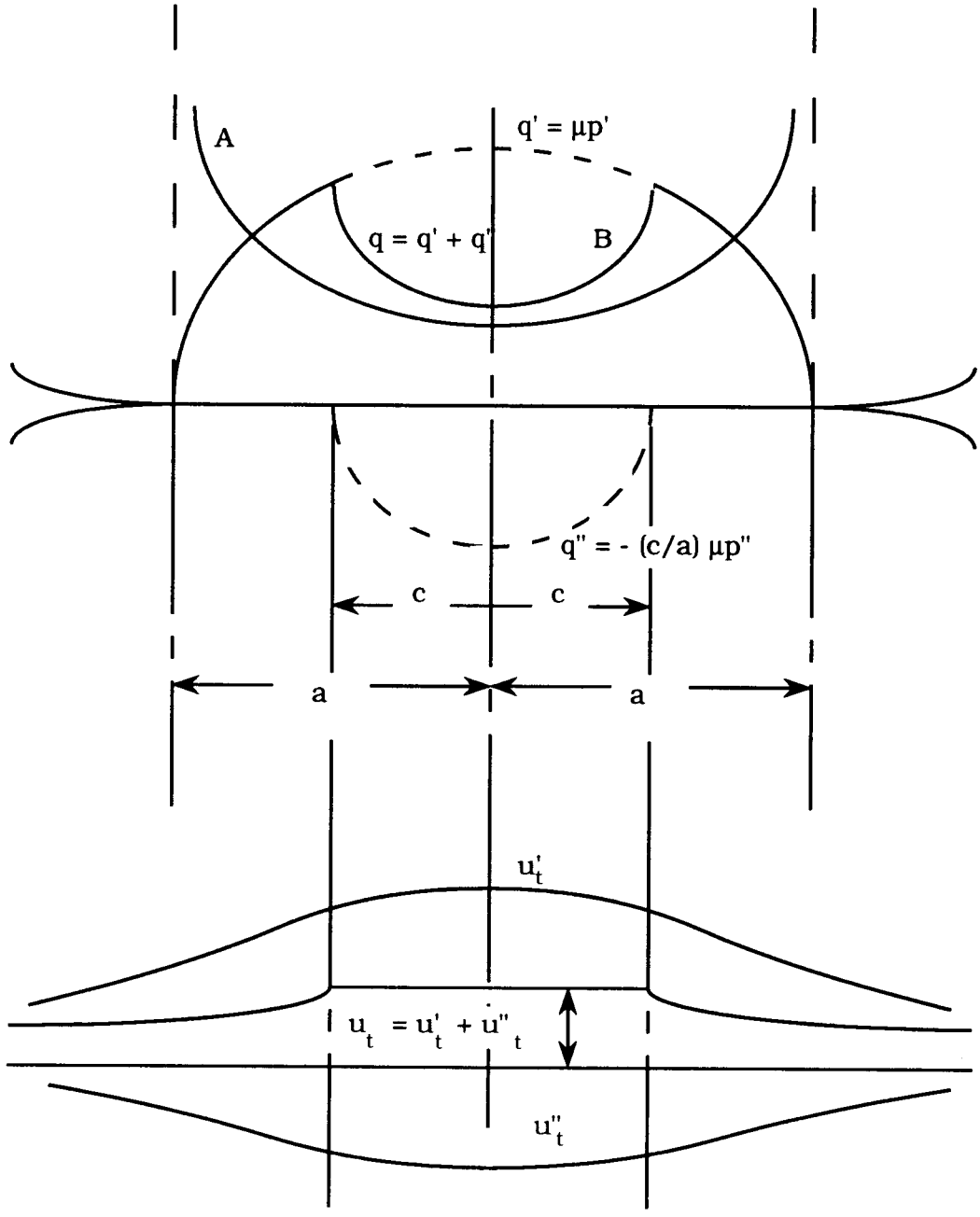

Figure 7. Surface tractions and displacements due to a tangential force less than limit friction

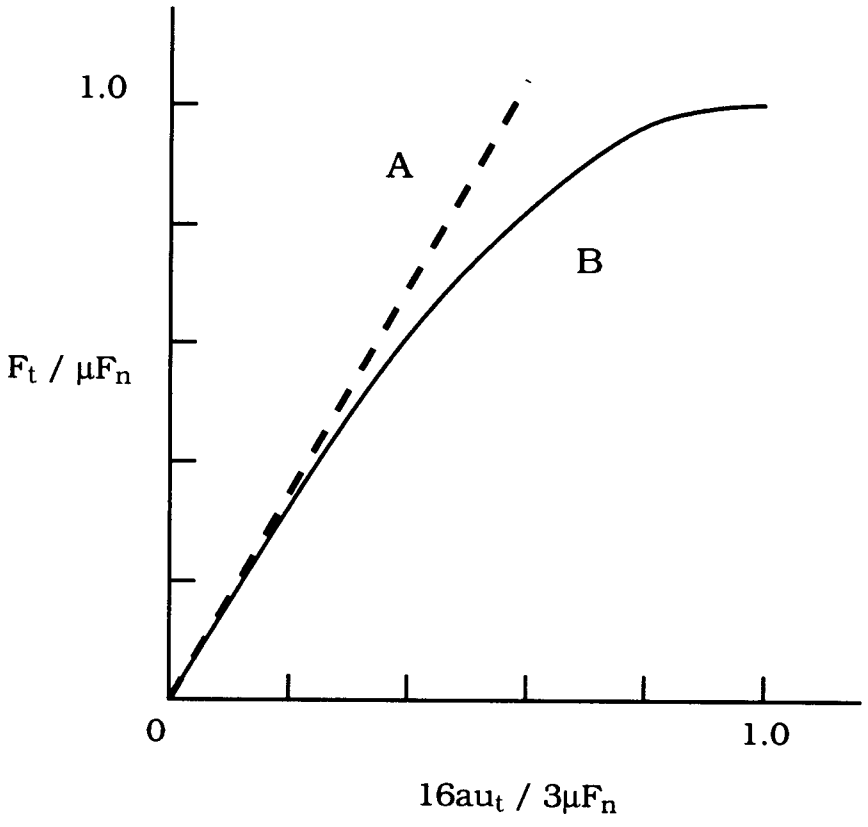

Figure 8. Tangential displacement u_t of a circular region by tangential force F_t; (A) with no slip, (B) with slip at the edge of the contact area

$$c_t = \frac{du_t}{dF_t} = \frac{2-\nu}{4Ga}\left(1 - \frac{F_t}{\mu F_n}\right)^{-1/3} . \qquad (3.17)$$

As the tangential force is increased from zero, keeping the normal force constant, the stick region is decreased in size in accordance with the equation (3.15b). An annulus of slip penetrates from the edge of the contact area until $F_t = \mu F_n$, where the stick region has dwindled to a single point at the origin and the bodies are at the point of sliding. While slip continues colliding bodies act as rigid and the elastic tangential displacement u_t^* at the contact point has the value

$$u_t^* = \frac{3\mu F_n}{16a}\left(\frac{2-\nu_1}{G_1} + \frac{2-\nu_2}{G_2}\right). \qquad (3.18)$$

By substituting F_n from equation (3.1) into equation (3.18) for the same elastic constant,

$$u_t^* = \frac{\mu(2-\nu)}{2R(1-\nu)}\, a^2 \qquad (3.19a)$$

and, by substituting a from equation (3.2) into equation (3.19a),

$$u_t^* = \frac{\mu(2-\nu)}{2(1-\nu)}\, u_n . \qquad (3.19b)$$

Now here the initial condition of tangential velocity which determines whether the bodies stick or slide at the beginning of impact is evaluated. By taking the derivative of equation (3.19b) with respect to time,

$$\dot{u}_t^* = \frac{\mu(2-\nu)}{2(1-\nu)}\, \dot{u}_n \qquad (3.20)$$

For $v_t < \dot{u}_t^*$, the bodies stay stuck at the beginning of impact, and the tangential compliance for small value of F_t ($<< \mu F_n$), when the

colliding bodies have the same material properties, is given by equations (3.9) and (3.17) as

$$C_t = \frac{du_t}{dF_t} = \frac{(2 - \nu)}{4Ga} \tag{3.21}$$

It is instructive to compare the tangential compliance for two bodies in equation (3.21) with the normal compliance given in Hertz theory as equation (3.6). Though both tangential and normal compliances are funtions of radius of contact area a, which continuously is changing during impact, the ratio of the tangential to normal compliance is a function of only the Poisson's ratio, and is independent of the normal load,

$$\frac{C_t}{C_n} = \frac{2 - \nu}{2\ (1 - \nu)} . \tag{3.22}$$

This ratio, ranging from unity to 3/2 for values of Poisson's ratio between zero and 0.5, plays an important role in analysis of elastic collisions.

Now, consider that after the tangential force has reached a value of F_t^* ($<\mu F_n$), the tangential force F_t is decreased, keeping the normal force F_n at constant P. Since the normal force remains constant at P, the contact area and the normal pressure will remain constant, as given in Hertz theory. The first application of F_t^* in a positive direction will cause partial slip in the annulus $c \le r \le a$ in the manner previously described. The distribution of tangential traction is shown by the curve A in Figure 9(a). The tangential displacement of the contact area is given by equation(3.15) and shown by the curve OA in Figure 9(b). At the point A on this curve, $F_t = + F_t^*$. It follows that a

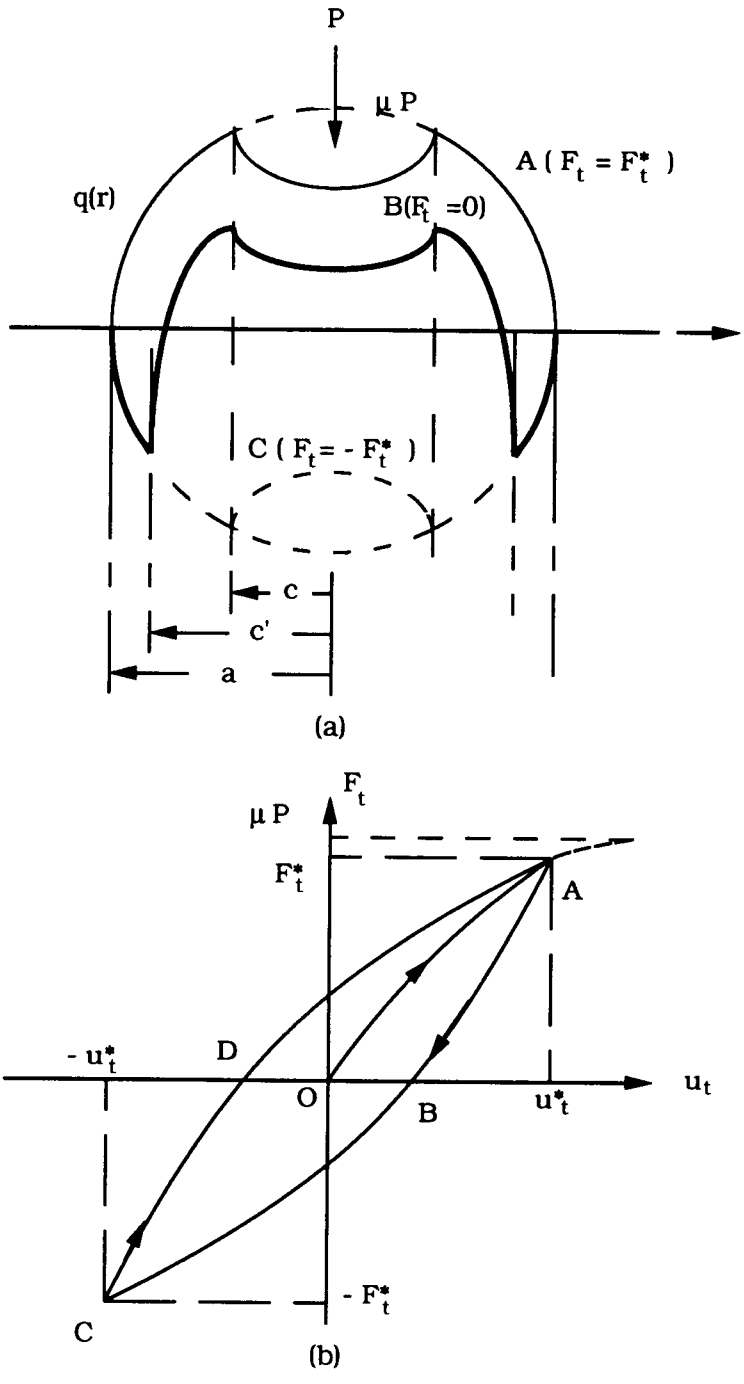

Figure 9. Oscillating tangential load of amplitude F_t^*: (a) traction distribution at A ($F_t=F_t^*$), B ($F_t=0$) and C ($F_t=-F_t^*$) (b) load-displacement cycle

decrease in tangential force is equivalent to the application of a negative increment in F_t. If there were no slip during this reduction, the increment in tangential traction would be negative and infinite at the edge of the contact area. Hence, there must be some negative slip immediately at the initiation of unloading, and the tangential traction near to the edge of the contact area must take the value $q(r) = -\mu p(r)$. During the unloading, the reverse slip penetrates to the radius c' and, within this radius, there is no reverse slip. The increment in tangential traction due to the unloading is therefore

$$\Delta q(r) = -2\,\frac{3\mu P}{2\pi a^3}\left(a^2-r^2\right)^{\frac{1}{2}}, \qquad c' \le r \le a$$

and

$$\Delta q(r) = -2\,\frac{3\mu P}{2\pi a^3}\left(a^2-r^2\right)^{\frac{1}{2}} - \left(c'^2-r^2\right)^{\frac{1}{2}}, \qquad r \le c' \tag{3.23}$$

The resultant traction at any point on the unloading curve can be then given by adding this increment to the traction at A, with the result

$$q(r) = \begin{cases} -\dfrac{3\mu P}{2\pi a^3}(a^2 - r^2)^{\frac{1}{2}}, & c' \le r \le a \\ -\dfrac{3\mu P}{2\pi a^3}\{(a^2 - r^2)^{\frac{1}{2}} - 2(c'^2 - r^2)^{\frac{1}{2}}\}, & c \le r \le c' \\ -\dfrac{3\mu P}{2\pi a^3}\{(a^2 - r^2)^{\frac{1}{2}} - 2(c'^2 - r^2)^{\frac{1}{2}} + (c^2 - r^2)^{\frac{1}{2}}\}, & r \le c \end{cases} \tag{3.24}$$

as shown by curve B in Figure 9(a). The radii of the stick regions may be determined from the equilibrium of the traction distribution described above for the applied force. At point A,

$$\frac{F_t^*}{\mu P} = 1 - \frac{c^{*3}}{a^3}\ , \tag{3.25}$$

and during unloading,

$$\frac{F_t}{\mu P} = \frac{F_t^*}{\mu P} - \frac{\Delta F_t}{\mu P} = \left(1 - \frac{c^{*3}}{a^3}\right) - 2\left(1 - \frac{c'^3}{a^3}\right), \tag{3.26}$$

which fixes the extent of reverse slip c'/a. At point B, when the tangential load is removed, $F_t = 0$, so that

$$\frac{c'^3}{a^3} = \frac{1}{2}\left(1 + \frac{c^{*3}}{a^3}\right), \tag{3.27}$$

and tangential displacement during unloading can be determined by application of equation(3.14):

$$u_t = u_t^* - \Delta u_t$$

$$= \frac{3\mu P}{16a^3}\left(\frac{2-\nu_1}{G_1} + \frac{2-\nu_2}{G_2}\right)\left\{(a^2 - c^2) - 2(a^2 - c'^2)\right\}$$

$$= \frac{3\mu P}{16a^3}\left(\frac{2-\nu_1}{G_1} + \frac{2-\nu_2}{G_2}\right)\left\{2\left(1 - \frac{F_t^* - F_t}{2\mu P}\right)^{\frac{2}{3}}\right.$$

$$\left. -\left(1 - \frac{F_t^*}{\mu P}\right)^{\frac{2}{3}} - 1\right\} \tag{3.28}$$

This expression is shown in Figure 9(b) as the curve ABC. At point C, when the tangential force is completely reversed, substituting $F_t = -F_t^*$ in equations (3.25) and (3.27) gives $c = c_*$ and $u_t = -u_t^*$. Thus, the

reverse slip has covered the original slip annulus and the distribution of tangential traction is equal to that at A, but of opposite sign. The conditions at C are the complete reversal of those of at A, so that a further reversal of F_t produces a sequence of events which is similar to unloading from A, but of opposite sign. The displacement curve CDA completes a symmetrical hysteresis loop.

To this point in the analysis, while keeping the normal force constant and contact area unchanged, unloading of tangential force within the friction limit has been considered. However, the conditions of contact area during an impact are considerably complicated by the fact that the normal force and contact area as well as tangential force are subject to continuous change. In a study which reflected a high degree of complexity, Mindlin and Deresiewicz [14] have investigated changes in surface traction and compliance between spherical bodies in contact arising from various possible combinations of incremental changes in load. For the purpose of this investigation, consider an increase in normal force accompanied by a decrease in tangential force. Apply F_n, increasing the tangential force from zero to F_t^* at A, then reduce it to F_t at B in Figure 10(b). Tangential traction is given in equation (3.12) and shown by curve **A** in Figure 10(a). Keeping the tangential load constant, increase the normal load to $F_n + \Delta F_n$. The radius a_1 of the new contact area is given as in equation (3.1). Then, keeping the normal force constant at $F_n + \Delta F_n$, reduce the tangential force by ΔF_t. The additional tangential traction is given by curve **B** with sign reversed. Thus, if $\Delta F_t = \Delta \mu F_n$ for $c_1 = a$, the resultant traction shown by curve **C** in Figure 10(a) is:

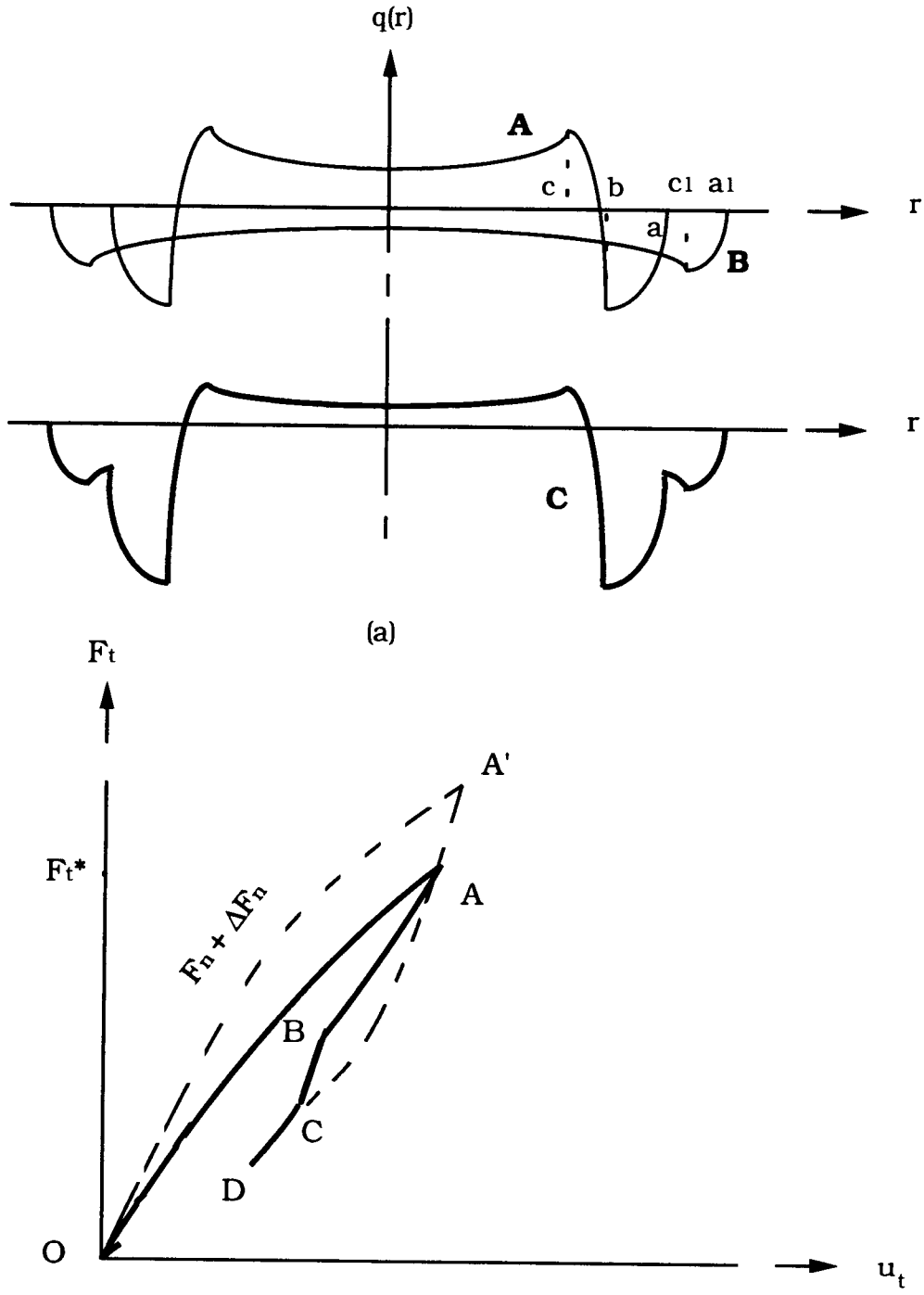

Figure 10. Increasing normal force and decreasing tangential force: (a) tangential traction (b) force-displacement cycle

$$q(r) = \begin{cases} -\dfrac{3\mu(F_n + \Delta F_n)}{2\pi a^3}(a^2 - r^2)^{\frac{1}{2}}, & c' \le r \le a \\ -\dfrac{3\mu(F_n + \Delta F_n)}{2\pi a^3}\{(a^2 - r^2)^{\frac{1}{2}} - 2(c'^2 - r^2)^{\frac{1}{2}}\}, & c \le r \le c' \\ -\dfrac{3\mu(F_n + \Delta F_n)}{2\pi a^3}\{(a^2 - r^2)^{\frac{1}{2}} - 2(c'^2 - r^2)^{\frac{1}{2}} + (c^2 - r^2)^{\frac{1}{2}}\}, & r \le c \end{cases} \tag{3.29}$$

Therefore, displacement has traversed the path O-A-B and would have reached point C, at which stage path O-A-B-C meets the path O-A'-C. When $\Delta F_t > \Delta\, \mu F_n$, additional displacement will follow the path C-D along the curve A'-D, and the tangential compliance becomes

$$C_t = \begin{cases} \dfrac{2 - \nu}{8Ga}\left\{\dfrac{\mu dF_n}{dF_t} + (1 - \dfrac{\mu dF_n}{dF_t})(1 - \dfrac{F_t^* - F_t}{2\mu F_n})^{-\frac{1}{3}}\right\}, & 0 < \mu dF_n < -dF_t \\ \dfrac{2 - \nu}{8Ga}, & \mu dF_n \ge -dF_t \end{cases} \tag{3.30}$$

Similarly, the tangential compliance for alternative cases could be obtained through application described previously:

1) Decreased normal force and tangential force

$$c_t = \frac{2 - \nu}{8Ga}\left[-\mu\frac{dF_n}{dF_t} + \left(1 + \mu\frac{dF_n}{dF_t}\right)\left(1 - \frac{F_t^* - F_t}{2\mu F_n}\right)\right], \quad \frac{dF_n}{dF_t} \ge 0 \tag{3.31}$$

2) Increased normal force and tangential force at $F_t = F_t^*$

$$C_t = \begin{cases} \dfrac{2 - \nu}{8Ga}\left\{\dfrac{\mu dF_n}{dF_t} + (1 - \dfrac{\mu dF_n}{dF_t})(1 - \dfrac{F_t^* - F_t}{2\mu F_n})^{-\frac{1}{3}}\right\}, & 0 > \mu dF_n < dF_t \\ \dfrac{2 - \nu}{8Ga}, & \mu dF_n \ge dF_t \end{cases} \tag{3.32}$$

3) Decreased normal force and tangential force at $F_t = F_t^*$

$$C_t = \begin{cases} \dfrac{2-\nu}{8Ga}\left\{\dfrac{\mu dF_n}{dF_t} + \left(1-\dfrac{\mu dF_n}{dF_t}\right)\left(1-\dfrac{F_t^* - F_t}{2\mu F_n}\right)^{-\frac{1}{3}}\right\}, & 0 > \mu dF_n > dF_t \\ \dfrac{2-\nu}{8Ga}, & \mu dF_n \le dF_t \end{cases} \tag{3.33}$$

and

4) Decreased normal force and increased tangential force at the point of unloading curve,

(a) for $\Delta F_t \ge 2\,\mu F_n$,

$$C_t = \frac{2-\nu}{8Ga}\,, \tag{3.34a}$$

(b) and for $\Delta F_t < 2\,\mu F_n$,

i) where $\mu\Delta F_n \le \Delta F_t < 2\,\mu\Delta F_n$,

$$C_t = \frac{2-\nu}{8Ga}\,, \tag{3.34b}$$

ii) and where $\Delta F_t < \mu\Delta F_n$,

$$C_t = \begin{cases} \dfrac{2-\nu}{8Ga}\left\{\dfrac{\mu dF_n}{dF_t} + \left(1-\dfrac{\mu dF_n}{dF_t}\right)\left(1-\dfrac{F_t^* - F_t}{2\mu F_n}\right)^{-\frac{1}{3}}\right\}, & \text{for} \quad \mu dF_n < -dF_t \\ \dfrac{2-\nu}{8Ga}, & \text{for} \quad 0 \ge \mu dF_n \ge -dF_t \end{cases} \tag{3.34c}$$

Since these tangential compliances are given only for a single body, "equivalent tangential compliance" should be taken for impact of two bodies.

The compliances considered above represent only a small number of possibilities for normal and tangential loadings. Consequently, the process of unloading is different from that of loading and this irreversibility implies that tangential compliance is dependent not only upon the initial stage of loading, but also upon the entire past history of loading as well as the instantaneous relative rates of change for the normal and tangential forces. In the impact problem, neither the normal nor the tangential force can be known a prior, since they both depend upon the interaction between the contact compliance and the motion of bodies subject to collision.

4. ANALYSIS OF LOCAL DEFORMATIONS

To account for the complexity of the tangential and normal force relationships, Maw et. al. [10] have developed a numerical technique for the solution of the oblique impact of elastic spheres. The contact area is divided into a series of n equally spaced centric circles. Stick and slip regions are assumed and they are tested to see whether the initial assumption is correct by solving n simultaneous equations. In stick regions the tangential traction must be below the limit at which slip occurs, whereas in slip regions, the relative incremental displacement must be correct in the sense of the assumed frictional traction. If these tests failed for any region, the assumption for that region is changed and new solution would be obtained. The solution should converge in each time interval of impact duration. For the impact problem of spheres, this solution demonstrated that tangential compliance of the contact surface under the action of Coulomb friction has a significant effect on the rebound angles of the sphere and the interface behaves as a two-degree of vibrating system with a pair of mutually perpendicular springs which react independently against the body.

Another approach to the analysis is by means of a finite element method, using ANSYS code, recently introduced by Liu [9]. Although predictions from a finite element method which include wave propagation are closer to the real system than simplified prediction procedures based on rigid body mechanics, they sometimes are

unstable under certain circumstances. Furthermore, the increase in computational load required for the use of this method is significant.

For this chapter, normal and tangential deformation is modeled with a single spring in each of the two directions. Three different force-displacement laws are used: linear, coupled and nonlinear springs. The model is shown in Figure 11.

A tangential force, the magnitude of which is less than the force of the limiting friction ($F_t < \mu F_n$), will not result in a sliding motion. Nevertheless, the effect of a tangential deformation is to cause a small relative motion. Any attempt to increase F_t in excess of μF_n will cause the contact to slide. Rigorously this model could not be used to represent the complexity of real collision process, but its ability to simplify the contact conditions during impact would contribute to reasonable solutions. As shown in Figure 11, $\mathbf{u}(t)$ is the relative displacement of the points on the interface, $\mathbf{F}(t)$ is the acting force on B at point P, and s(t) is the extension of tangential spring. Where $\mathbf{v}$ is a given initial approach velocity at the incident angle α, $\bar{\mathbf{v}}(t)$ is the velocity of the contact point P at any instant time during impact, and $\mathbf{w}$ is the separating velocity after impact.

Each result obtained is compared to those obtained by the application of the Maw et al.[10,11,12] solution for the oblique impact of elastic spheres.

4.1 Modelling tangential stiffness

The influence of tangential traction upon normal pressure in the

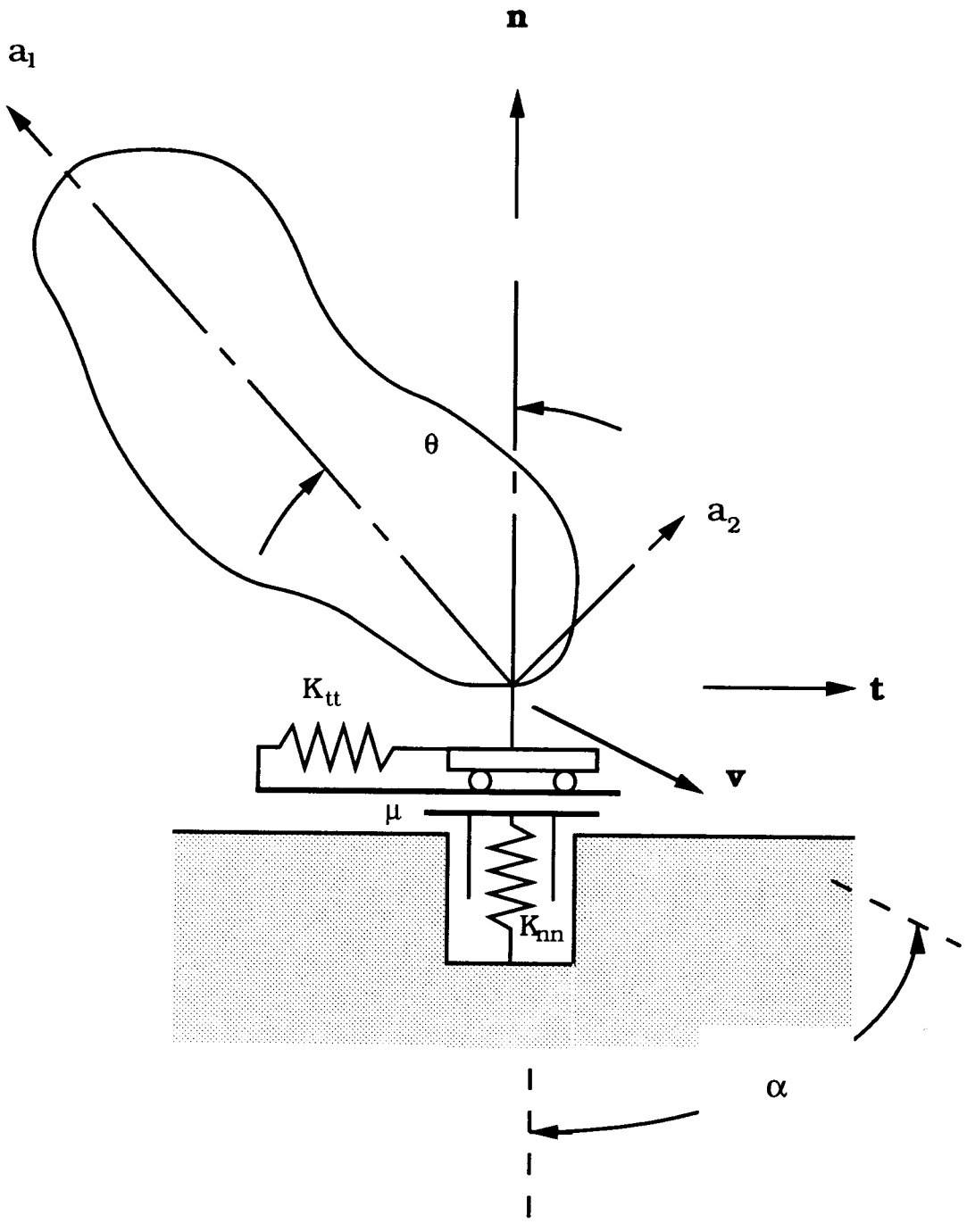

Figure 11. Modelling normal and tangential deformation during impact

contact area is generally small, particularly when the coefficient of limiting friction is less than unity [5,10]. Therefore, for the analysis of problems involving tangential traction, this interaction is neglected: it is assumed that the stress and deformation due to the normal force and tangential force are independent of each other, but that they could be superposed to find the resultant stress and deformation. In other words, the coefficients for K_{tn} and K_{nt} would be zero in the stiffness matrix of a local deformation.

4.1.1 Linear spring

As shown in equation (3.3), Hertz theory can be used to predict a nonlinear force-displacement relationship in the normal direction. However, by linearization, the stiffness of the normal spring K_{nn} may be considered to be an "equivalent constant",

$$K_{nn} = \frac{4}{3}\sqrt{R}E \ . \tag{4.1}$$

Then, from the relationship between normal and tangential compliance in a constant contact area for a small tangential force, as given in equation (3.22), the tangential stiffness becomes

$$K_{tt} = \frac{8\,(1-\nu)}{3\,(2-\nu)}\sqrt{R}E \ . \tag{4.2}$$

The spring forces in the normal and tangential direction may then, respectively, be expressed in terms of coefficients of stiffness as

$$F_n = - K_{nn}\, u_n \tag{4.3}$$

and

$$F_t = - K_{tt}\, s \,. \tag{4.4}$$

If the tangential force is less than the limiting friction force, the tangential velocity for elastic colliding bodies becomes the derivative of the extension of tangential spring,

$$\bar{v}_t(t) = \dot{s}(t) \,. \qquad \text{for} \quad |F_t| < \mu F_n \tag{4.5a}$$

If the tangential force reaches the limiting friction force, then the colliding bodies begin to slip, the tangential force becomes

$$F_t = - \mu \frac{(\bar{v}_t - \dot{s})}{|\bar{v}_t - \dot{s}|} F_n \,, \tag{4.6}$$

and the system effectively acts as a rigid body once gross slip has occured. (i.e., $\dot{s}(t) \neq \bar{v}_t(t)$).

The relation of impulse-momentum and for the colliding system indicated in equation (2.17) is recalled,

$$\begin{Bmatrix} \bar{v}_t - v_t \\ \bar{v}_n - v_n \end{Bmatrix} = \begin{bmatrix} N_{tt} & N_{tn} \\ N_{nt} & N_{nn} \end{bmatrix} \begin{Bmatrix} g_t \\ g_n \end{Bmatrix} \tag{4.7}$$

and the relationship of force-impulse in the normal and tangential directions are, respectively, $\dot{g}_t = F_t$ and $\dot{g}_n = F_n$. Then, combining the equations (4.3), (4.4), (4.5) and (4.7),

$$\dot{g}_t = - K_{tt}\ s \,, \tag{4.8a}$$

$$\dot{g}_n = - K_{nn}\, u_n \,, \tag{4.9a}$$

$$\dot{u}_t = \bar{v}_t = v_t + N_{tt}\, g_t + N_{tn}\, g_n \,, \tag{4.10a}$$

and

$$\dot{u}_n = \bar{v}_n = v_n + N_{nt}\, g_t + N_{nn}\, g_n \,. \tag{4.11a}$$

Thus, for stick, if $|s| < \left(\frac{\mu K_{nn}}{K_{tt}}\right)(-u_n)$, then

$$\dot{u}_t = \dot{s} \ ,$$

that is,

$$\bar{v}_t = v_t + N_{tt}g_t + N_{tn}g_n \ ;$$

otherwise, for gross slip,

$$s = -\left(\frac{\mu K_{nn}}{K_{tt}}\right) u_n \ . \tag{4.12}$$

Substituting equations (4.1) and (4.2) into equation (4.12), the displacement and velocity of the tangential spring during slip may be given as

$$s = -\frac{\mu\,(2 - \nu)}{2\,(1 - \nu)}\, u_n \tag{4.13}$$

and

$$\dot{s} = -\frac{\mu\,(2 - \nu)}{2\,(1 - \nu)}\, \dot{u}_n \ . \tag{4.14}$$

It is of interest to note that these displacement and velocity of the tangential spring, as obtained through linearization, are in agreement with the result from equations (3.19) and (3.20) for the nonlinear relationship of the tangential displacement of a circular contact to a tangential force, as given in equation (3.16).

For generality, non-dimensional quantities may be formulated by the introduction of the length

$$\eta = \left(\frac{mv^2}{ER}\right)^{\frac{1}{2}} \ ,$$

and expression of the initial velocity in terms of α, the incident angle $\mathbf{v} = v\,(\sin\alpha\ \mathbf{t} - \cos\alpha\,\mathbf{n})$. Impulse, displacement and duration of

impact are expressed in terms of non-dimensional quantities as follows:

$$g_i = mv\,\gamma_i\,, \tag{4.15}$$

$$u_i = \eta\,\delta_i\,, \tag{4.16}$$

$$s = \eta\,\varepsilon \tag{4.17}$$

and

$$t = \frac{\eta}{v}\tau\,, \tag{4.18}$$

where the subscript i represents the normal and tangential directions, respectively, t and n. By following chain rule for the differentiating with respect to time,

$$\dot{\phi} = \frac{d\tau}{dt}\frac{d\phi}{d\tau} = \frac{v}{\eta}\phi'\,,$$

the equations governing non-dimensional force and displacement of the contact point are given as follows:

$$\gamma_t' = \frac{-8(1-\nu)}{3(2-\nu)}\varepsilon\,, \tag{4.8b}$$

$$\gamma_n' = -\frac{4}{3}\delta_n\,, \tag{4.9b}$$

$$\delta t' = \sin\alpha + (1+\lambda\cos 2\theta)\gamma_t + (\lambda\sin 2\theta)\gamma_n \tag{4.10b}$$

and

$$\delta n' = -\cos\alpha + (\lambda\sin 2\theta)\gamma_t + (1-\lambda\cos 2\theta)\gamma_n\,. \tag{4.11b}$$

Thus, for stick, if $|\varepsilon| < \frac{\mu(2-\nu)}{2(1-\nu)}(-\delta_n)$, then

$$\varepsilon' = \delta t' \tag{4.5b}$$

otherwise, for gross slip,

$$\varepsilon^* = -\frac{\mu\,(2-\nu)}{2\,(1-\nu)}\,\delta_n \tag{4.19}$$

and

$$\varepsilon'^* = -\frac{\mu\,(2-\nu)}{2\,(1-\nu)}\,\delta_n' \,. \tag{4.20}$$

The initial conditions (at $\tau = 0$) become

$$\delta_t = 0 \,,$$

$$\delta_t' = \sin\alpha \,,$$

$$\delta_n = 0 \,,$$

and

$$\delta_n' = -\cos\alpha \,.$$

The contact area sticks at the beginning of impact, if

$$\frac{\delta'_t}{-\delta'_n} < \frac{\mu(2-\nu)}{2(1-\nu)} \quad \left(\text{i.e., } \tan\alpha < \frac{\mu(2-\nu)}{2(1-\nu)}\right) .$$

The system equations would be rearranged in matrix form as:

$$\frac{d}{d\tau}\begin{Bmatrix}\delta_t'\\ \delta_n'\end{Bmatrix} = \begin{bmatrix}N_{tt} & N_{tn}\\ N_{nt} & N_{nn}\end{bmatrix}\begin{Bmatrix}\gamma'_t\\ \gamma'_n\end{Bmatrix}$$

that is,

$$\begin{Bmatrix}\delta_t''\\ \delta_n''\end{Bmatrix} = \begin{bmatrix}-\frac{8(1-\nu)}{3(2-\nu)}(1+\lambda\cos 2\theta) & -\frac{4}{3}\lambda\sin 2\theta\\ -\frac{8(1-\nu)}{3(2-\nu)}\lambda\sin 2\theta & -\frac{4}{3}(1-\lambda\cos 2\theta)\end{bmatrix}\begin{Bmatrix}\delta_t\\ \delta_n\end{Bmatrix} ; \tag{4.21}$$

otherwise, for

$$\frac{\delta_t'}{-\delta_n'} > \frac{\mu(2-\nu)}{2(1-\nu)} \,,$$

the tangential force has a limiting friction force ($F_t = \mu F_n$) and sliding takes place at the beginning of impact. The system equation is then

$$\begin{Bmatrix}\delta_t''\\ \delta_n''\end{Bmatrix} = \begin{bmatrix}-\frac{4\mu}{3}(1+\lambda\cos 2\theta) & -\frac{4}{3}\lambda\sin 2\theta\\ -\frac{4\mu}{3}\lambda\sin 2\theta & -\frac{4}{3}(1-\lambda\cos 2\theta)\end{bmatrix}\begin{Bmatrix}\delta_n\\ \delta_n\end{Bmatrix} , \tag{4.22}$$

acting as if it were a rigid body.

The initial slide may stop and stick at some point during the impact. For slip, the tangential velocity should be greater than the velocity of tangential spring for limiting friction force,

$$\delta_t' > \varepsilon^{*'} \tag{4.23}$$

Sliding action ceases when effective rigid body velocity is equal to the rate of extension of the tangential spring for limiting friction force, that is, $\delta_t' = \varepsilon^{*'}$. Once slide ceases and the contact points stick, tangential compliance in contact conforms to the behavior of the spring-mass system indicated in equation (4.21). This tangential oscillation is cut short by the occurrence of gross slip when F_t reaches the value $-\mu F_n$ and the direction of slip is opposite to the velocity at incidence.

If, under certain circumstances, the sliding velocity does not decrease to reach the rate of extension of the tangential spring for limiting friction during impact (i.e., $\delta_t' > \varepsilon^{*'}$), gross slip persists throughout the impact. In this case, the tangential impulse g_t has a limiting value of $-\mu g_n$ and is substituted into equations (4.10a) and (4.11a) as

$$\bar{v}_t = v_t - \mu N_{tt} g_n + N_{tn} g_n \tag{4.24}$$

and

$$\bar{v}_n = v_n - \mu N_{nt} g_n + N_{nn} g_n \,. \tag{4.25}$$

While gross slip continues and impact motion is analyzed with respect to the rigid body mechanics, displacement and the velocity of tangential spring still exist as a function of normal displacement and

velocity as given in equation (4.13) and (4.14), respectively. At the termination of impact, the normal velocity will have an equal magnitude and opposite direction of the initial normal velocity. Substituting $-v_n$ for $\bar{v}_n$ into equation (4.25), normal impulse and final tangential velocity for complete slip may be expressed in terms of the initial normal velocity v_n:

$$-v_n = v_n - \mu N_{nt}\, g_n + N_{nn}\, g_n ,$$

$$g_n = \frac{2v_n}{\mu N_{nt} - N_{nn}} , \tag{4.26}$$

and substituting equation (4.26) into equation (4.24),

$$w_t = v_t + \frac{2(N_{tn} - \mu N_{tt})v_n}{\mu N_{nt} - N_{nn}} . \tag{4.27}$$

Moreover, for the necessary condition of complete slip, at the end of impact the tangential velocity must be kept greater than the rate of extension of the tangential spring $\dot{s}$ as given in equation (4.14). For complete gross slip,

$$v_t + \frac{2(N_{tn} - \mu N_{tt})v_n}{\mu N_{nt} - N_{nn}} - \frac{\mu\,(2 - \nu)}{2\,(1 - \nu)}\, v_n \;> 0 ,$$

that is,

$$v_t + \frac{2(N_{tn} - \mu N_{tt})v_n}{\mu N_{nt} - N_{nn}} > \frac{\mu(2 - \nu)}{2(1 - \nu)} v_n . \tag{4.28}$$

The ratio of the initial tangential and normal velocities may be defined as tangent function of the incident angle α, $v_t/(-v_n) = \tan\alpha$. Applying parameters of inertia coupling as given in equation (2.31), the necessary condition for complete gross slip is then

$$\tan\alpha > \frac{2[\mu(1+\lambda\cos 2\theta)-\lambda\sin 2\theta]}{1-\lambda(\cos 2\theta+\mu\sin 2\theta)} - \frac{\mu(2-\nu)}{2(1-\nu)} \qquad (4.29)$$

From this point in the analysis, predictions for planar collision could be determined by the parameters: friction coefficient μ, two inertia coupling factors λ and θ, and the incident angle α. For the equations used in this analysis, curvature of contact shape R and other material properties of Young's modulus E and mass density ρ are excluded from non-dimensional formulations. Incident angle conditions for stick and slip at the initial state of impact could be expressed in terms of friction coefficient μ and inertia coupling parameters λ and θ, and summarized as follows.

i) $\tan\alpha > \frac{2[\mu(1+\lambda\cos 2\theta)-\lambda\sin 2\theta]}{1-\lambda(\cos 2\theta+\mu\sin 2\theta)} - \frac{\mu(2-\nu)}{2(1-\nu)}$

When the incident velocity is satisfied with this relation, the initial tangential force reaches the limiting friction force. The bodies slide at the beginning of impact and slip persist throughout entire impact. In this case, the motion of the system is identical to that given for rigid body mechanics;

ii) $\frac{\mu(2-\nu)}{2(1-\nu)} < \tan\alpha \le \frac{2[\mu(1+\lambda\cos 2\theta)-\lambda\sin 2\theta]}{1-\lambda(\cos 2\theta+\mu\sin 2\theta)} - \frac{\mu(2-\nu)}{2(1-\nu)}$:

For this range of incident angles, the bodies slide at the initiation, then at some point tend to stick as the tangential force decreases due to the friction resistance during the cycle. The motion is then completed by the tangential and normal stiffness governed by stick region; and

iii) $\tan\alpha \le \dfrac{\mu(2-\nu)}{2(1-\nu)}$:

For this incident angle condition, the initial tangential force is less than the limiting friction force, and the bodies stick at the beginning of impact. In general, tangential motion at impact, considered to be distinct from the half-cycle of normal motion, is completed within one cycle.

However, there could be circumstances in which there is conflict between conditions for stick and slip. Consider the situation where

$$\frac{2[\mu(1+\lambda\cos 2\theta)-\lambda\sin 2\theta]}{1-\lambda(\cos 2\theta+\mu\sin 2\theta)} - \frac{\mu(2-\nu)}{2(1-\nu)} < \frac{\mu(2-\nu)}{2(1-\nu)} ,$$

that is,

$$\frac{2[\mu(1+\lambda\cos 2\theta)-\lambda\sin 2\theta]}{1-\lambda(\cos 2\theta+\mu\sin 2\theta)} < \frac{\mu(2-\nu)}{(1-\nu)} . \qquad (4.30)$$

In this circumstanc, due to the effect of inertia coupling of the system, the tangential force increases and reaches the limit friction force in either the initial tangential direction or the opposite direction. The bodies, which stick initially, begin to slide at some point and slip persists throughout impact.

4.1.2 Coupled spring

Based upon the assumption of entire stick throughout the contact area, the relative tangential displacement of two bodies in contact was given in equation (3.9). Substituting equation(3.2) into

equation(3.9), the displacement of the tangential spring becomes coupled with the displacement of the normal spring,

$$s = \frac{-F_t}{8\sqrt{R(-u_n)}}\left(\frac{2-\nu_1}{G_1}+\frac{2-\nu_2}{G_2}\right). \tag{4.31}$$

Normal and tangential force may be expressed as

$$F_n = K_{nn}\,(-u_n)^{\frac{3}{2}} \tag{4.32}$$

and

$$F_t = -\,K_{tt}\,s(-u_n)^{\frac{1}{2}}, \tag{4.33}$$

and the stiffness of the normal and tangential spring, respectively, are

$$K_{nn} = \frac{4}{3}\sqrt{R}\,E \tag{4.34}$$

and

$$K_{tt} = 8\,G\sqrt{R}\,, \tag{4.35}$$

where

$$G = \frac{1}{\frac{2-\nu_1}{G_1}+\frac{2-\nu_2}{G_2}}\,.$$

When the contact area is subject to sticking, and the tangential force is less than the limiting friction force, the tangential velocity of colliding bodies is equal to the extension rate of the tangential spring; that is, if

$$K_{tt}\,|s|\,\sqrt{-u_n} < \mu\,K_{nn}(-u_n)^{\frac{3}{2}},$$

then $\bar{v}_t(t) = \dot{s}(t)$. As the tangential force reaches the limiting friction force, elastic deformation and the velocity of tangential direction, respectively, become

$$s = \frac{\mu\,E}{6\,G}\,(-u_n) \tag{4.36}$$

and

$$\dot{s} = \frac{\mu E}{6 G} (-\dot{u}_n) . \tag{4.37}$$

Following each step for the non-dimensional formulation for the linearized model, the equations of motion may then be formulated in non-dimensional terms as

$$\gamma_t' = -\frac{8G}{E} \varepsilon\sqrt{-\delta_n} , \tag{4.38}$$

$$\gamma_n' = \frac{4}{3}(-\delta_n)^{\frac{3}{2}} , \tag{4.39}$$

$$\delta_t' = \sin\alpha + (1+\lambda\cos 2\theta)\,\gamma_t + (\lambda \sin 2\theta)\,\gamma_n , \tag{4.40}$$

and

$$\delta_n' = -\cos\alpha + (\lambda \sin 2\theta)\,\gamma_t + (1-\lambda\cos 2\theta)\,\gamma_n . \tag{4.41}$$

Thus, for stick, if $|\varepsilon| < \frac{\mu E}{6 G}(-\delta_n)$, then

$$\varepsilon' = \delta t' ; \tag{4.42}$$

otherwise, for slip,

$$\varepsilon' = -\frac{\mu E}{6 G} \delta_n' . \tag{4.43}$$

Initially, $\delta t = \delta_n = 0$, $\delta_t' = \sin\alpha$, and $\delta_n' = -\cos\alpha$. The condition for stick and slip would be decided by the incident angle α. For

$$\tan\alpha \le -\frac{\mu E}{6 G} \delta_n ,$$

the bodies stick at the beginning of impact and tangential velocity is as determined by equation (4.38); otherwise, slide occurs at the beginning of impact and equation (4.22) is used for representation of elastic tangential velocity.

In the manner developed from the linearized analysis given in 4.1.1, conditions for stick and slip for the bodies with the same material constants could be summarized as follows.

i) For gross slip,

$$\tan\alpha > \frac{2[\mu(1+\lambda\cos 2\theta)-\lambda\sin 2\theta]}{1-\lambda(\cos 2\theta+\mu\sin 2\theta)} - \frac{\mu(2-\nu)}{3(1-\nu)} ;$$

ii) For slip and stick,

$$\frac{\mu(2-\nu)}{3(1-\nu)} < \tan\alpha \le \frac{2[\mu(1+\lambda\cos 2\theta)-\lambda\sin 2\theta]}{1-\lambda(\cos 2\theta+\mu\sin 2\theta)} - \frac{\mu(2-\nu)}{3(1-\nu)} ;$$

iii) For stick,

$$\tan\alpha \le \frac{\mu(2-\nu)}{3(1-\nu)} .$$

4.1.3 Nonlinear spring

Elastic deformations of normal and tangential directions may be approximated to the same dimensions and the relationship indicated in equation (3.22) then would be applied for an analysis of spring stiffness. In terms of their displacements, the normal and tangential spring force both are nonlinear, expressed as

$$F_t = - K_{tt}\, s\, \sqrt{|s|} \qquad (4.44)$$

and

$$F_n = K_{nn}\, (-u_n)^{\frac{3}{2}} , \qquad (4.45)$$

where the stiffness of the normal and tangential springs is identical to the equivalent conditions considered in section 4.1.1 in equation (4.1) and (4.2), respectively:

$$K_{nn} = \frac{4}{3}\sqrt{R}E \quad \text{and} \quad K_{tt} = \frac{8(1-\nu)}{3(2-\nu)}\sqrt{R}E \ .$$

By observing the procedures previously given for non-dimensional formulation, the equations of motion are expressed in terms of non-dimensional quantities as

$$\gamma_t' = -\frac{8(1-\nu)}{3(2-\nu)}\varepsilon|\varepsilon|^{\frac{1}{2}} \ , \tag{4.46}$$

$$\gamma_n' = -\frac{4}{3}(-\delta_n)^{\frac{3}{2}} \ , \tag{4.47}$$

$$\delta_t' = \sin\alpha + (1+\lambda\cos 2\theta)\,\gamma_t + (\lambda\sin 2\theta)\,\gamma_n \tag{4.48}$$

and

$$\delta_n' = -\cos\alpha + (\lambda\sin 2\theta)\,\gamma_t + (1-\lambda\cos 2\theta)\,\gamma_n \ . \tag{4.49}$$

Thus, for stick, if $|\varepsilon| < \left[\frac{\mu(2-\nu)}{2(1-\nu)}\right]^{\frac{2}{3}}(-\delta_n)$, then

$$\varepsilon' = \delta t' \ ; \tag{4.50}$$

otherwise, for gross slip,

$$\varepsilon' = -\left[\frac{\mu(2-\nu)}{2(1-\nu)}\right]^{\frac{2}{3}} \ . \tag{4.51}$$

Similarly the conditions of stick and slip could be summarized as follows.

i) For gross slip,

$$\tan\alpha > \frac{2[\mu(1+\lambda\cos 2\theta) - \lambda\sin 2\theta]}{1-\lambda(\cos 2\theta + \mu\sin 2\theta)} - \left[\frac{\mu(2-\nu)}{2(1-\nu)}\right]^{\frac{2}{3}} \ ;$$

ii) For slip and stick,

$$\left[\frac{\mu(2-\nu)}{2(1-\nu)}\right]^{\frac{2}{3}} < \tan\alpha \leq \frac{2[\mu(1+\lambda\cos 2\theta)-\lambda\sin 2\theta]}{1-\lambda(\cos 2\theta+\mu\sin 2\theta)} - \left[\frac{\mu(2-\nu)}{2(1-\nu)}\right]^{\frac{2}{3}} ;$$

iii) For stick,

$$\tan\alpha \leq \left[\frac{\mu(2-\nu)}{2(1-\nu)}\right]^{\frac{2}{3}} .$$

4.2. Oblique impact of elastic spheres

In this section, the oblique impact of elastic spheres is investigated, using the methods developed in the previous section. A sphere colliding with a massive flat surface is taken for example. The parameters of inertia coupling for the collision system are $\lambda = 5/9$ and $\theta = 0$. From the system equations for the non-dimensional formulation, it may be seen that only the incident velocity and friction coefficient characterize the motion of impact for a given value of Poisson's ratio. Consider a sphere with $\nu = 0.3$ and $\mu = 0.5$ striking on a flat surface as shown in Figure 9. Since there is no inertia coupling for the sphere, the motion of impact in the normal and tangential direction could be solved independently. Only tangential velocity is considered in this example since normal velocity returns to its initial value without energy dissipation.

As shown in Figure 12, the angles are related to the velocity components as

$$\alpha_1 = \tan^{-1}\left(\frac{v_t}{-v_n}\right) \tag{4.53}$$

and

$$\alpha_2 = \tan^{-1}\left(\frac{w_t}{w_n}\right), \tag{4.54}$$

where v_t, v_n, w_t and w_n are the incident and reflecting velocities of the point P, respectively, in the tangential and normal directions.

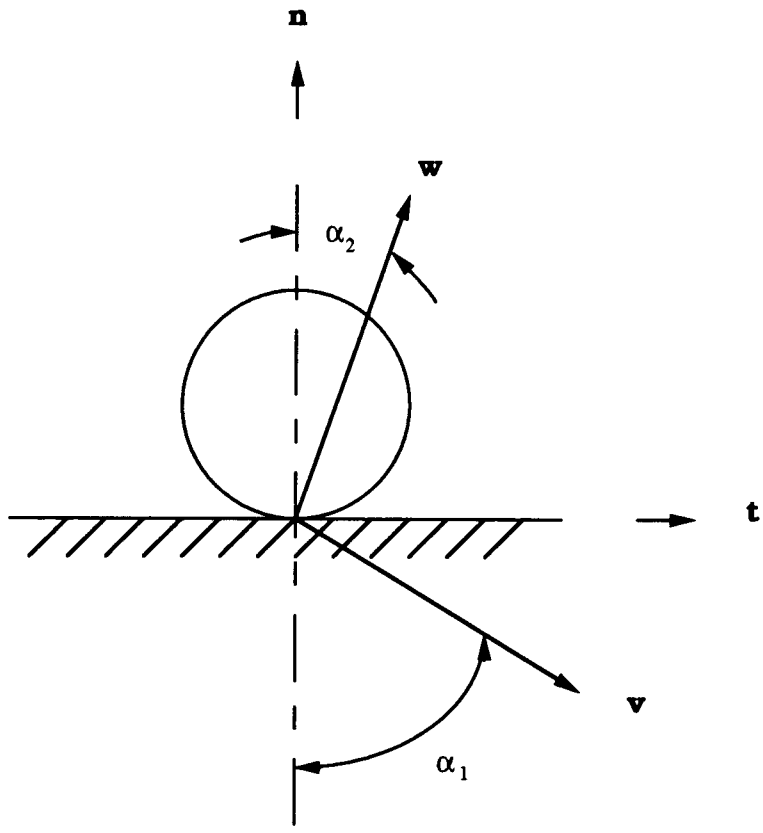

Figure 12. The definitions of the angle of incidence and the angle of reflection

Given the above material constants, Maw et al. [10] introduced a non-dimensional quantitiy for incident velocity,

$$\Psi = \frac{2(1-\nu)}{\mu(2-\nu)} \tan\alpha \ , \tag{4.52}$$

where the values of Ψ and α that correspond to incidence will be denoted as Ψ_1 and α_1 and those that correspond to the reflection as Ψ_2 and α_2. Since Ψ is proportional to the ratio between tan α and the coefficient of friction μ, Ψ_1 and Ψ_2 are referred to, respectively, as the non-dimensional angle of incidence and the non-dimensional angle of reflection.

To examine the model for a linear spring over the collision of elastic spheres, the coefficients of stiffness for the normal and tangential spring in the equation of motion in non-dimensional quantities are, respectively,

$$K_{nn} = 4/3 \sqrt{R}E$$

and

$$K_{tt} = 2(1-\nu)/(2-\nu)\, K_{nn}\sqrt{R}E$$
$$= 1.09804\sqrt{R}E$$

The value of w_n is equal to the value of v_n since there was no energy dissipation in normal direction. The computed values of w_t are then used for the evaluation of the corresponding values of Ψ_2, and non-dimensional tangential force and time are defined, respectively, as

$$\Phi_t = \frac{F_t}{\mu F_{n,max}} \tag{4.55}$$

and

$$\tau = \frac{t}{T} \ , \tag{4.56}$$

where t is any instant time during the contact and T is the duration of contact. For the linearized model, the plot of nondimensional tangential force Φ_t with respect to the dimensionless time τ for different value of Ψ_1 is given in Figure 13.

Accoding to the section 4.1, the condition for gross slip is compared to those from the analysis given by Maw et al. [10,11]. For the sphere (θ=0), condition for gross slip given in equation (4.29) becomes

$$\tan \alpha_1 > \frac{2\mu(1+\lambda)}{1-\lambda} - \frac{\mu(2-\nu)}{2(1-\nu)}$$

Then, introducing another nondimensional quantity,

$$\chi = \frac{(1-\nu)(1+\lambda)}{(2-\nu)(1-\lambda)} ,$$

which is independent of the friction coefficient and a function of the Poisson ratio for a given value of λ, the condition for gross slip could be expressed as

$$\Psi_1 > 4\chi - 1 \qquad (4.57)$$

and this is identical to the condition for gross slip developed by Maw. Gross slip occurs throughout impact if $\Psi_1 > 4.765$ as indicated in equation (4.57). In the stick region, Ψ_1<1.0, the value of tangential force should stay less than limiting friction force throughout the impact. However, from Figure 13, the tangential force is limited by an opposite friction force discontinously and this unsmooth change for tangential force is caused by the linearization of stiffness, which actually is both nonlinear and dependent on previous load history.

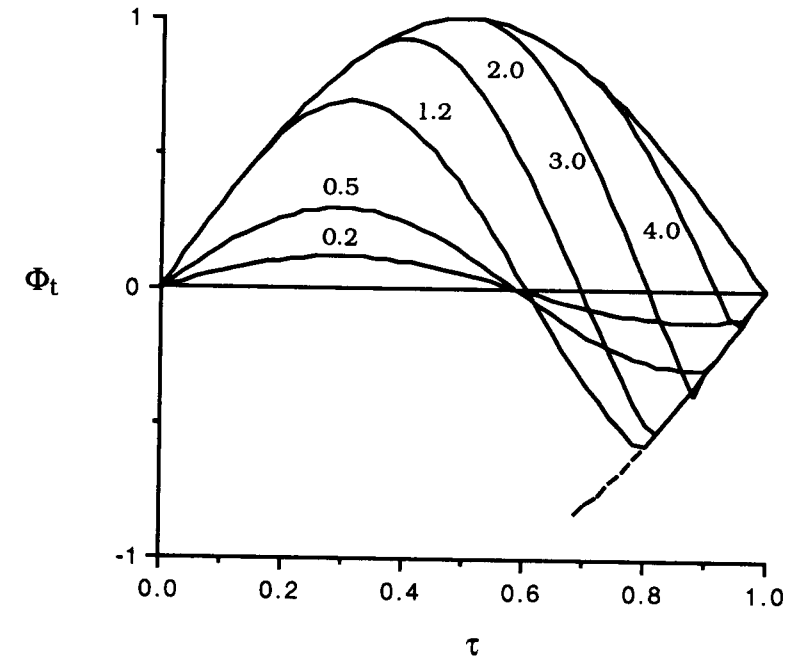

(a)

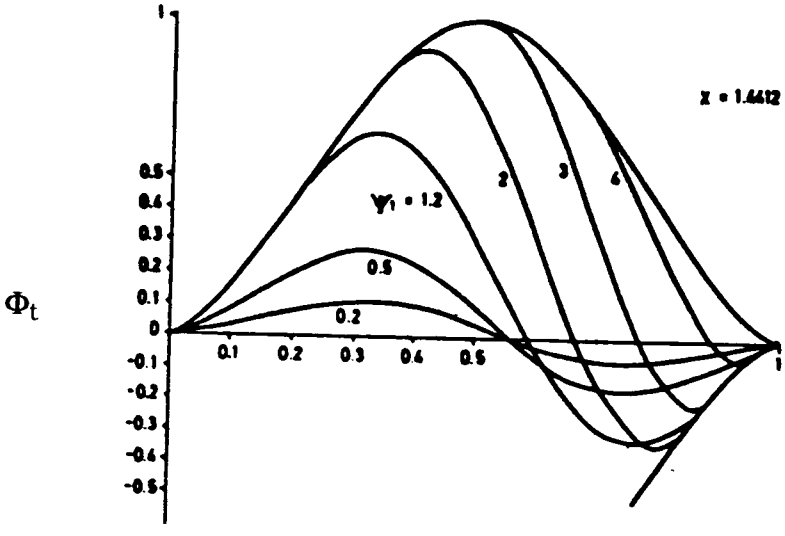

(b)

Figure 13. Nondimensional tangential force during impact for various nondimensional incident angle Ψ_1:
(a) analysis for linear spring (b) Maw's analysis [10]

Though there are no smooth changes in tangential forces into the direction of opposite slip, there is little effect upon rebound velocity. In Figure 14, the effect of linearization of stiffness is noticeable in the region of transit from stick to slip (i.e., $0.5 < \Psi_1 < 1.5$). Since the tangential elastic recovery of the surfaces can maintain relative motion even when the contact patch of the body has been brought to rest, the range of Ψ_1, over which gross-slip can be expected throughout the cycle, exceeds that from simple rigid body theory. Referring to the equations (4.20) and (4.23) for gross slip, the velocity of the tangential spring has a negative value during restitution and that is the reason tangential velocity at seperation become negative in the range Ψ_1 between 4.765 and 5.765. Consequently, the results from the linearized analysis for the impact of elastic spheres are in close agreement with those from Maw's method, which has been verified experimentally.

For $\Psi_1 = 1.2$, the tangential compliance is examined throughout the entire period of impact, as given in Figure 15. Since the nondimensional incident angle Ψ_1 is greater than one, slip occurs at the initiation of impact from point O to A. Since both normal and tangential force increase as $\mu dF_n \geq dF_t$ in the path A to B, from equation (3.30), the tangential compliance is given as (2-ν)/4Ga. The normal force increases and the tangential force decreases as $\mu dF_n \leq -dF_t$ from B to C, and referring to equation (3.29), the tangential compliance does not have the value of (2-ν)/4Ga. However, this could be approximated to the value of (2-ν)/4Ga, since there is no big difference between F_t^* and F_t in equation (3.29). In the path C to

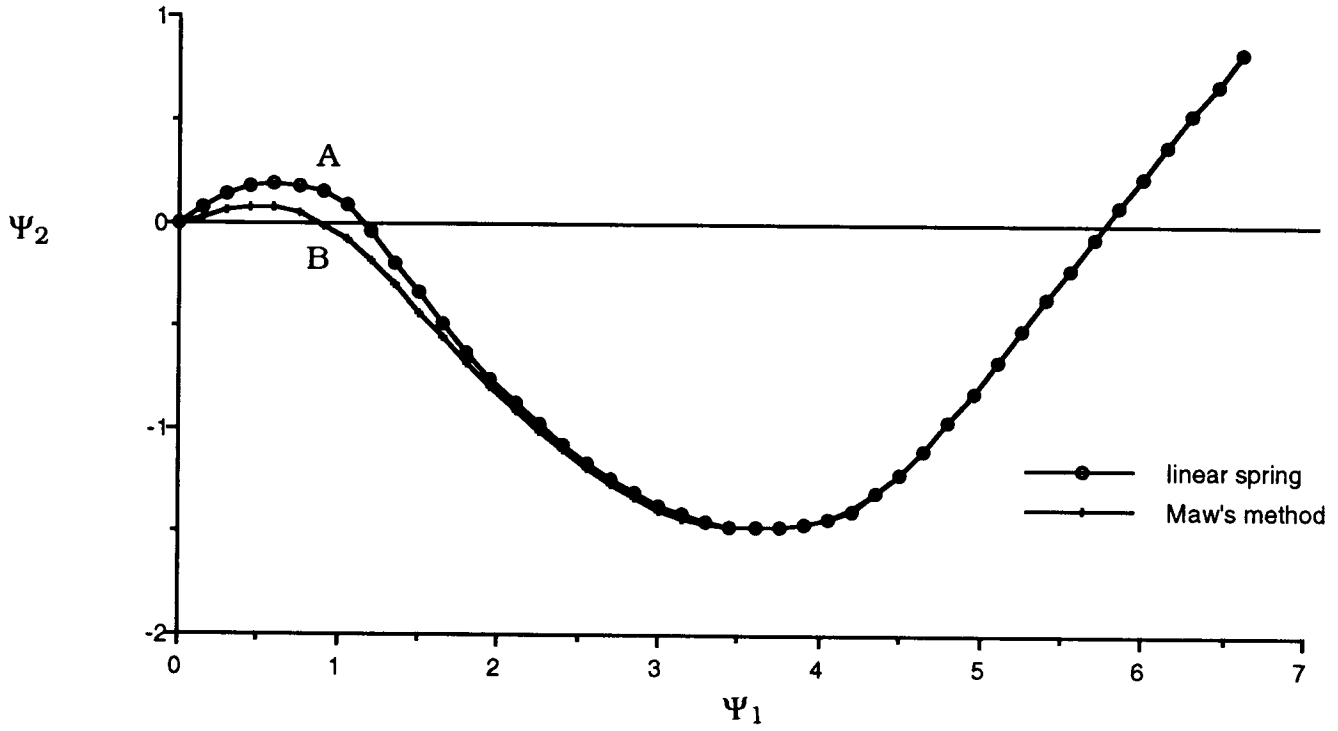

Figure 14. Nondimensional angle of reflection Ψ_2 and angle of incidence Ψ_1 for a sphere with Poisson's ratio 0.3: Path A from analysis for linear spring and path B from Maw's result

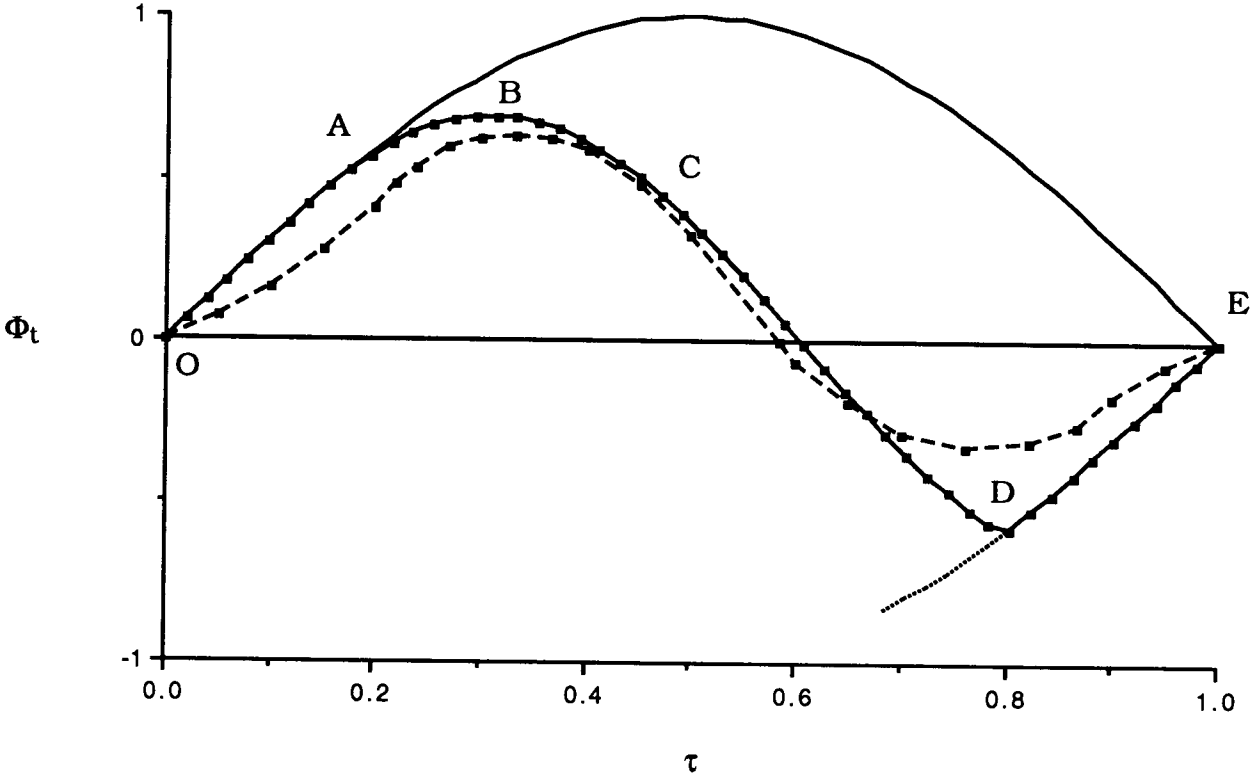

Figure 15. Nondimensional tangential force during impact at Ψ_1 = 1.2: Solid line from analysis for linear spring and dashed line from Maw's result

D, both normal and tangential forces decrease and tangential compliance has the value from equation (3.30). As the path approaches to D, the tangential compliance can not be approximated to the value of (2-ν)/4Ga, since there is more difference between F_t^* and F_t in equation (3.30). Comparing with Maw's result shown in Figure 13 (b), there are some discrepancies caused by linearization and constant tangential compliance. As the tangential force decreases to reach the limiting friction force, slip takes place in an opposite direction to initial slip from D to E.

The value of non-dimensional incident velocity Ψ_1 for stick and slip depends on the method applied. In Table 1, the conditions for stick and slip are summarized for each analysis.

Table 1. Conditions for stick and slip at the beginning of impact

Analysis\Condition	Stick	Slip and Stick	Slip
Linear spring	$0 \le \Psi_1 < 1.0$	$1.0 \le \Psi_1 < 4.675$	$\Psi_1 \ge 4.675$
Coupled spring	$0 \le \Psi_1 < 0.67$	$0.67 \le \Psi_1 < 5.20$	$\Psi_1 \ge 5.20$
Nonlinear spring	$0 \le \Psi_1 < 1.18$	$1.18 \le \Psi_1 < 4.59$	$\Psi_1 \ge 4.59$

For $\Psi_1 = 1.2$, the values for displacement, velocity, force, and impulse at the contact points for the linearized analysis are plotted nondimensionally in Figures 16 to 22. Moreover, changes in the constant value of normal stiffness, k_{nn}, are influenced only by the duration of contact, and not the behavior of impact motion. However,

the ratio of the tangential to normal stiffness given in equations (4.1) and (4.2) is important to the prediction of impact motions.

The results from analyses for the coupled and nonlinear spring are shown in Figure 23. Roughly there are no significant discrepancies between the methods considered in this study and Maw's method.

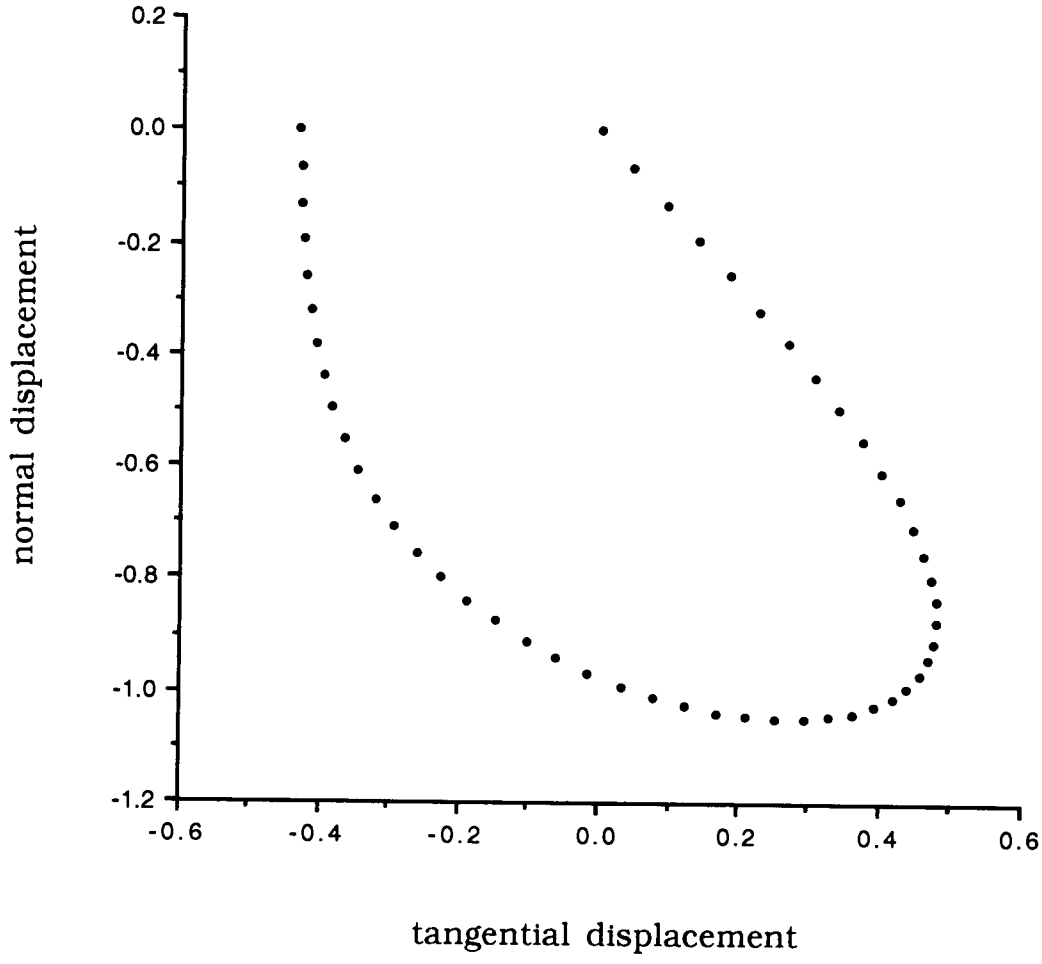

Figure 16. Nondimensional normal and tangential displacement of contact point at Ψ_1=1.2

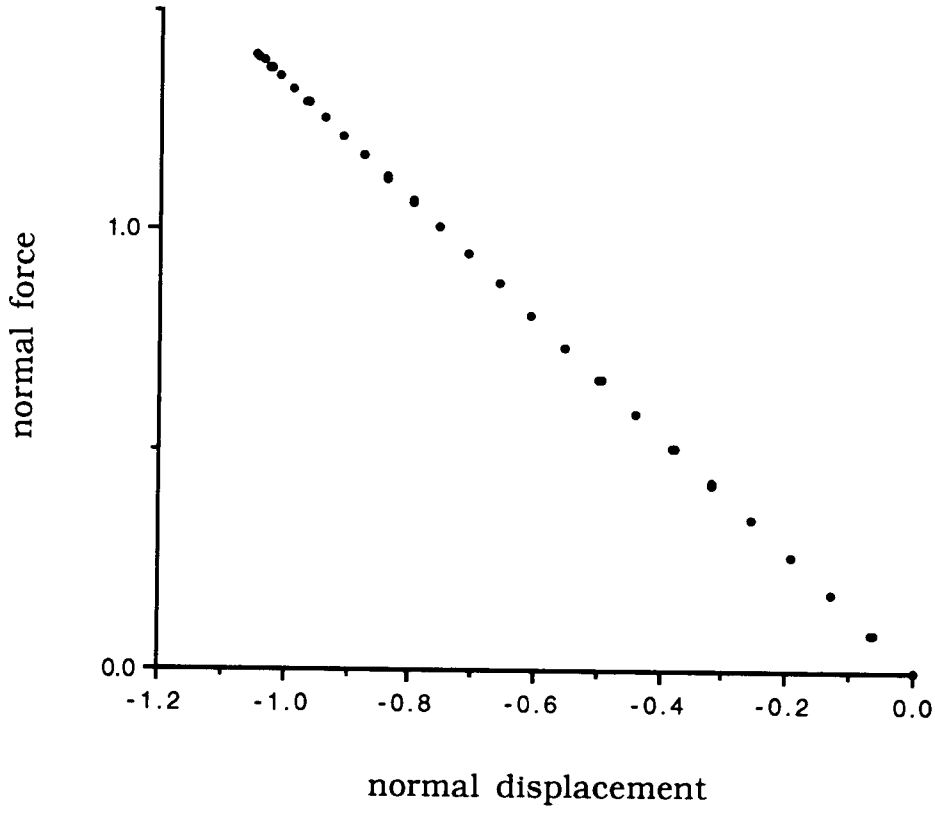

Figure 17. Nondimensional normal displacement and normal force of contact point at Ψ_1=1.2

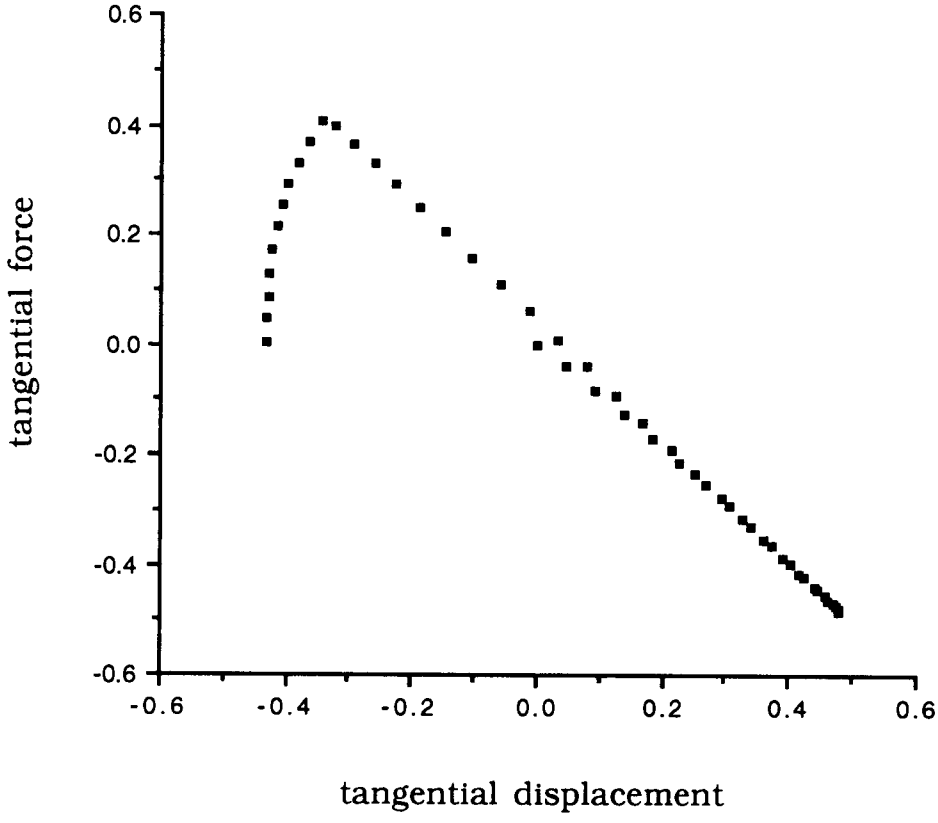

Figure 18. Nondimensional tangential displacement and tangential force of contact point at Ψ_1=1.2

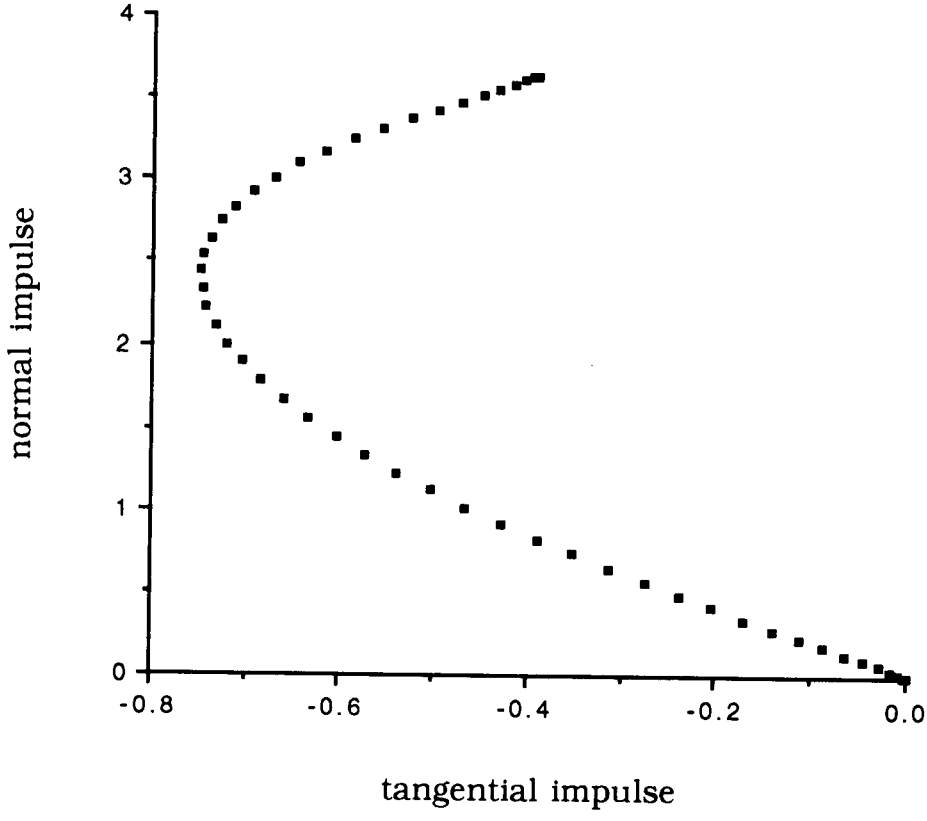

Figure 19. Nondimensional normal and tangential impulse of contact point at Ψ_1=1.2

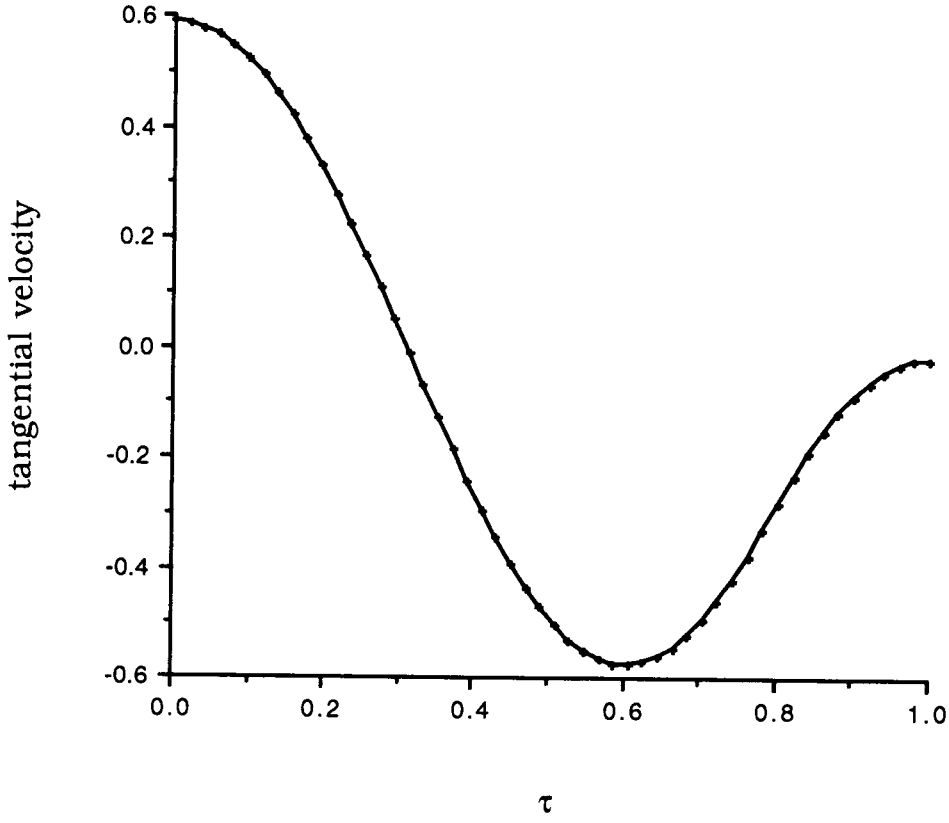

Figure 20. Nondimensional tangential velocity of contact point at Ψ_1=1.2

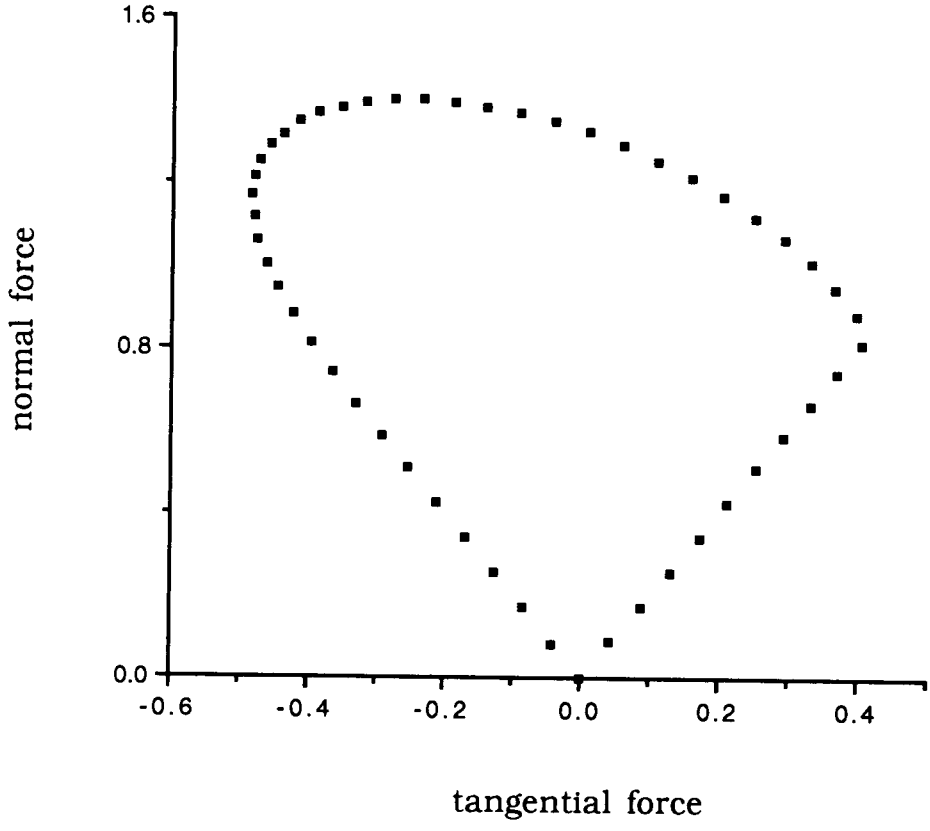

Figure 21. Nondimensional tangential and normal force of contact point at Ψ_1=1.2

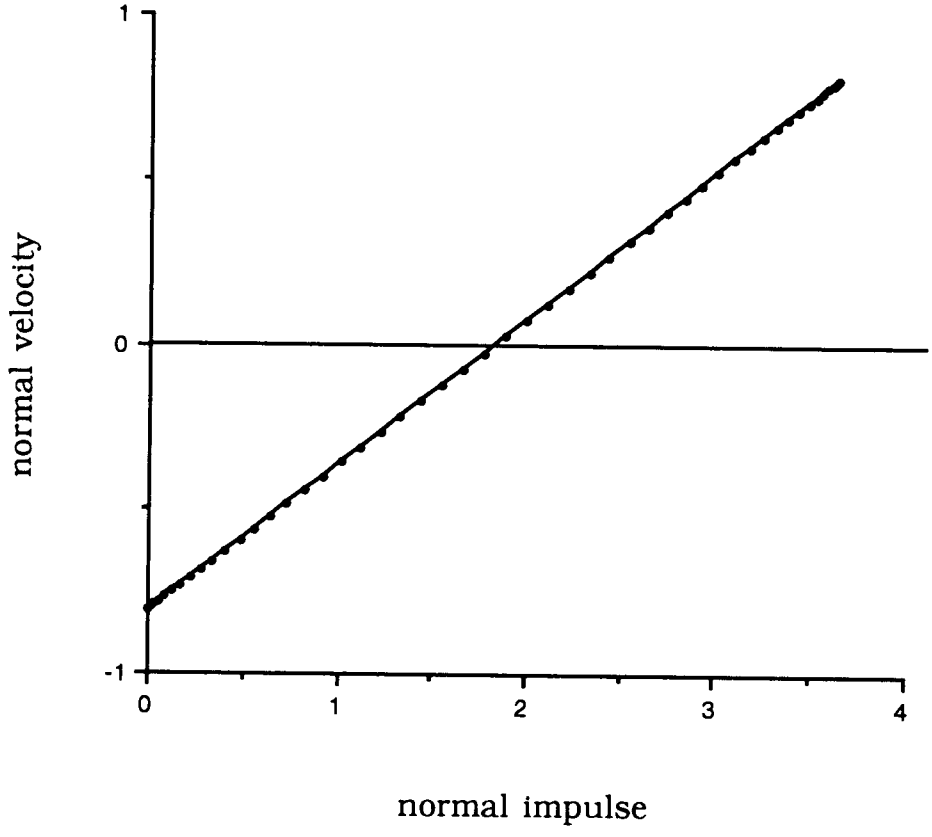

Figure 22. Nondimensional normal impulse and normal velocity of contact point at $\Psi_1=1.2$

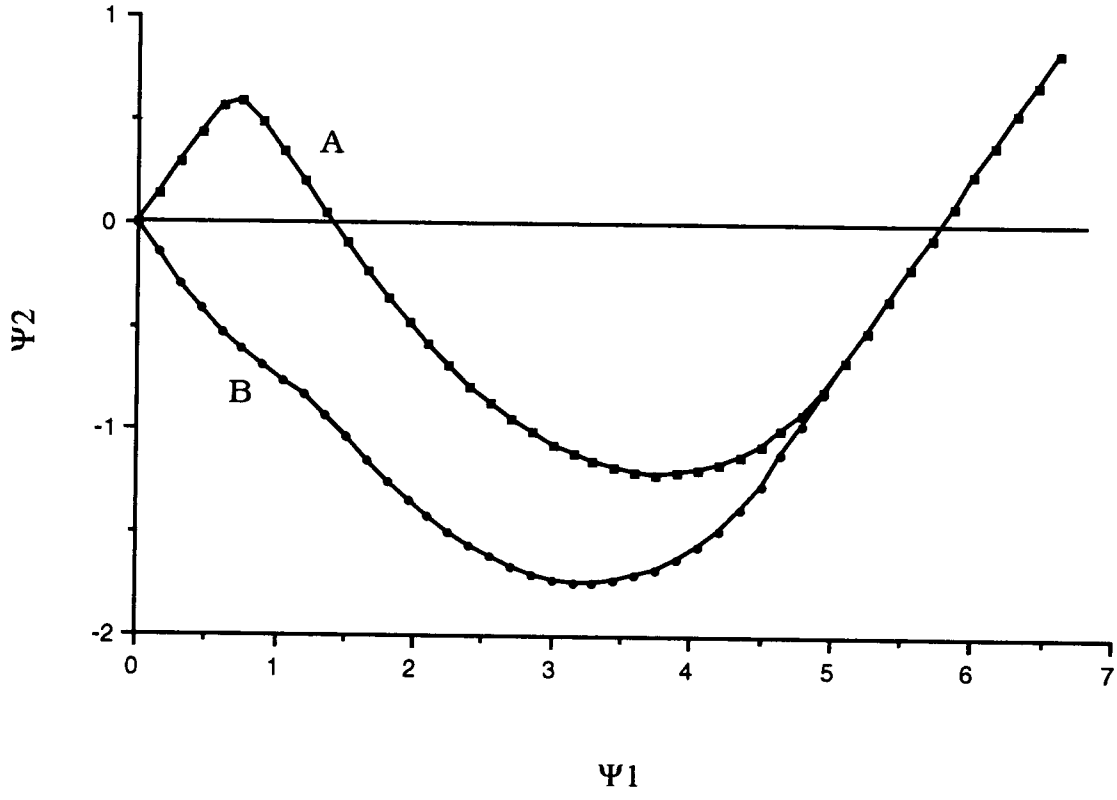

Figure 23. Nondimensional angle of reflection Ψ_2 and angle of incidence Ψ_1 for a sphere with Poisson's ratio 0.3: (A) analysis for coupled spring (B) analysis for nonlinear spring

5. PARAMETERS OF COLLISION SYSTEM

It is common to define a quantity, called the coefficient of restitution, which can be used to predict the final state of contact. In this chapter, three coefficients of restitution are compared for non-collinear collisions. In addition, parameters obtained through application of the non-dimensional formulation in Chapter 4 are investigated for the characterization of a variety of mechanical collisions.

5.1 Coefficients of restitution

The duration of impact is separated into a compression phase and a restitution phase. The duration from first contact to the instant at which the normal component of the relative velocity reaches zero is called the compression phase. The restitution phase follows the compression phase and terminates at the end of contact. In this definition, the motions of P and P' are understood to belong to "rigid" bodies B and B', even though it is recognized that deformation is necessary to preclude penetration. Thus, the instant that separates the compression and restitution phases is that at which maximum penetration (even in the rigid-body idealization) is reached. The three definitions for the coefficient of restitution are considered as follows:

The first definition is given as

$$c = \frac{g_{nr}}{g_{nc}} , \tag{5.1}$$

where g_{nc} is the normal component of impulse $\mathbf{g}$ accumulated during the compression phase and g_{nr} is that accumulated during the restitution phase.

The second definition is given as

$$e = \frac{\mathbf{n} \cdot \mathbf{w}}{-\mathbf{n} \cdot \mathbf{v}} , \tag{5.2}$$

where $\mathbf{v}$ and $\mathbf{w}$ are the relative velocities at the beginning of contact and at the end of contact, respectively.

The inertia operator $\mathbf{N}$ plays an important role in the work done by the contact force at P and P'. The force exerted on B by B' at P denoted $\mathbf{F}$, the sum of the works of this force at any time may be expressed as

$$\begin{aligned} W &= \int \mathbf{F} \cdot d\mathbf{u} \\ &= \int \bar{\mathbf{v}} \cdot \mathbf{F}\, dt \\ &= \int \bar{\mathbf{v}} \cdot d\mathbf{g} \\ &= \int (\mathbf{v} + \mathbf{g} \cdot \mathbf{N}) \cdot d\mathbf{g} \\ &= \mathbf{v} \cdot \mathbf{g} + \frac{1}{2} \mathbf{g} \cdot \mathbf{N} \cdot \mathbf{g} \\ &= \left[\mathbf{v} + \frac{1}{2} (\bar{\mathbf{v}} - \mathbf{v}) \right] \cdot \mathbf{g} \\ &= \frac{\mathbf{v} + \bar{\mathbf{v}}}{2} \cdot \mathbf{g} \end{aligned} \tag{5.3}$$

in agreement with equation (2.22 c). An alternative expression for the change in kinetic energy at any time is equation (2.22c), which can be written with the help of equation (2.19) as

$$\Delta K = \frac{1}{2}(\bar{\mathbf{v}} \cdot \mathbf{N}^{-1} \cdot \bar{\mathbf{v}} - \mathbf{v} \cdot \mathbf{N}^{-1} \cdot \mathbf{v}) . \tag{5.4}$$

Because $\mathbf{x} \cdot \mathbf{N}^{-1} \cdot \mathbf{x}$ is a positive definite function of $\mathbf{x}$, this indicates that the greatest possible loss of kinetic energy during contact would occur if $\bar{\mathbf{v}} = 0$ (i.e., if the point P and P' have the same velocity). For planar collisions the maximum possible loss in kinetic energy could be expressed in terms of the parameters as

$$|\Delta K|_{max} = \frac{1}{2} \mathbf{v} \cdot \mathbf{N}^{-1} \cdot \mathbf{v} \tag{5.5 a}$$

and for planar collisions it can be expressed in terms of parameters as given in equations (2.47), (2.48), (2.49) and (2.50).

$$|\Delta K|_{max} = \frac{[1 + \lambda \cos 2(\alpha - \theta)] m v^2}{2(1 - \lambda^2)} \tag{5.5 b}$$

Recently, a third coefficient of restituion was introduced by Stronge [18] as

$$d = \sqrt{\frac{W_{nr}}{-W_{nc}}} , \tag{5.6}$$

where W_{nc} and W_{nr} are the sums of the work done by the normal components of the reaction forces at the contact point during the compression phase and during the restitution phase, respectively. Displacements in the definition of work used here must be understood to be those of points of "rigid" bodies (which would imply an artificial penetration, as mentioned above).

From equation (5.3) the normal component of work done by contact force then becomes

$$W_n = \int \bar{\mathbf{v}}_n \cdot dg_n \tag{5.7}$$

during the compression and restitution phases, respectively. From equation (5.7), the sum of the work done by the normal impulse is proportional to the area under the curve shown in Figure 24, which is the path in the diagram of normal velocity $\bar{v}_n$ versus normal impulse g_n. If there is no inertia coupling between the normal and tangential directions (i.e., **n** is parallel to the principal direction of **N**) or if the tangential component of the reaction force is zero (as when the surfaces are smooth), the variations of $\bar{v}_n(t)$ and $g_n(t)$ are linear:

$$\bar{v}_n = v_n + N_{nn}\, g_n \,. \tag{5.8}$$

In either case, then,

$$W_n = \int (v_n + N_{nn} g_n) dg_n = \frac{v_n + \bar{v}_n}{2}\, g_n \tag{5.9}$$

and, as can be seen from Figure 24, c = d = e. The presence of **t-n** inertia coupling, however, permits tangential impulse to affect normal velocity, so that the v_n- g_n curve may be nonlinear. In general, the sum of the works done by the normal components of the contact forces is not equal to $g_n(v_n + \bar{v}_n)/2$ and the values of c, d, and e may be expected to differ.

5.2 Prediction of planar collisions

Parameters such as the coefficient of friction and incident velocity, in addition to the inertia coupling expressed in **N**, already have been determined for the formulation of the non-dimensional

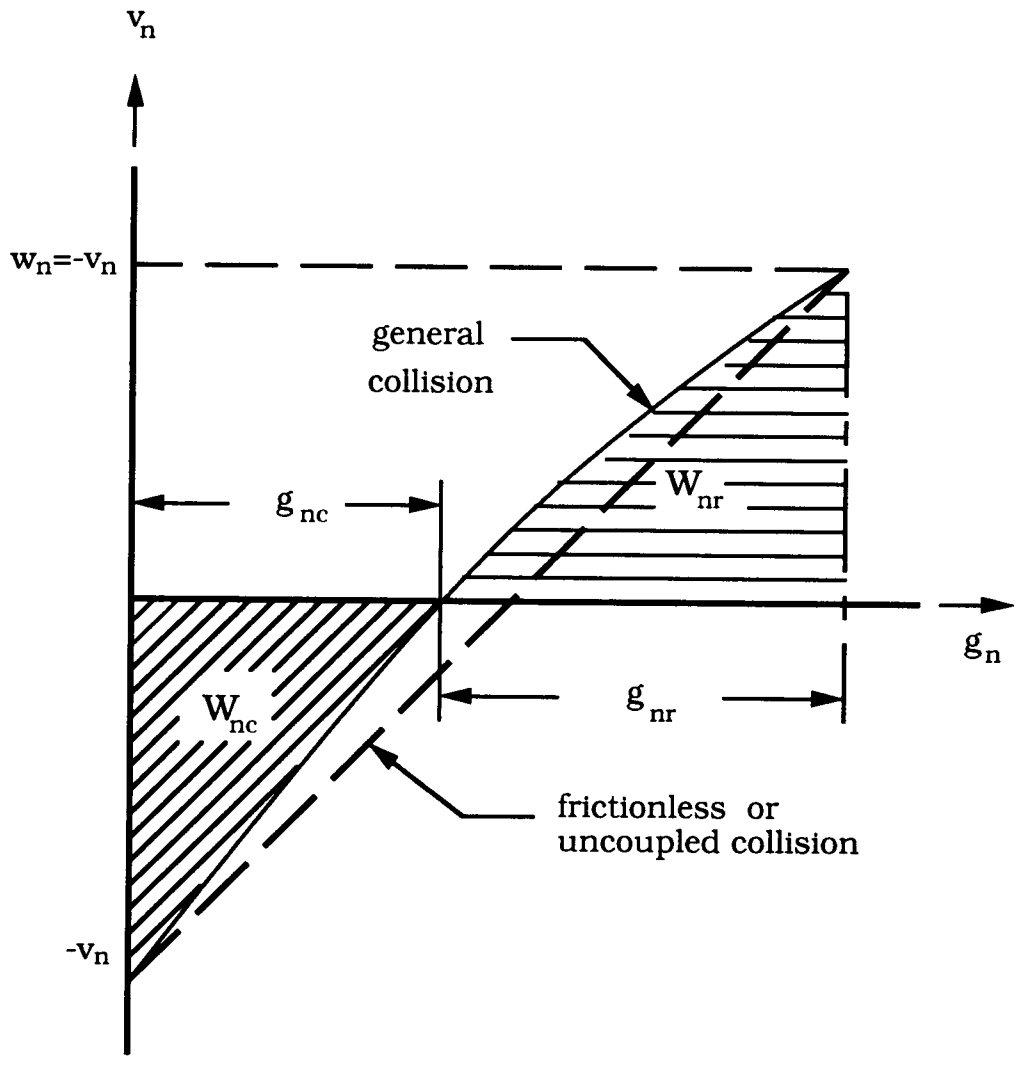

Figure 24. Work done during the compression and restitution of impact

system equations considered in Chapter 4. The results of several examples are presented and effects of the concerned parameters are investigated for a variety of collisions.

Consider the example shown in figure 25, in which a rod of uniform density colliding against a flat plane has a circular cylindrical portion with hemospherical ends. With respect to the dimensions given in Fgure 2, identical quantities as applied to this example are:

$$b^2 = \frac{L^2}{4} + LR\cos\phi + R^2 \,, \tag{5.10}$$

$$k_3{}^2 = \frac{\frac{8}{15}R^3 + \frac{3}{4}R^2L + \frac{1}{3}RL^2 + \frac{1}{12}L^3}{\frac{4}{3}R + L} \,, \tag{5.11}$$

and

$$\phi = \theta + \sin^{-1}\left(\frac{R\sin\theta}{L/2}\right). \tag{5.12}$$

Equations (5.10), (5.11) and (5.12) indicate that the parameter

$$\lambda = \left(1 + \frac{2k_3{}^2}{b^2}\right)^{-1} \tag{5.13}$$

is a function of L/R and ϕ. All dimensions and material constants are taken to be the same as those in Liu [9], namely L/R=5.0 and the ν = 0.28. For a rod at L/R=5.0, the inertia coupling parameter λ has a value in the range 0.48 to 0.63 and is dependent on θ. The extreme values of (e/d) and (d/c), as introduced by Smith and Liu [17] for a simplified analysis based on rigid body dynamics,have been defined to have maximum value for positive θ and minimum value for negative θ. The approach angle α^* for $(e/d)_{extr}$ or $(d/c)_{extr}$ has been found as

$$\tan\,\alpha^* = \frac{\mu(1+\lambda\cos2\theta) - \lambda\sin2\theta}{(1-\lambda\cos2\theta) - \mu\lambda\sin2\theta} \,,$$

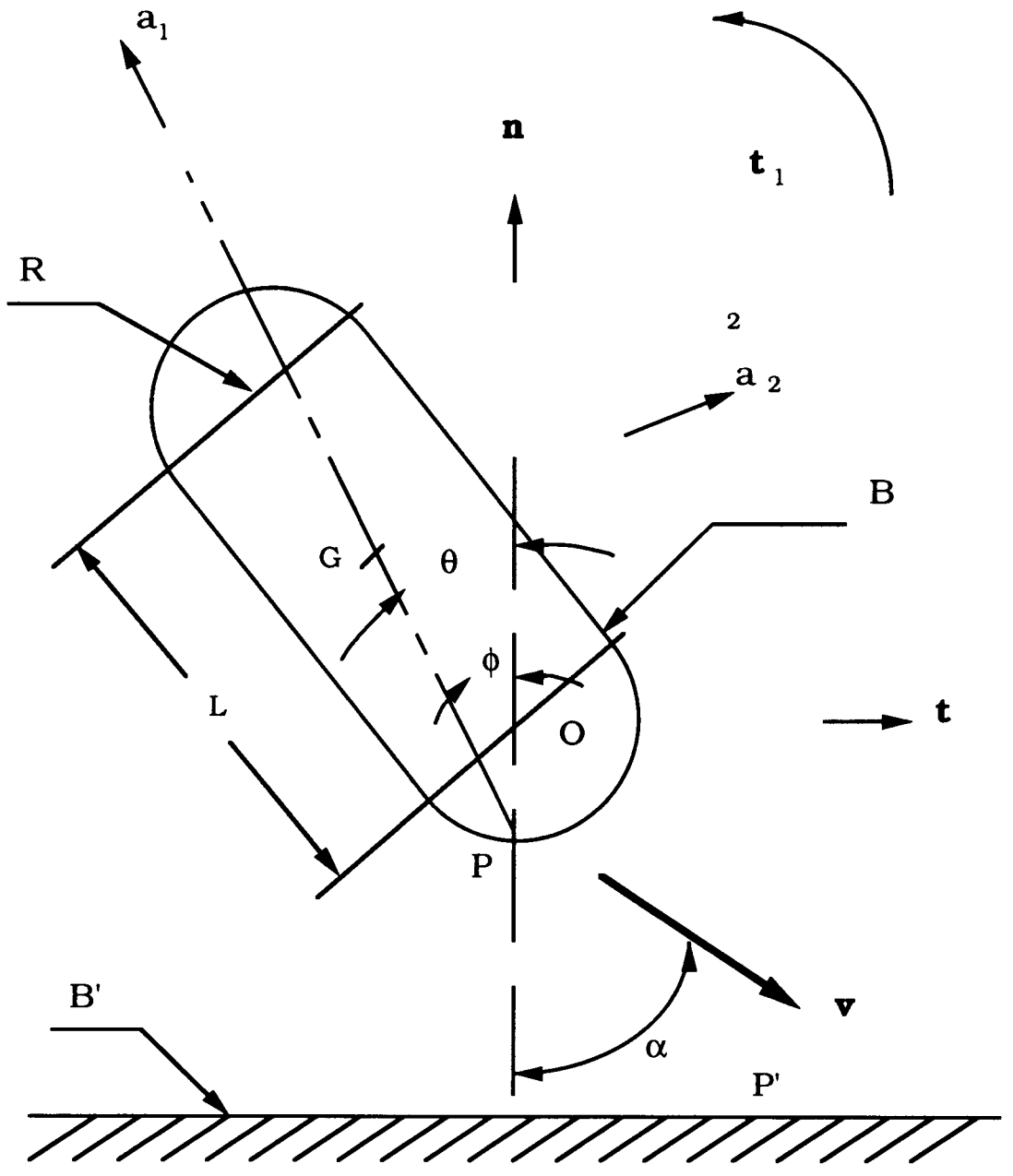

Figure 25. Collision between a cylindrical rod and a flat plane

where, for the value of α^*, initial slip stops at the end of compression phase and stick persists throughout the restitution phase.

The linear spring analysis for normal and tangential stiffness developed in Chapter 4 has been applied to this example. By trial and error to the incident angle α, for the coupling parameters λ and θ and various coefficients of friction μ, extreme values of e ($w_n/-v_n$) have been determined and plotted in Figure 26 for the range $-\pi/2$ to $\pi/2$ for θ. The first coefficient of restitution c, ratio of normal impulse during compression to restitution, has a value less than one for positive θ and greater than one for negative θ. The coefficient of restitution e has a value greater than one for certain circumstances, and is dependent upon the inertia coupling parameter λ and θ, the angle of incident velocity α, and the friction coefficient μ. This implies that the second definition of the coefficient of restitution is not a material constant for elastic collisions. As the coefficient of friction has a larger value, extreme values of e become higher for the maximum value and lower for the minimum value. From Figure 27, it also is shown that the ratio of incident velocity ($\tan \alpha = v_t/-v_n$) is less than or equal to the value of $\tan \alpha^*$ for the entire range of θ.

In table 2 and 3, the results of eight cases for the extreme values of e are examined, and a number of plots for impulse, contact force, displacement, velocity at contact point and work done during impact for cases A, C, A' and C' are shown in Figures 28 to 43. The losses of kinetic energy are also computed using equations (5.4) and (5.5). According to the simplified prediction [9,17] there is a sudden change to the opposite direction in the tangential and normal impulse.

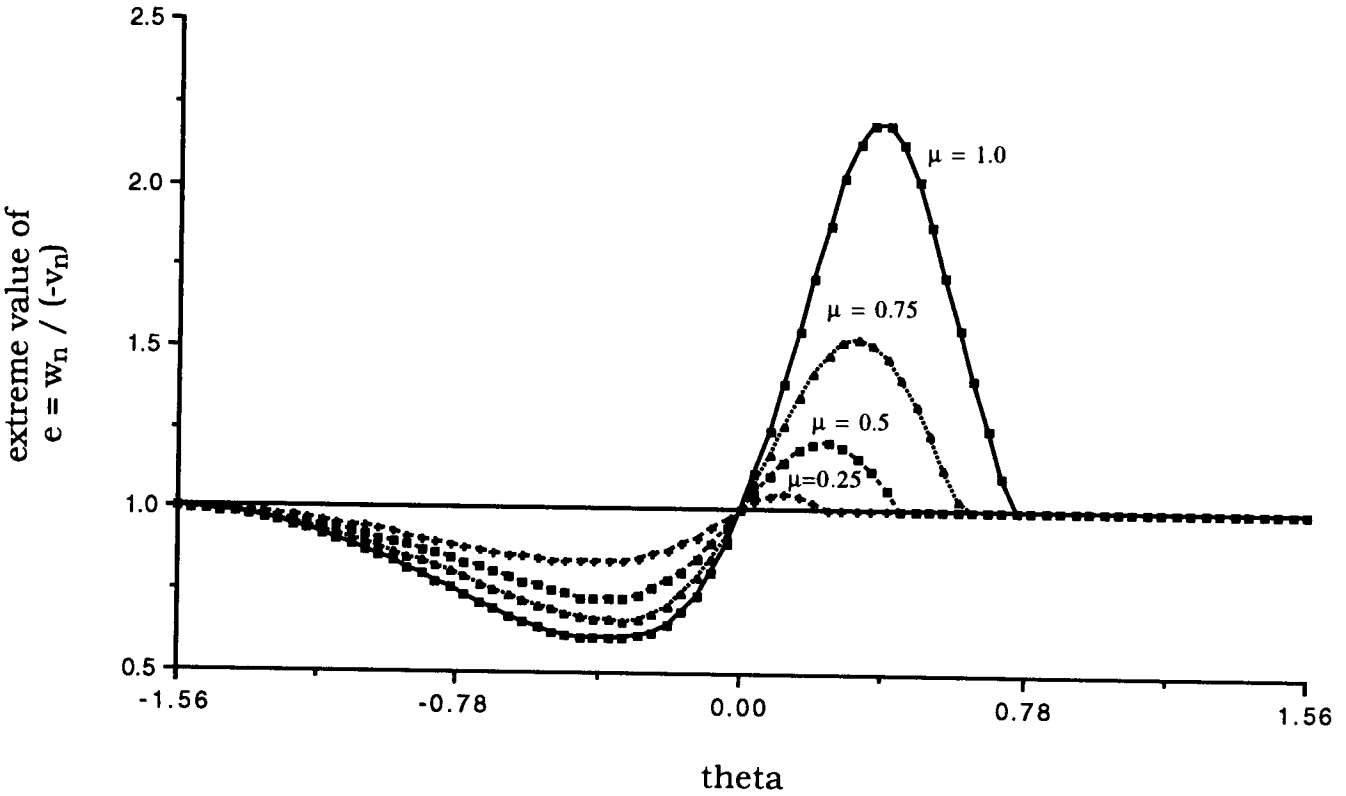

Figure 26. Extreme value of coefficient of restitution for bar with L/R = 5.0

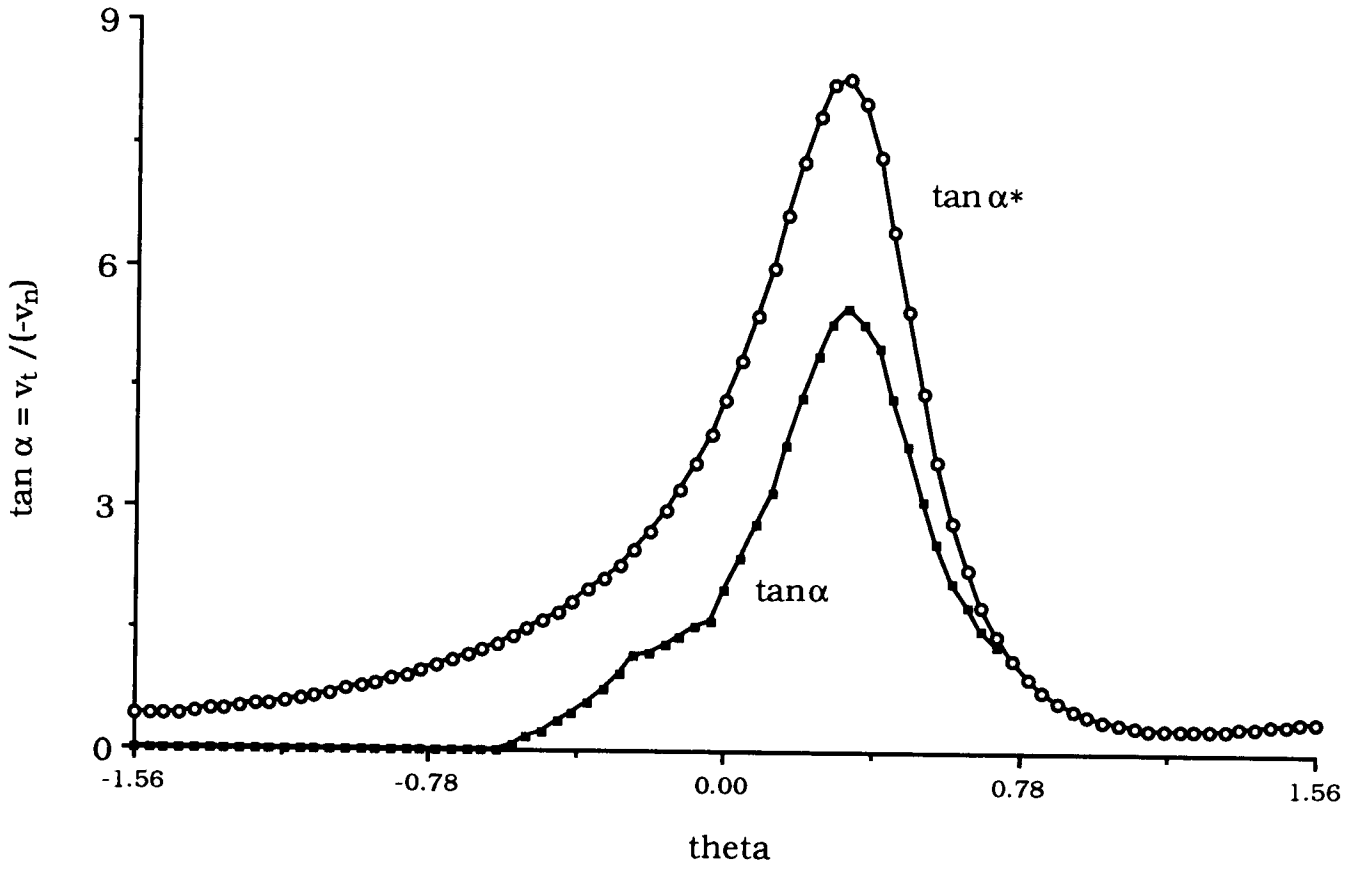

Figure 27. Ratio of incident velocity $v_t/-v_n$, tanα, for extreme value of e with friction coefficient μ=1.0

Table 2. Maximum value of e for various friction coefficients

CASE	A	B	C	D
μ	1.0	0.75	0.5	0.25
λ	0.614	0.618	0.622	0.626
θ	0.38	0.32	0.24	0.12
tan α	5.177	2.066	1.030	0.460
c	0.628	0.807	0.940	0.973
d	0.990	0.990	0.989	0.989
e	2.202	1.531	1.213	1.051
$\Delta K/\lvert\Delta K\rvert_{max}$	-0.603	-0.425	-0.115	-0.051

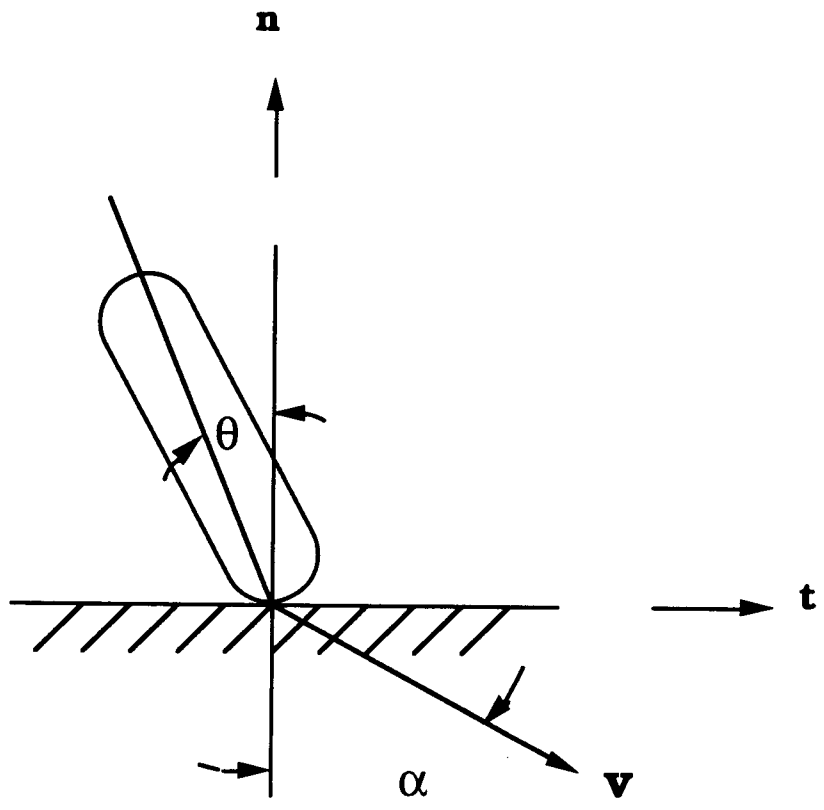

Table 3. Minimum value of e for various friction coefficients

CASE	A'	B'	C'	D'
μ	1.0	0.75	0.5	0.25
λ	0.614	0.618	0.615	0.611
θ	-0.38	-0.32	-0.36	-0.42
tan α	0.508	0.877	0.630	0.495
c	1.240	1.231	1.159	1.105
d	0.988	0.987	0.987	0.986
e	0.606	0.657	0.724	0.837
$\Delta K/\lvert\Delta K\rvert_{max}$	-0.687	-0.570	-0.477	-0.299

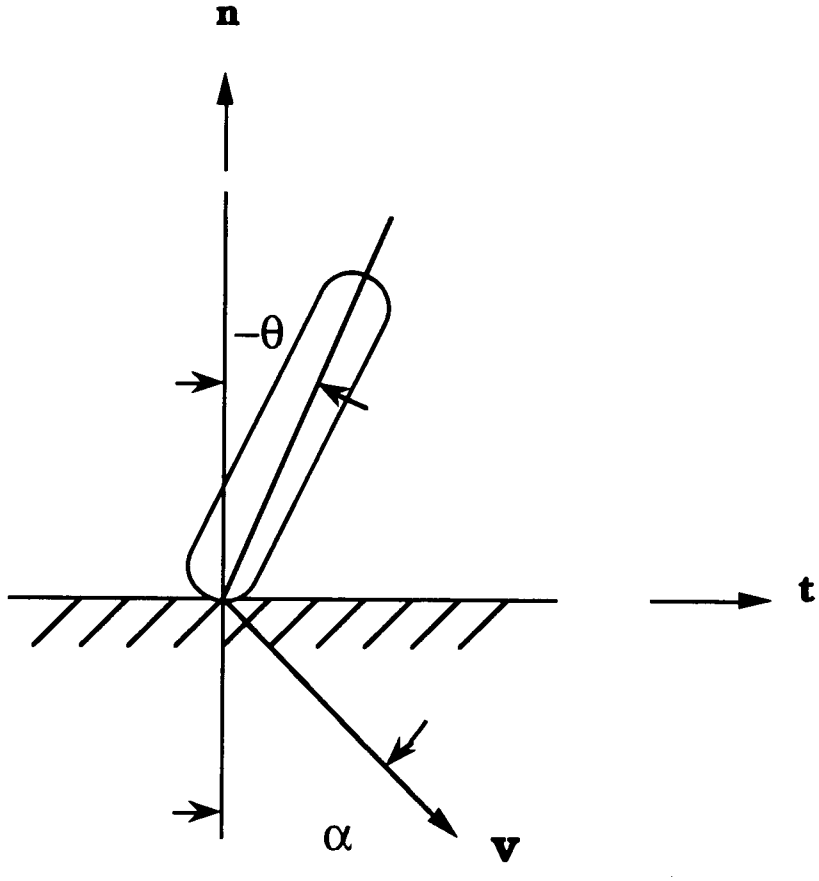

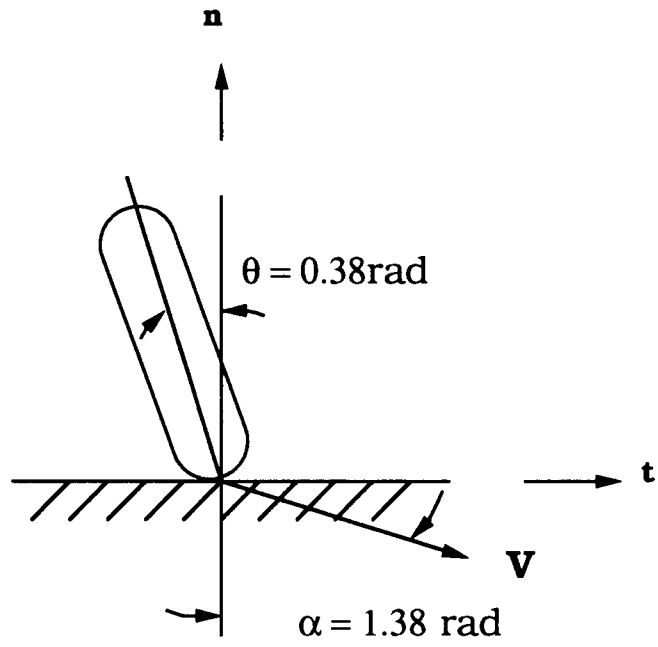

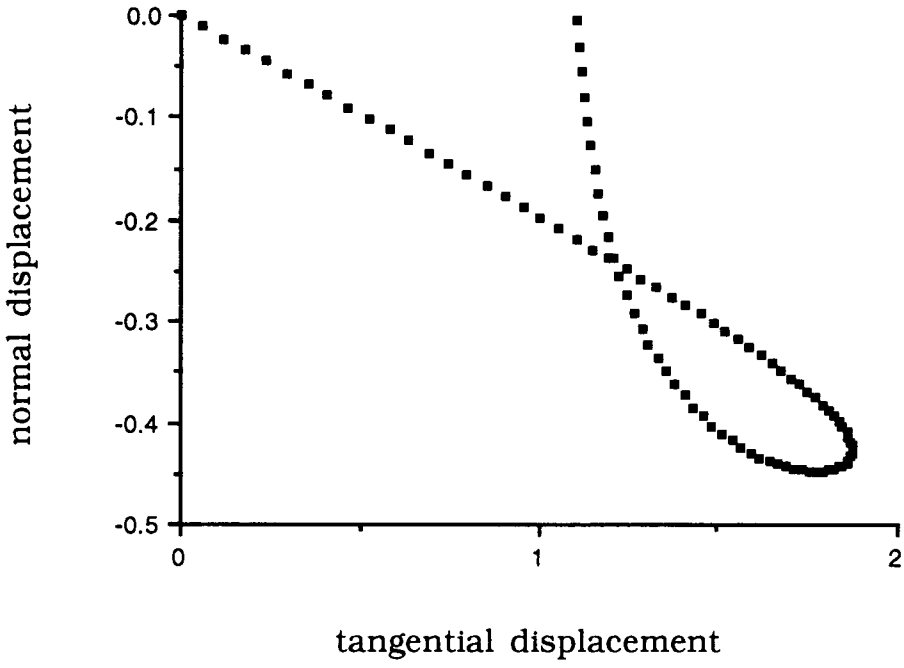

Figure 28. Nondimensional tangential and normal displacement for case A

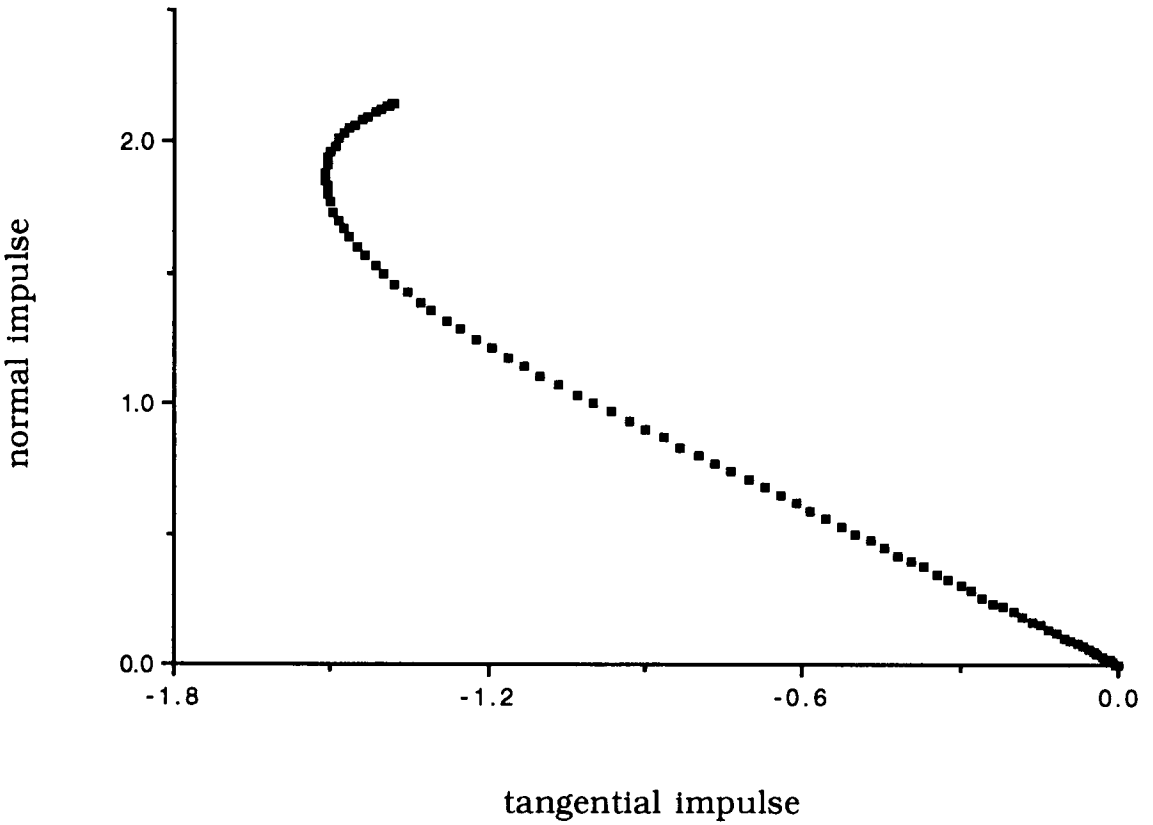

Figure 29. Nondimensional tangential and normal impulse for case A

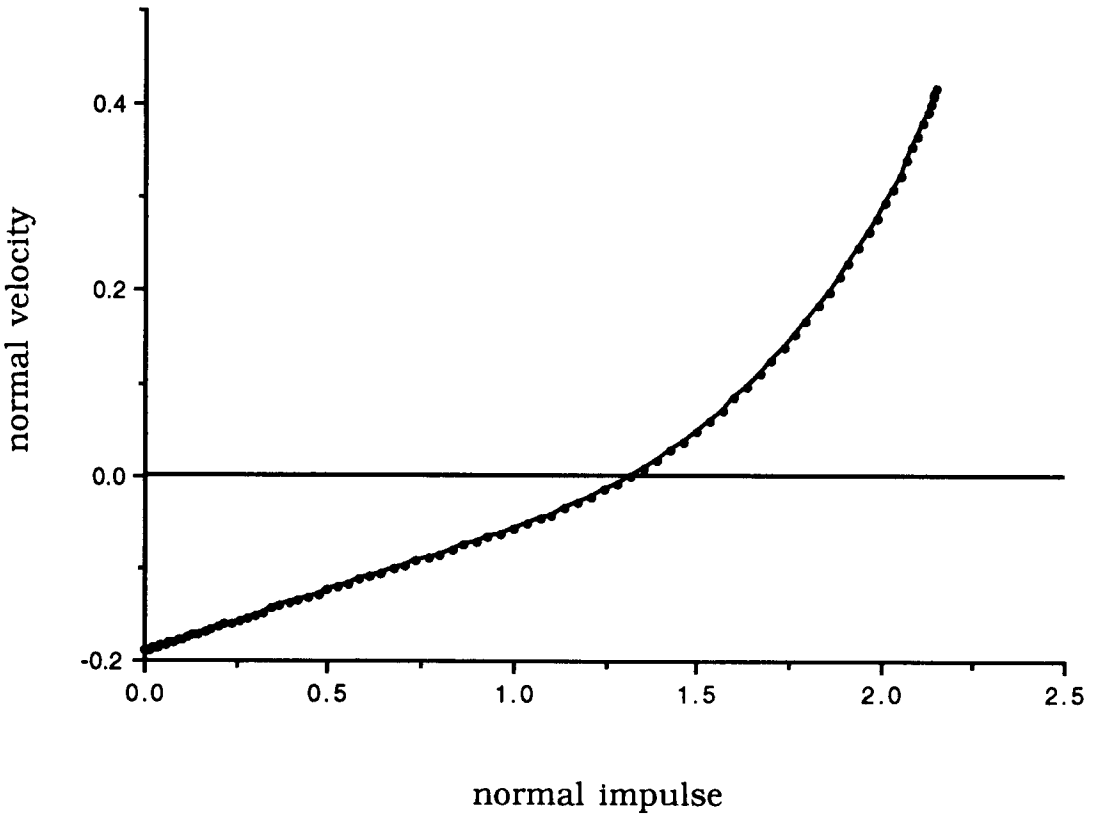

Figure 30. Nondimensional normal impulse and normal velocity for case A

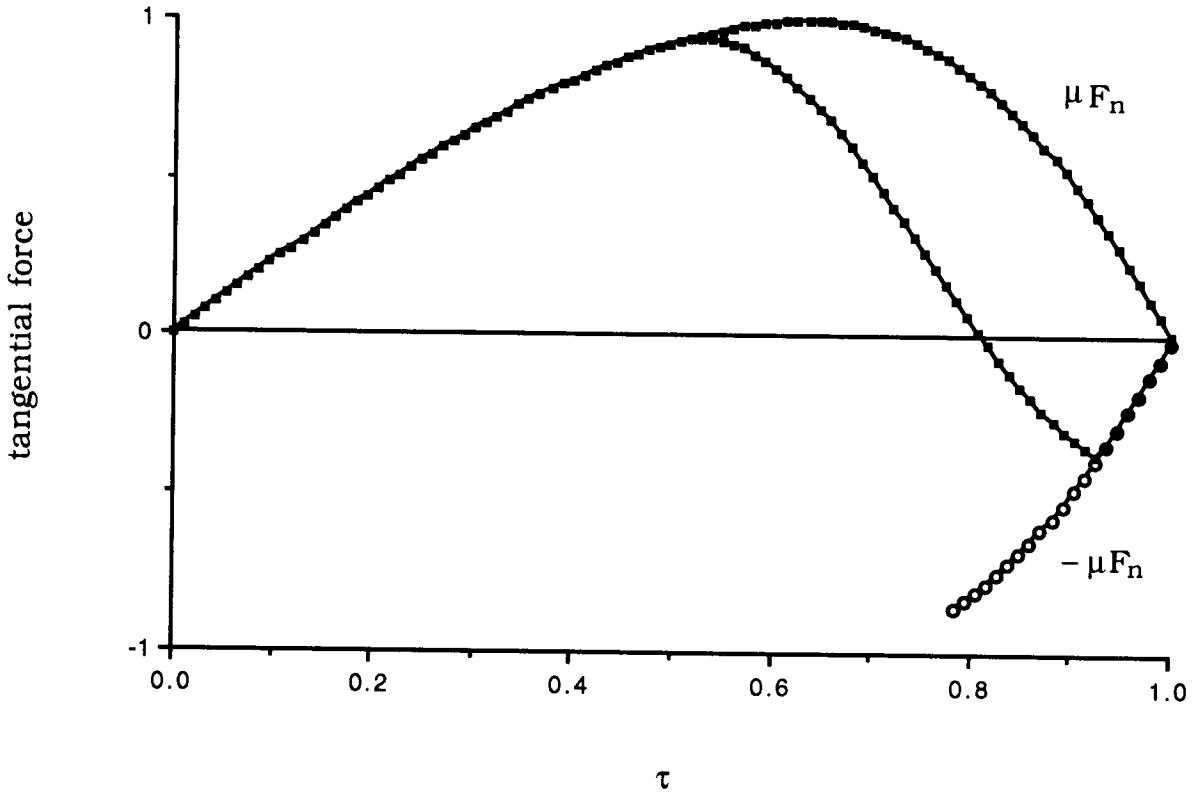

Figure 31. Nondimensional tangential force during impact for case A

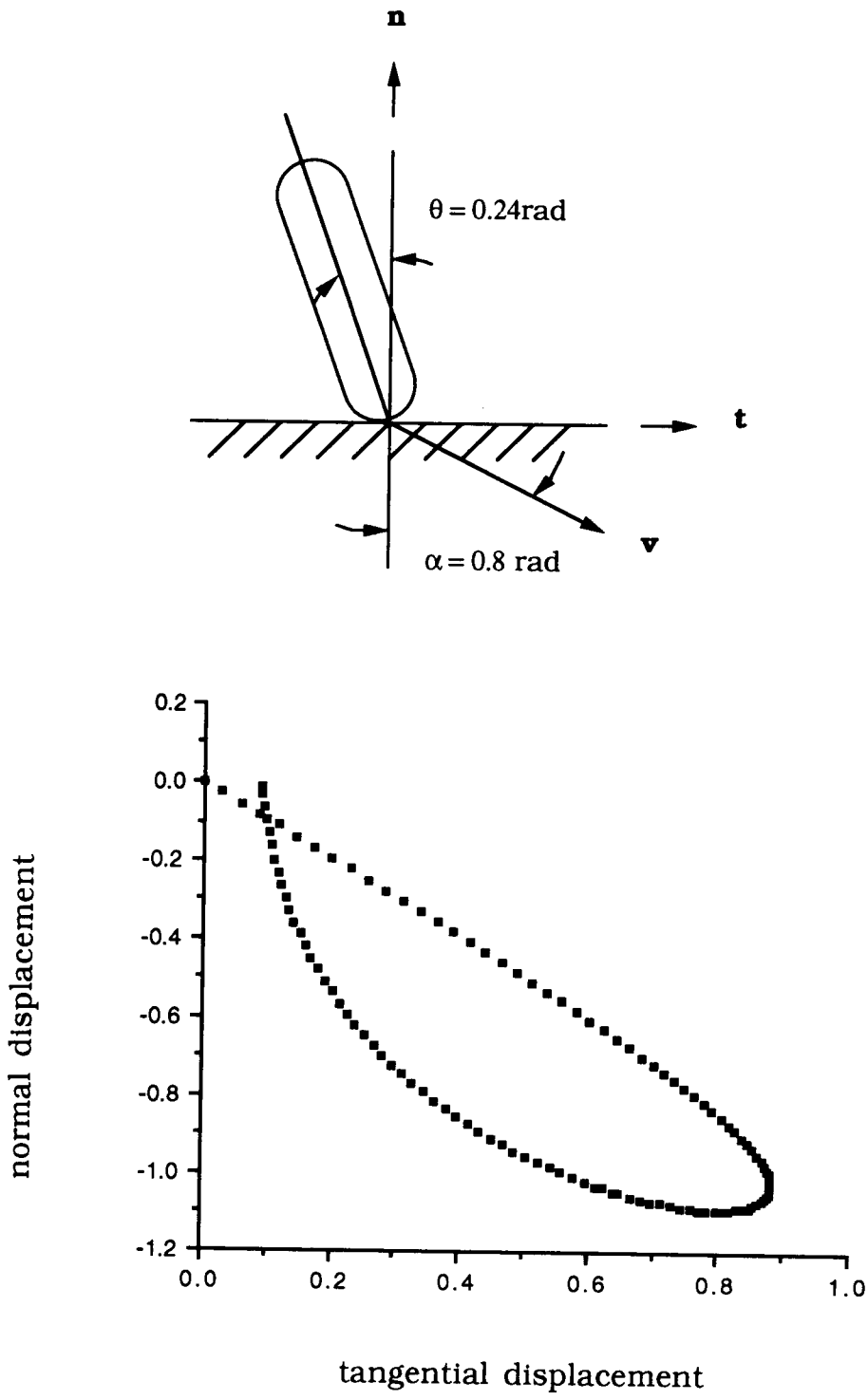

Figure 32. Nondimensional tangential and normal displacement for case C

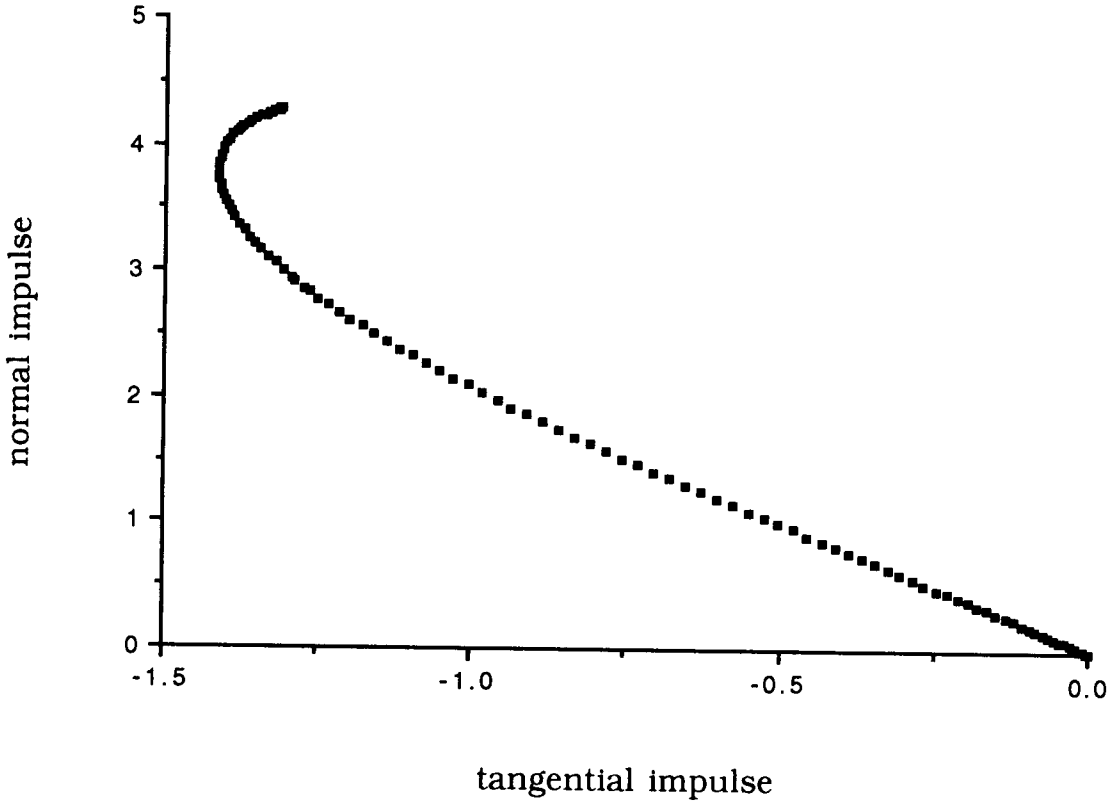

Figure 33. Nondimensional tangential and normal impulse for case C

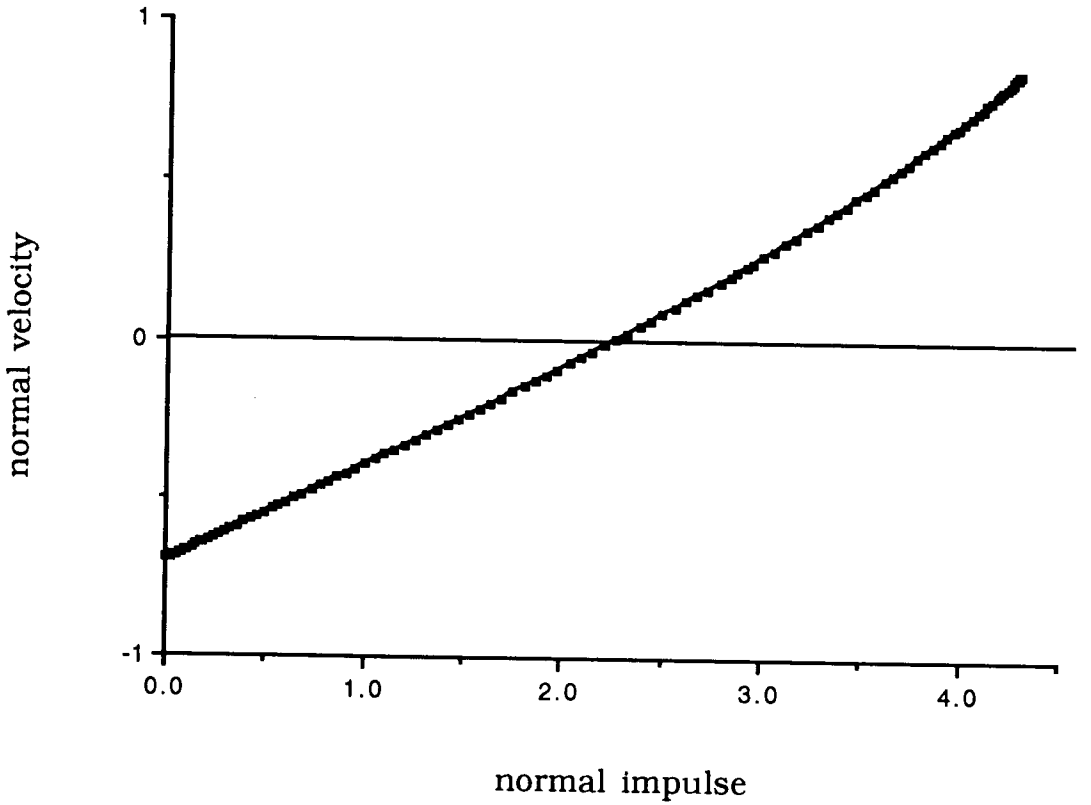

Figure 34. Nondimensional normal impulse and normal velocity for case C

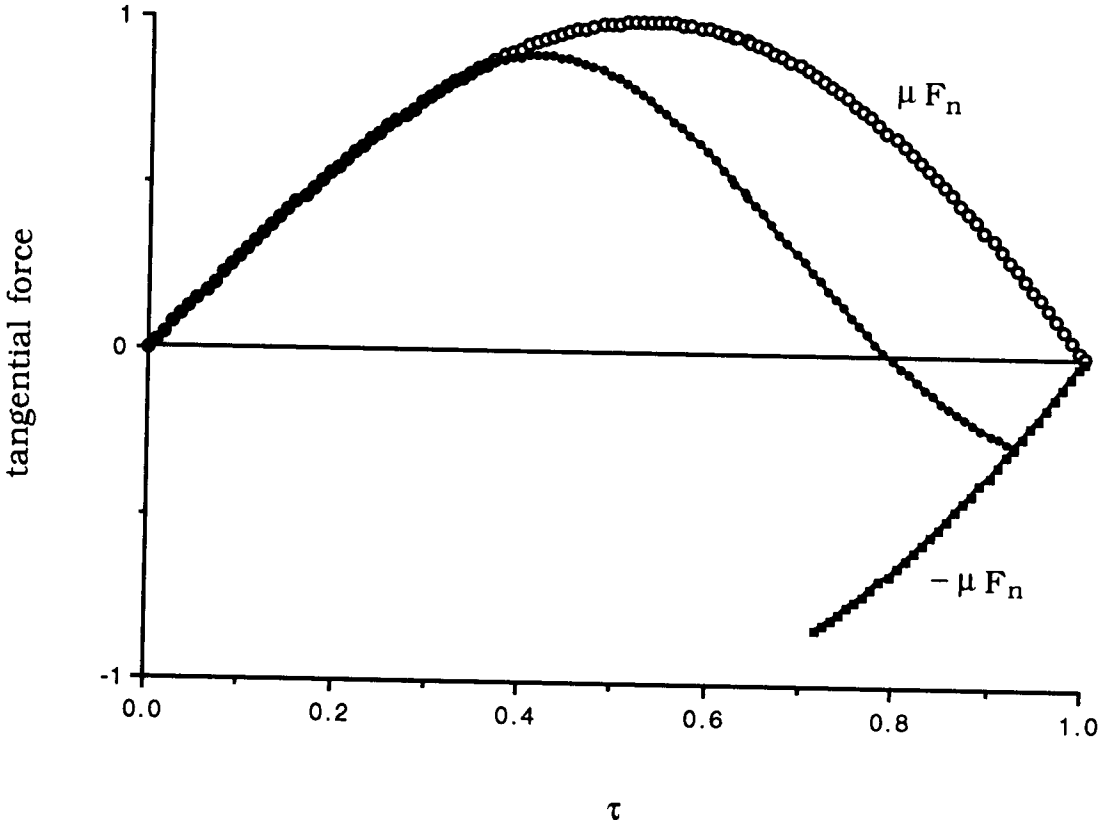

Figure 35. Nondimensional tangential force during impact for case C

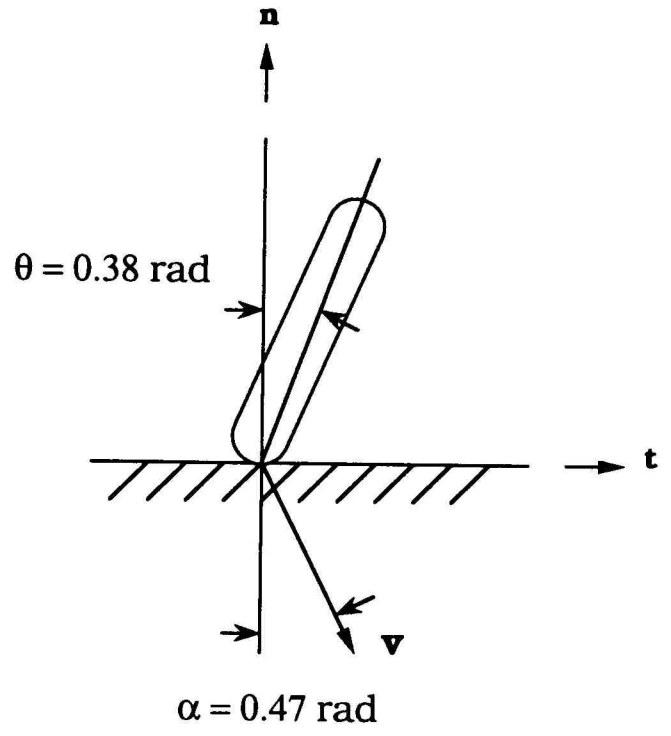

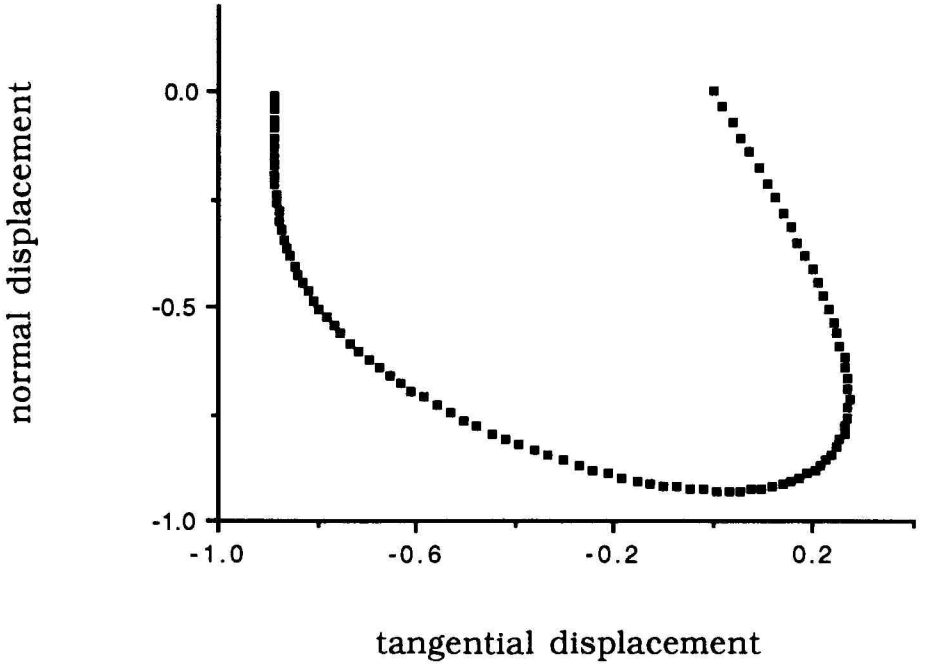

Figure 36. Nondimensional tangential and normal displacement for case A'

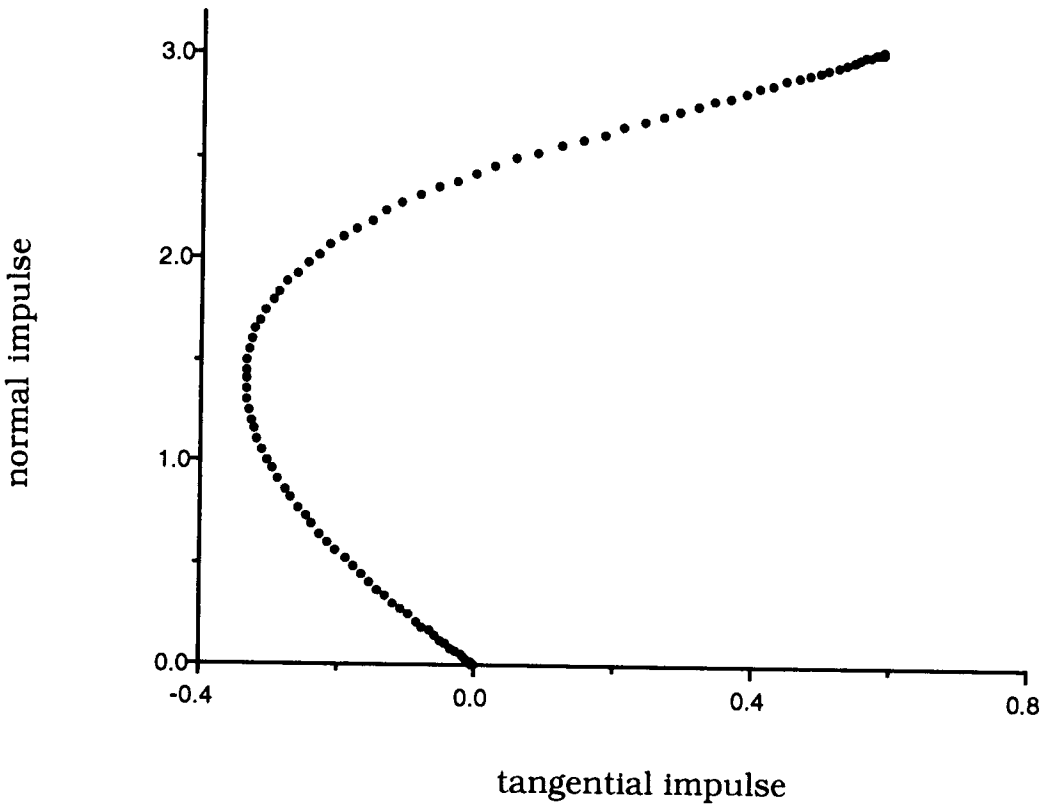

Figure 37. Nondimensional tangential and normal impulse for case A'

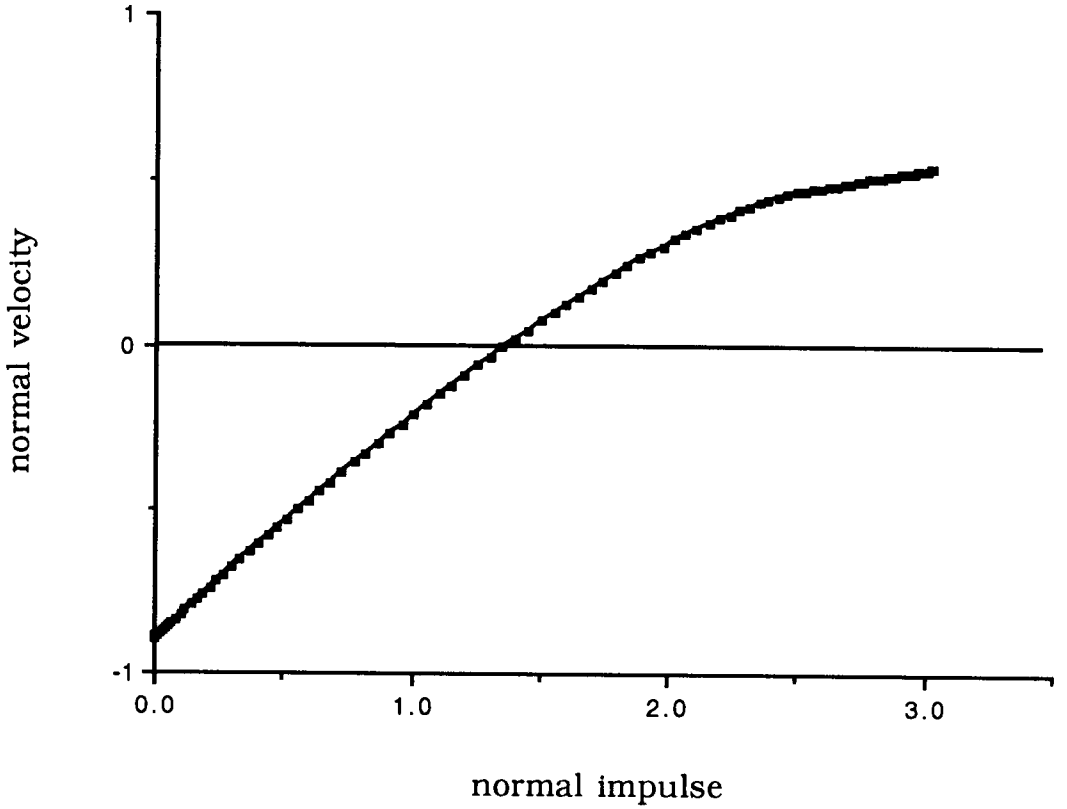

Figure 38. Nondimensional normal impulse and normal velocity for case A'

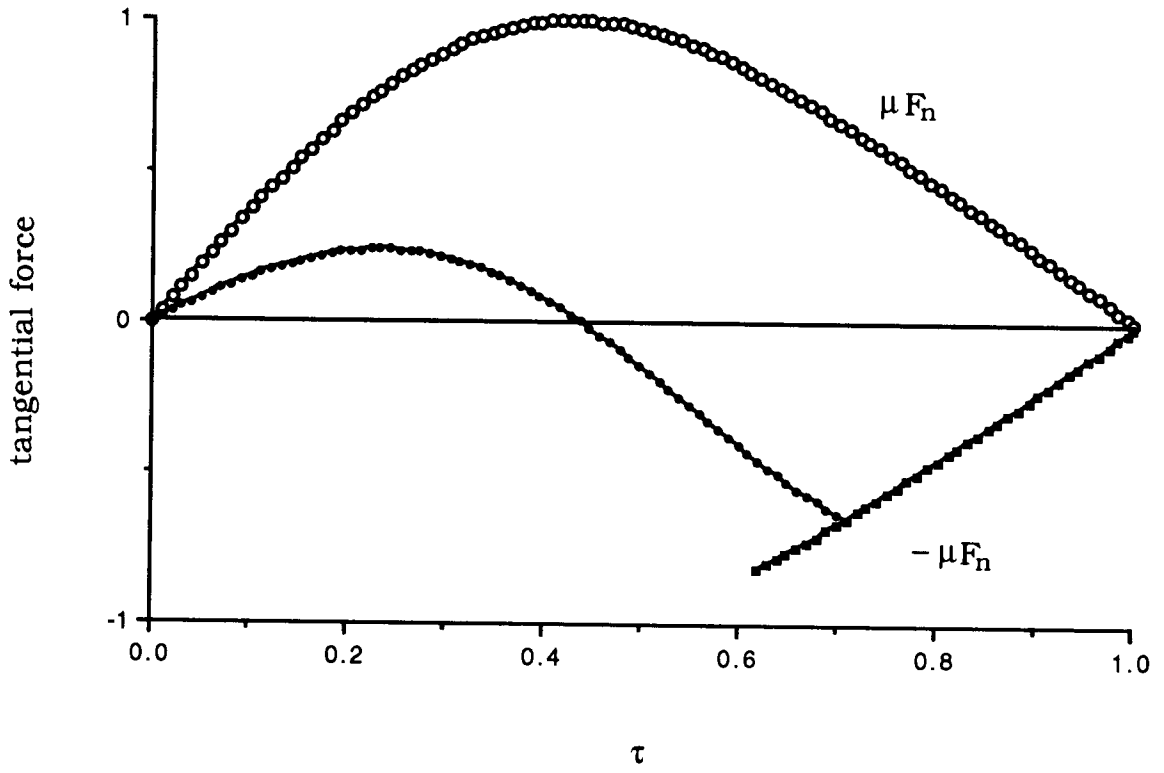

Figure 39. Nondimensional tangential force during impact for case A'

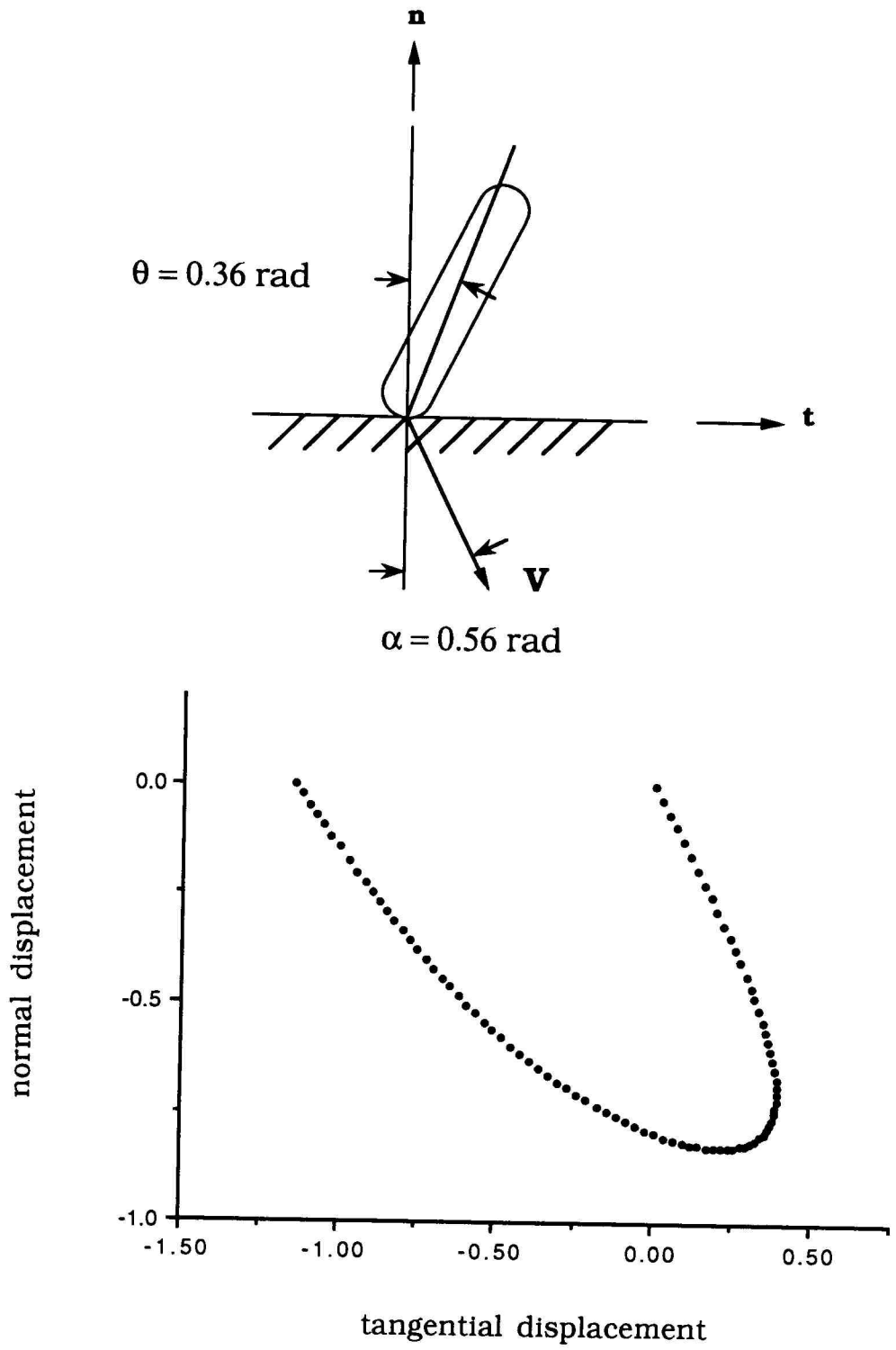

Figure 40. Nondimensional tangential and normal displacement for case C'

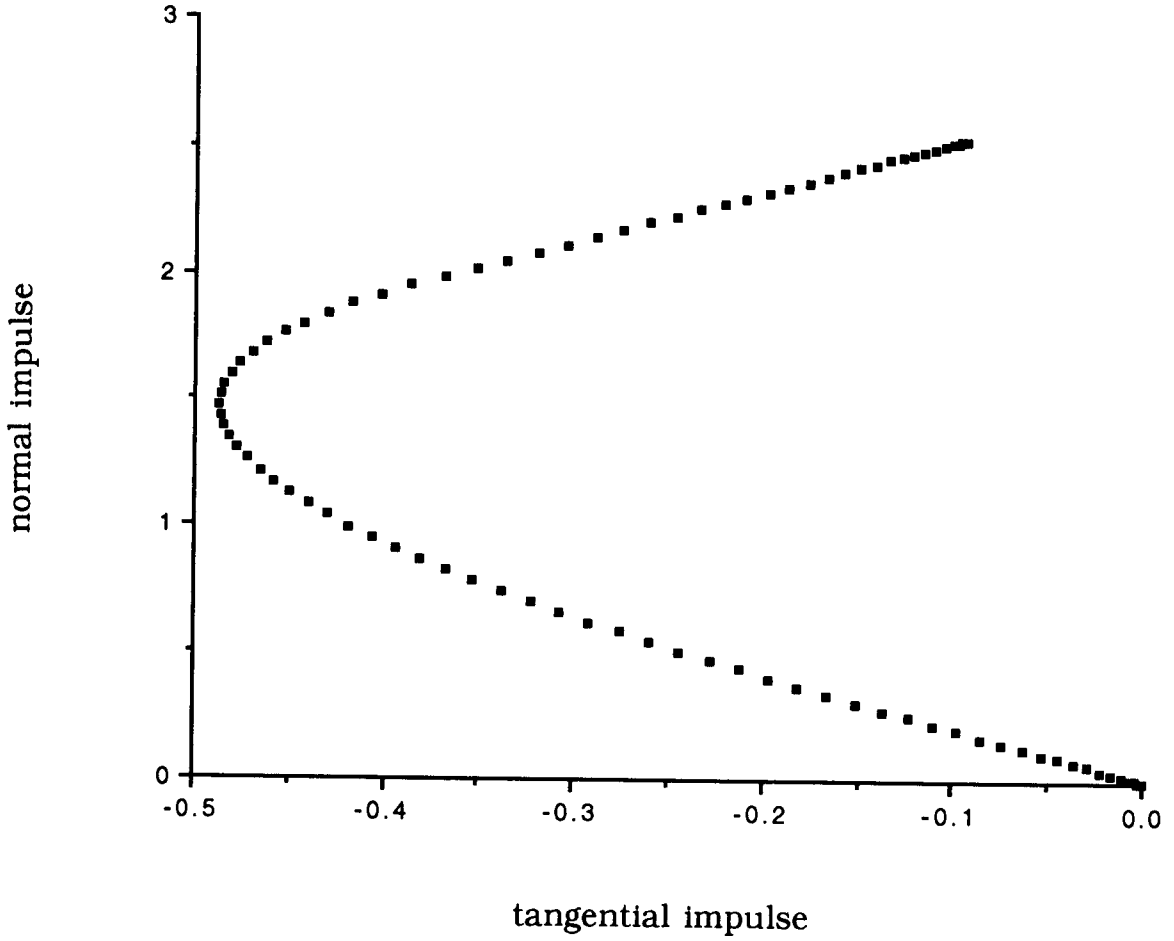

Figure 41. Nondimensional tangential and normal impulse for case C'

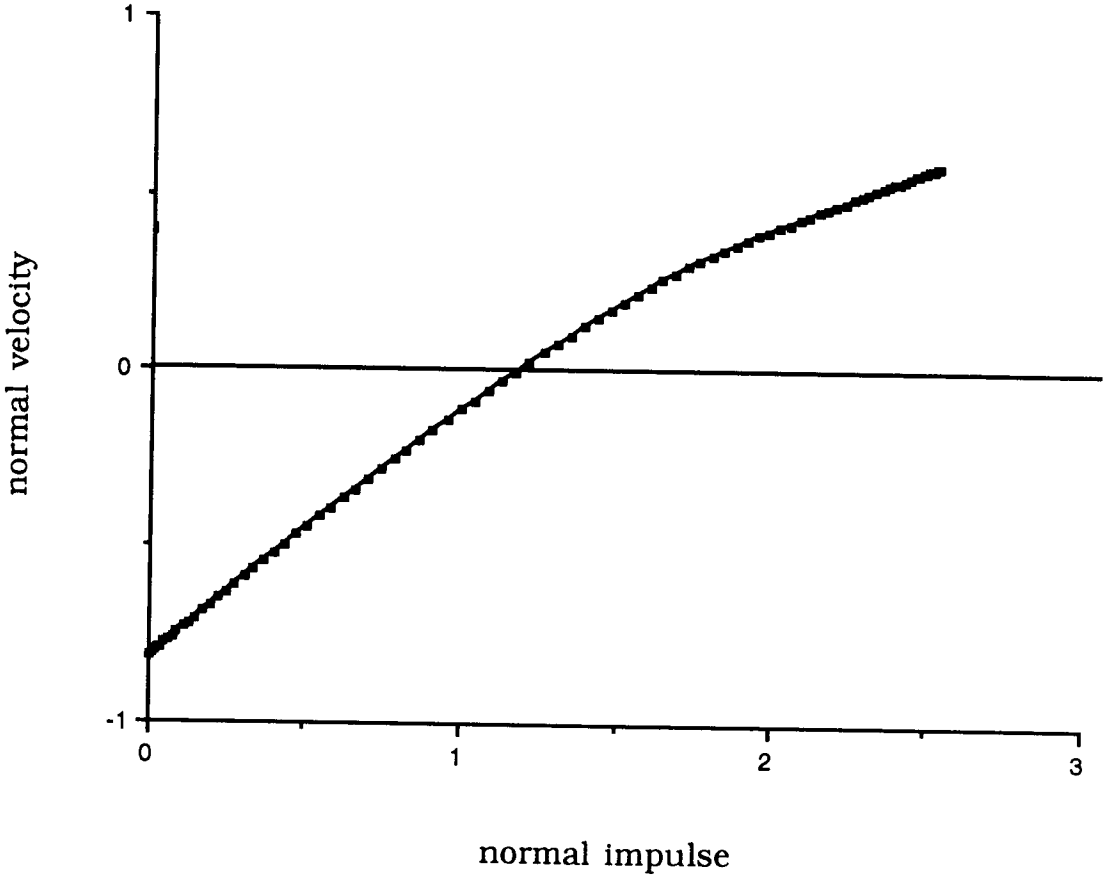

Figure 42. Nondimensional normal impulse and normal velocity for case C'

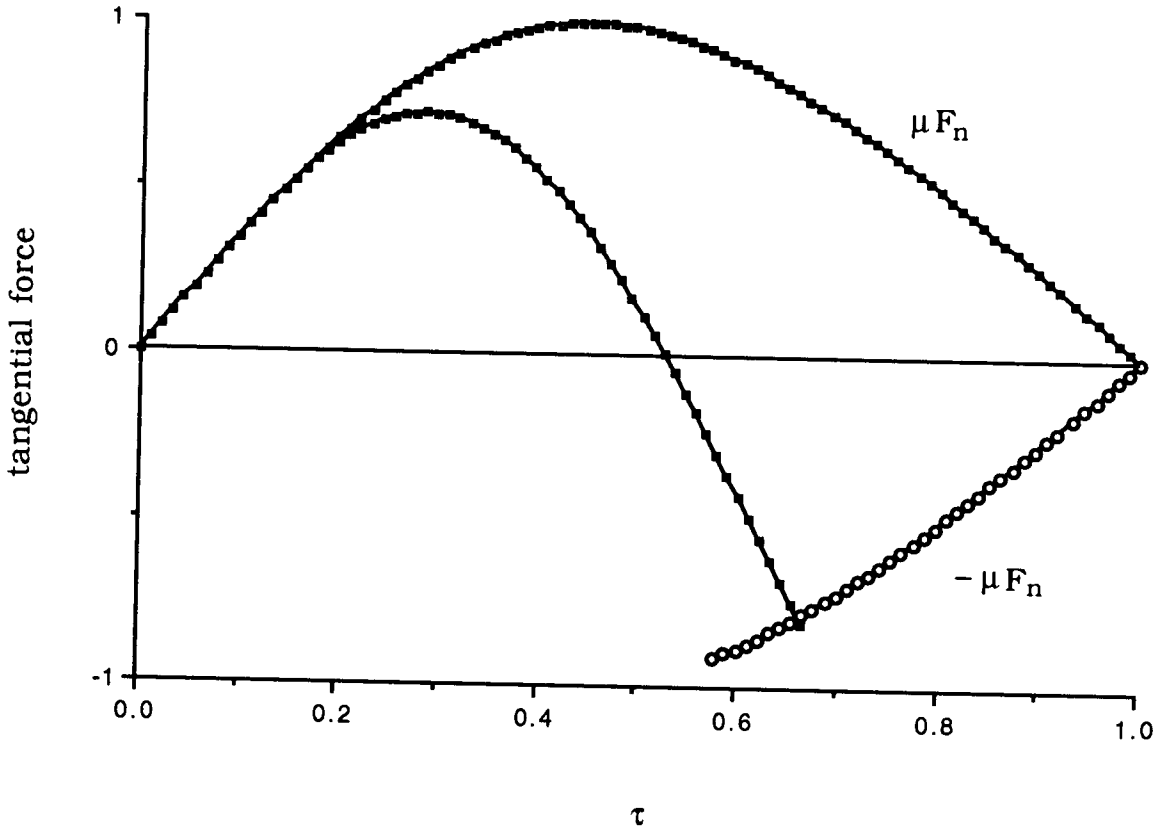

Figure 43. Nondimensional tangential force during impact for case C'

There are no abrupt changes in tangential and normal impulse for the linearized spring system during impact. Trajectories are similar to those from ANSYS code [9] for maximum e in positive θ, but there are some discrepancies for minimum e in negative θ. The value of the third definition of the coefficient of restitution d, the ratio of work of the normal force during compression to that during restitution, is close to unity for all cases. As may have been expected, based upon the assumption of elastic material, there is no energy dissipation in the normal direction. The coefficient of restitution d is more consistent and could be accepted as representation of the concept of energy conservation.

Different values for the inertia coupling parameter λ are investigated and plotted for various coefficients of friction in Figures 44 and 45. Results indicate that the higher the inertia coupling of colliding bodies, the greater the coefficient of restitution e. For the inertia coupling parameter λ=0.8 in Figure 45, the maximum value of e exceeds three, whereas the minimum value is zero (i.e., there is no rebound in normal direction). At λ = 0.8, the maximum incident angle α has been limited to 1.4 rad (80.2°) since the ratio of rebound of normal velocity has excessive high theoritical value for the incident angle approaching 90° and with $0.2 < \theta < 0.6$ and μ=1.0 and 0.75. Any approach angle in excess of 80° is unusual and meaningless in practice. In general, the coefficient of restitution e is highly dependent upon the inertia coupling parameters λ and θ, the angle of incident velocity α, and the friction coefficient μ.

Results from the coupled spring method also are shown in

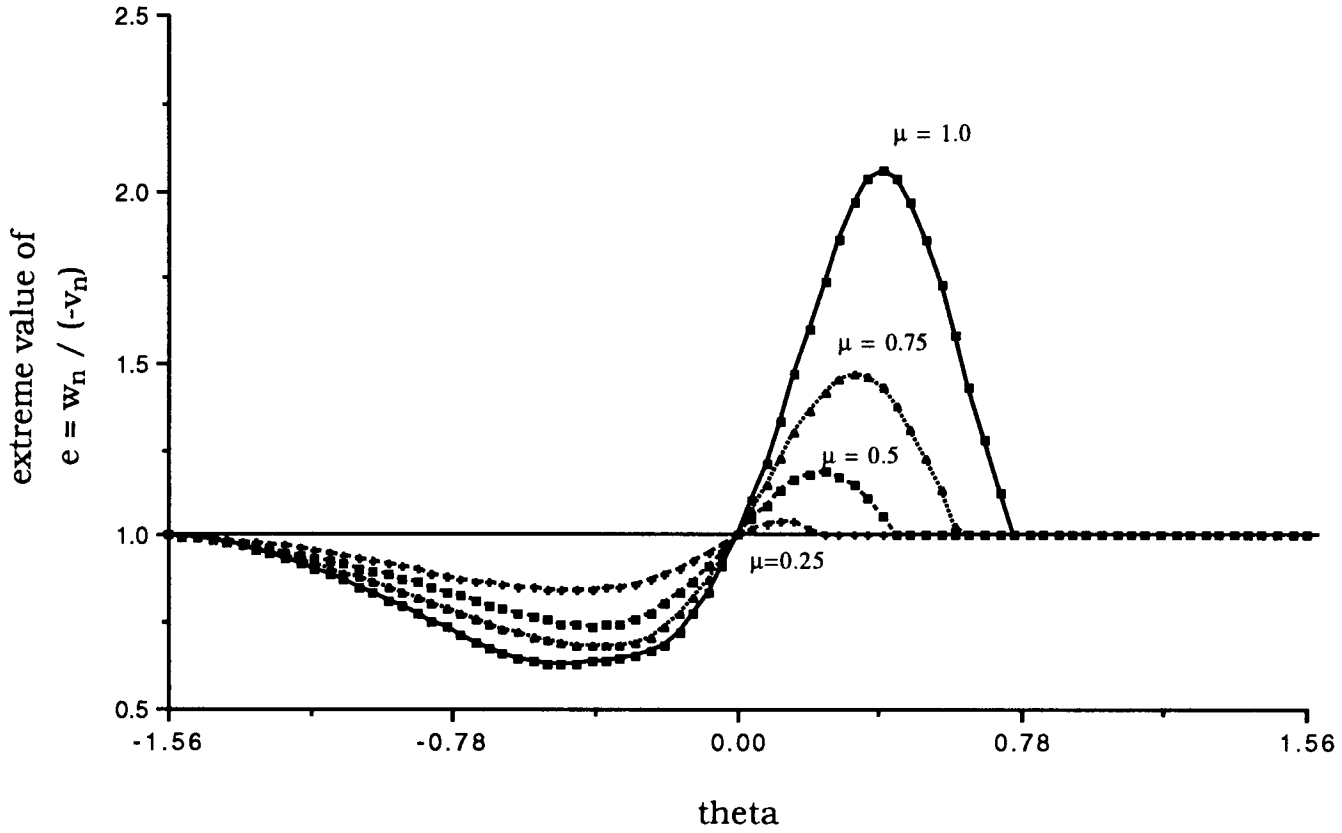

Figure 44. Extreme value of coefficient of restitution e for λ=0.6 by analysis of linear spring

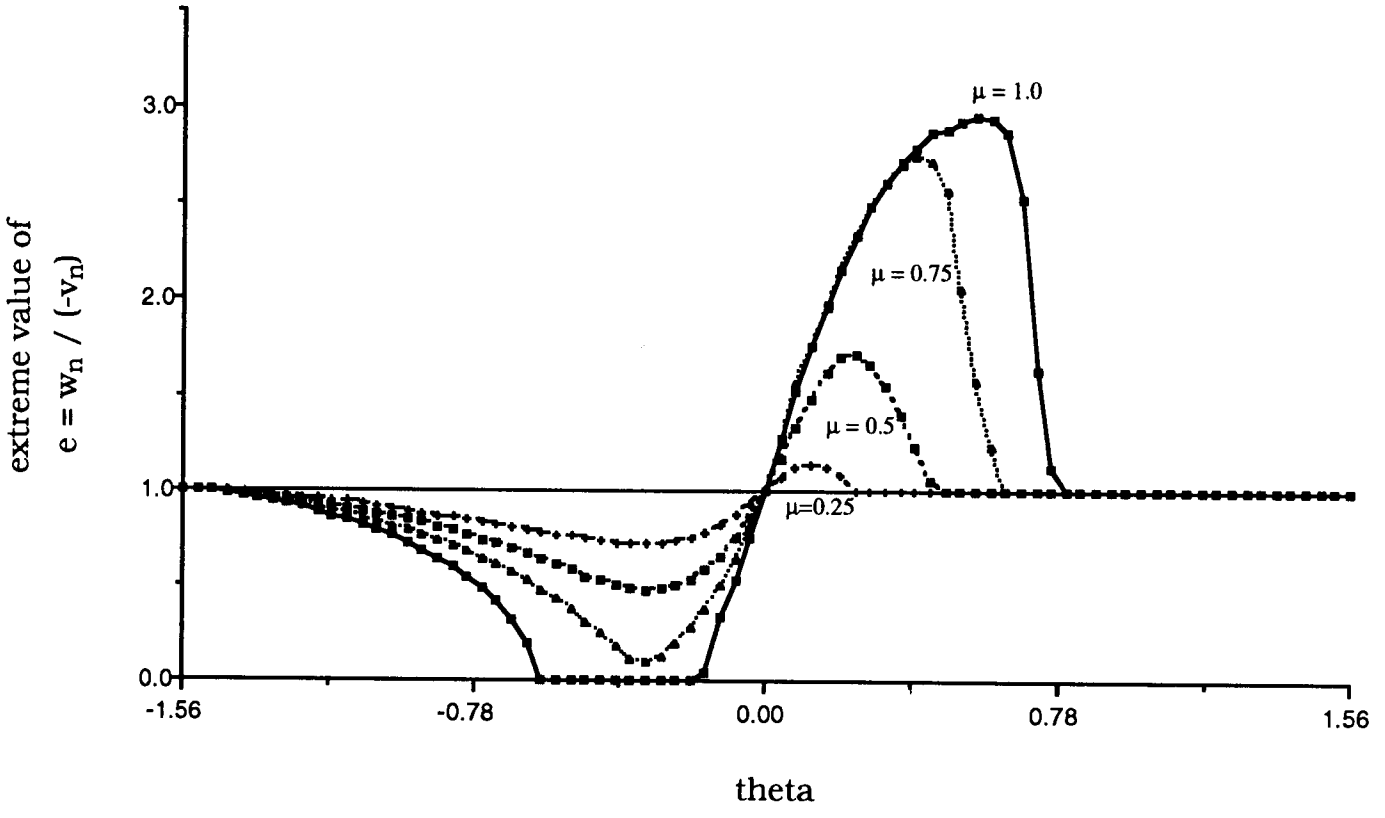

Figure 45. Extreme value of coefficient of restitution e for λ=0.8 with maximum approach angle α=1.4 rad. by analysis of linear spring

Figures 46 and 47. Compared to the analysis for the linear spring method, there is little discrepancy in the values for the coefficient of restitution e. For given friction coefficient 0.75 and the coupling inertia patameter $\lambda = 0.6$, results for all three methods are plotted in Figure 48. Even though these results are in close agreement, there may be different input values for incident velocity ($\tan \alpha = v_t/-v_n$) for most of the range of θ.

The Poisson ratio ν, as the material constant, has been examined to determine its effect on impact motion in cases A and A' shown in Figure 49 The smaller value of Poisson ratio for colliding bodies is, the greater will be the extreme values of e. However, this difference is not significant for all ranges of the Poisson's ratio ν from 0.0 to 0.5.

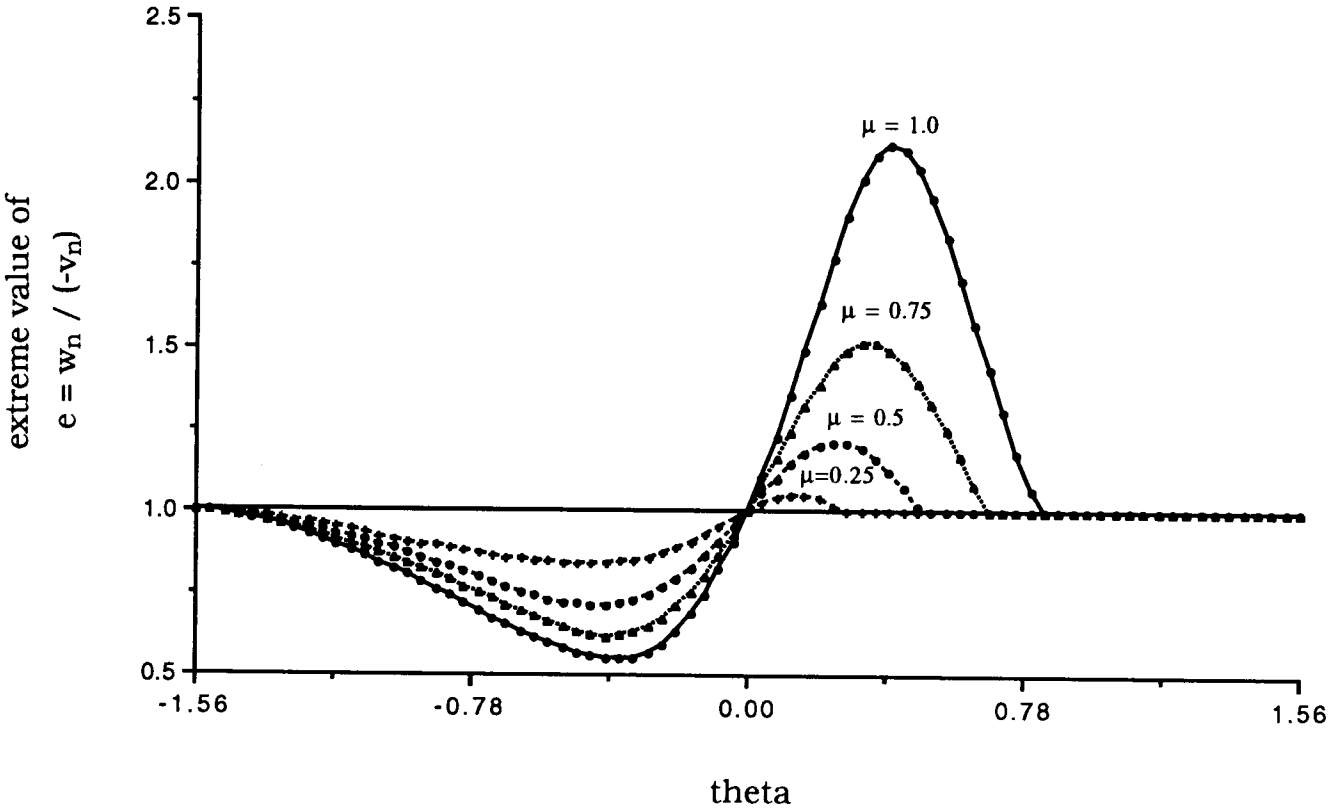

Figure 46. Extreme value of coefficient of restitution e for λ=0.6 by analysis of coupled spring

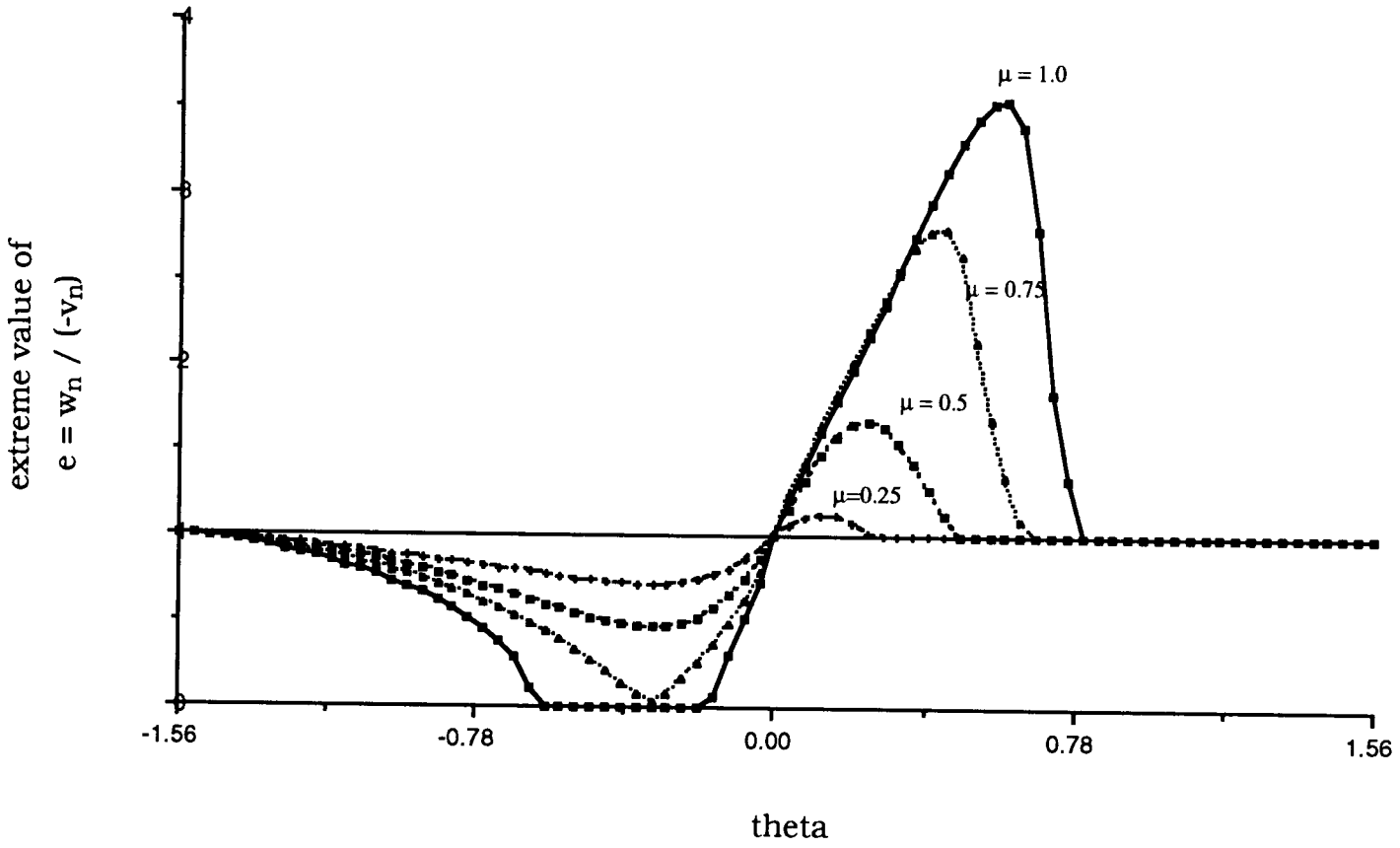

Figure 47. Extreme value of coefficient of restitution e for λ=0.8 with maximum approach angle α=1.4 rad. by analysis of coupled spring

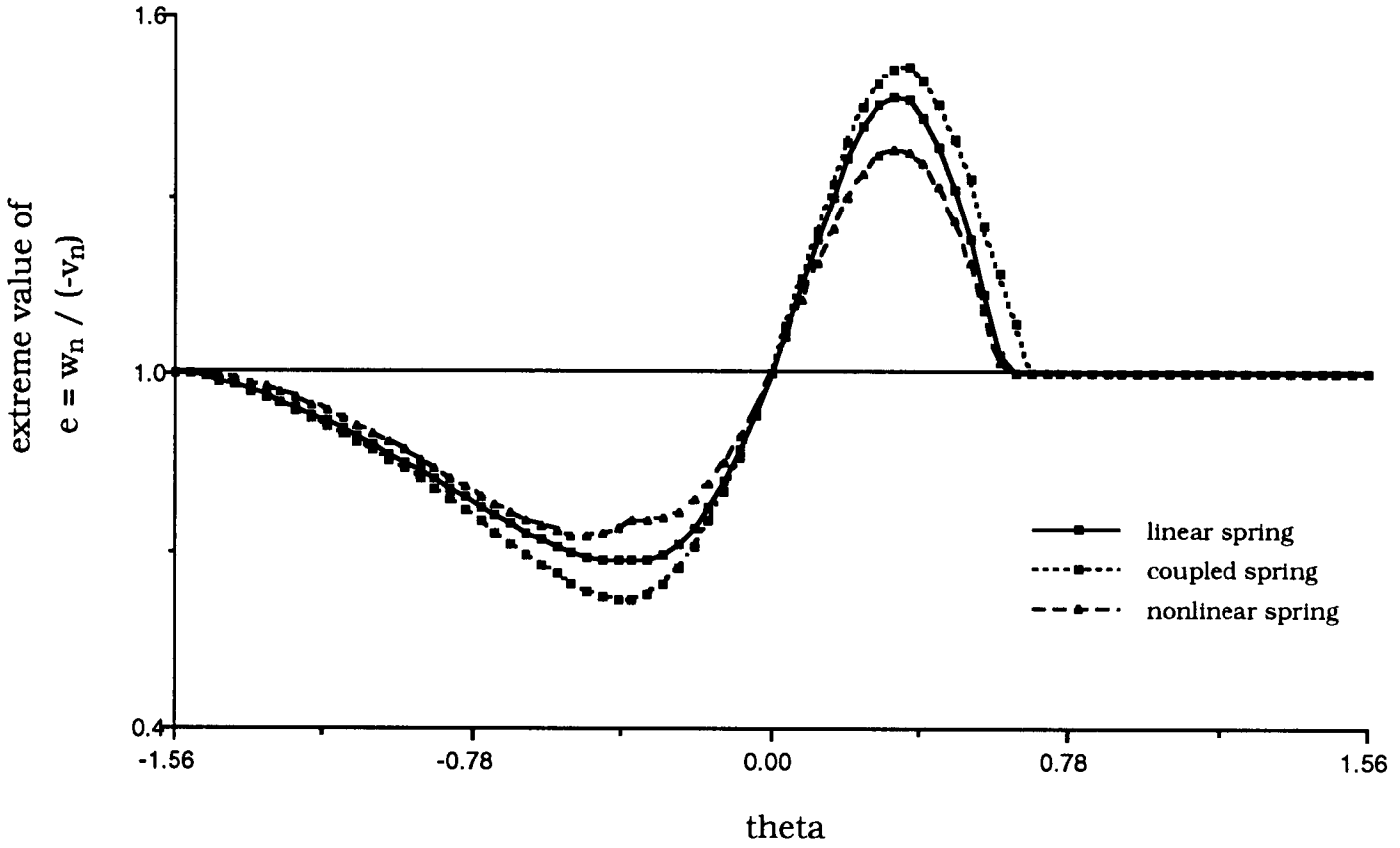

Figure 48. Extrem values of e from three modelling of spring for λ=0.6 with friction coefficient μ=0.75

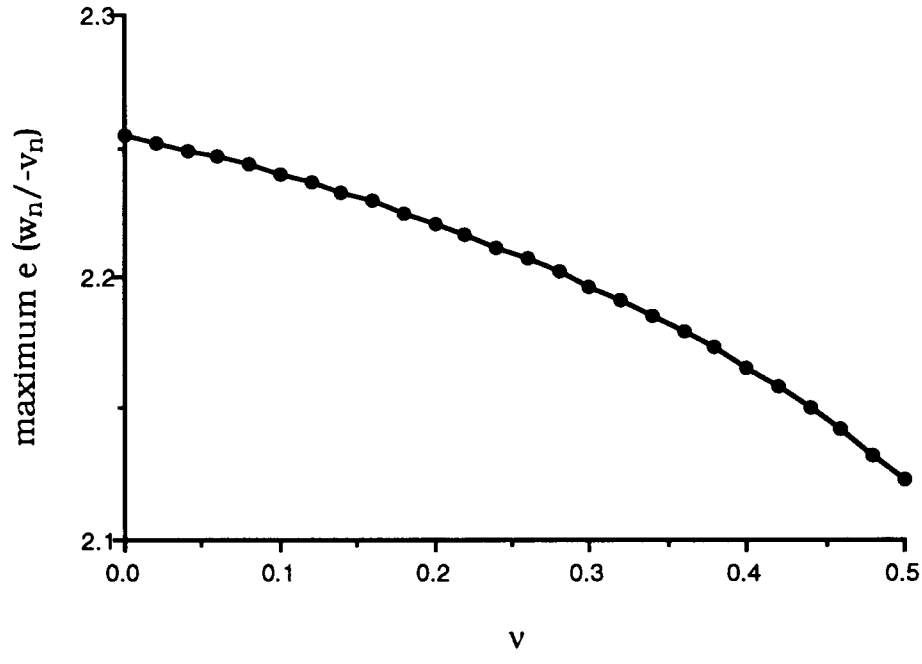

(a)

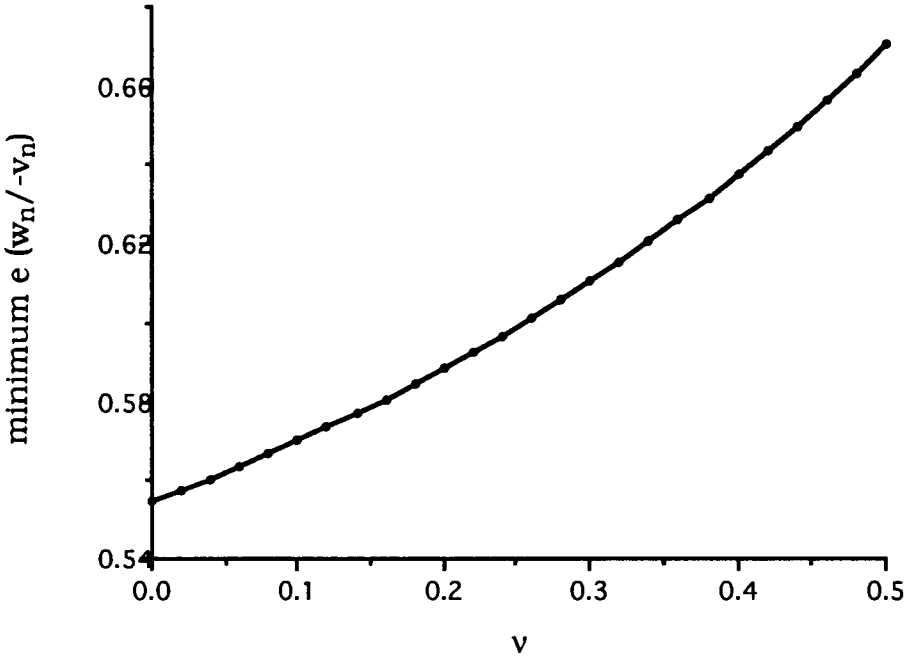

(b)

Figure 49. Extreme value of e for various Poisson's ratio: (a) for case A (b) for case A'

6. SUMMARY AND DISCUSSION

Analysis of collision is improved by the consideration of the elastic deformations at contact surface of the bodies concerned and is further simplified by application of the concept of the "spring" which represent the deformation on elastic half-space. Herzt theory for normal contact and other contact mechanics for tangential friction, which originally are developed for stactic loading, have been applied for the analysis of elastic collision in quasi-static sense. Post-collision motions of mechanical systems could be predicted from spring-mass vibrating system with appropriate friction analysis. There can be little doubt that the spring-mass system constitutes the most simple model for complex elastic collisions without sacrifying an accuracy even when tangential compliance is irreversible and dependent on actual past loading conditions. As obseved from the example problems, all trajectory can be monitored throughout even short duration of impact entirely.

Even though Maw has developed a numerical method which included consideration of tangential deformations, and verified this method through experimental results, the approach was confined to collisions of sphere. Thus the present approach constitutes an effort to analyze the impact motions for general configurations analytically. It was determined that for given Poisson ratio of colliding bodies, only four parameters, including the inertia coupling λ and θ, friction coefficient μ and the ratio of incident velocity tan α, can have an effect upon the prediction of the motion of mechanical collisions. Other

material properties, including Young's modulus and mass density, will thus no effects upom collision motions. All slip and stick conditions of incident velocity at the initial state of impact for general configuration have been found in terms of inertia coupling parameters λ, θ and friction coefficient μ. Among three different spring models, linear spring analysis is stable under all circumstances and its conditions of stick and slip are identiacal to those by Maw et al. [10] for the impact of elastic spheres. Despite consistency of third coefficient of restitution d, other two coefficients of restitution c and e are highly dependent upon four input parameters λ, θ, μ and α.

Numerical method frequently limits the time increments and requires long running time in calculation. In certain circumstances, moreover, the result from the use of ANSYS code are unstable with respect to energy consideration. Distinct from these difficulty in calculation and instability, analysis of spring-mass system also provides a great advantage in simplicity and stability upon all occasions.

This means of analysis developed for the current investigation can be extended to the three dimensional cases without any further complexity. Based upon the assumption that the contact area is a circle and compliances in the two tangential direction $\mathbf{t}_1$ and $\mathbf{t}_2$ are independent each other, the nondiagonal coefficients of stiffness for local deformation are zero and only diagonal terms remain. In general, however, shape of contact area will be elliptical and there will be two principal directions, $\mathbf{t}_1$ and $\mathbf{t}_2$. Elliptical integration should be involved in the calculation of tangential displacement, in which case the stiffness of the two tangential deformations become coupled and

offdiagonal terms exist. Thus, determination for the coefficients of tangential stiffness would be much complicated and tedious job.

If permanent deformations exist at the contact area for high incident velocity, then the assumption of elastic colliding material would no longer be valid. In this circumstance there is an energy dissipation due to permanent deformation in normal direction. For the analysis of this energy loss, the addition of damping term to the system equations could be considered. In this case it would be possible for the third coefficient of restitution, d (the ratio of work done during compression and restitution in normal direction), to be far smaller than one. The determination of the coefficients of damping in the normal and even tangential direction could constitute the subject of further study in impacts. Similarly, the effect of wave propagation within colliding bodies also forms the basis for a future study of interest.

BIBLIOGRAPHY

1. Brach, R. M. , 1984, " Friction, Restitution, and Energy Loss in Planar Collisions," ASME Journal of Applied Mechanics, Vol. 51, pp. 164-170.

2. Brach, R. M. , 1989, " Rigid Body Collisions," ASME Journal of applied Mechanics, Vol. 56, pp. 133-138.

3. Engel, P. A. , 1976 , Impact Wear of Material, Amsterdam, New York.

4. Goldsmith, W. , 1960, Impact , Edward Arnold LTD. , London.

5. Hunter, S. C., 1957, " Energy Absorbed By Elastic Waves During Impact," Journal of the Mechanics and Physics of Solids, Vol. 5, pp. 162-171.

6. Johnson, K. L., 1985, Contact Mechanics, Cambridge, London.

7. Kane, T. R. and Levinson, D. A., 1985, Dynamics: Theory and Applications, McGraw-Hill, New York.

8. Keller, J. B., 1986, " Impact with Friction," ASME Journal of applied Mechanics, Vol. 53, pp. 1-4.

9. Liu, P., 1991, " Rebound Predictions for Elastic Collision," Ph.D. Dissertation, Oregon State University, Corvallis , Oregon.

10. Maw, N., Barber, J. R. and Fawcett, J. N., 1976, " The Oblique Impact of Elastic Spheres," Wear, Vol. 38, No. 1, pp. 101-114.

11. Maw, N., Barber, J. R. and Fawcett, J. N., 1977, " The Rebound of Elastic Bodies in Oblique Impact," Mech. Res. Comm., Scientific Communication, Vol.4, pp. 17-22.

12. Maw, N., Barber, J. R. and Fawcett, J. N., 1981. " The Role of Elastic Tangential Compliance in Oblique Impact," ASME Journal of Lubrication Technology, Vol. 103, pp. 74-80.

13. Mindlin, R. D., 1949, " Compliance of Elastic Bodies in Contact," ASME Journal of Applied Mechanics, Vol. 71, pp. 259-268.

14. Mindlin, R. D. and Deresiewicz, H., 1953," Elastic Spheres in Contact Under Varying Oblique Forces," ASME Journal of Applied Mechanics, Vol. 75, pp. 327-344.

15. Routh, E.J. , 1905, Dynamics of a System of Rigid Bodies, Vol. 1, Macmillan & Co., London.

16. Smith, C. E., 1991 ," Prediction Rebounds Using Rigid Body Dynamics," ASME Journal of Applied Mechanics, Vol. 58, pp. 754-758.

17. Smith, C. E. and Liu, P. 1992, " Coefficients of Restitution," ASME Journal of Applied Mechanics (scheduled fior publication).

18. Stronge, W. J., " Rigid Body Collisions with Friction," Proc. R. Soc. London A., Vol. 431, pp. 169-181.

19. Timoshenko, S. P. and Goodier, J. N., 1970, Theory of Elasticity, 3rd edn., McGraw-Hill, New York.

20. Whittaker , E. T., 1904, A Treatise on the Analytical Dynamics of Particles and Rigid Bodies, Cambridge.